UNCLASSIFIED

AD 453219

DEFENSE DOCUMENTATION CENTER

FOR

SCIENTIFIC AND TECHNICAL INFORMATION

CAMERON STATION ALEXANDRIA, VIRGINIA

Reproduced From
Best Available Copy

UNCLASSIFIED

NOTICE: When government or other drawings, specifications or other data are used for any purpose other than in connection with a definitely related government procurement operation, the U. S. Government thereby incurs no responsibility, nor any obligation whatsoever; and the fact that the Government may have formulated, furnished, or in any way supplied the said drawings, specifications, or other data is not to be regarded by implication or otherwise as in any manner licensing the holder or any other person or corporation, or conveying any rights or permission to manufacture, use or sell any patented invention that may in any way be related thereto.

Reproduced From
Best Available Copy

FDL-TDR-64-81
PHASE I

CATALOGED BY DDC
AS AD No. 453219

INVESTIGATION OF VARIOUS TEXTILE PARACHUTES AND CONTROL SYSTEMS TO ACHIEVE STEERABILITY

TECHNICAL DOCUMENTARY REPORT No. FDL-TDR-64-81, PHASE I

OCTOBER 1964

AIR FORCE FLIGHT DYNAMICS LABORATORY
RESEARCH AND TECHNOLOGY DIVISION
AIR FORCE SYSTEMS COMMAND
WRIGHT-PATTERSON AIR FORCE BASE, OHIO

Project No. 6065, Task No. 606502

(Prepared under Contract No. AF 33(657)-10646 by
Northrop Corporation, Ventura Division, Newbury Park, California;
V. F. Riley and E. M. Linhart, Authors)

NOTICES

When Government drawings, specifications, or other data are used for any purpose other than in connection with a definitely related Government procurement operation, the United States Government thereby incurs no responsibility nor any obligation whatsoever; and the fact that the Government may have formulated, furnished, or in any way supplied the said drawings, specifications, or other data, is not to be regarded by implication or otherwise as in any manner licensing the holder or any other person or corporation, or conveying any rights or permission to manufacture, use, or sell any patented invention that may in any way be related thereto.

DDC release to OTS not authorized.

Qualified requesters may obtain copies of this report from the Defense Documentation Center (DDC), (formerly ASTIA), Cameron Station, Bldg. 5, 5010 Duke Street, Alexandria, Virginia, 22314.

Copies of this report should not be returned to the Research and Technology Division, Wright-Patterson Air Force Base, Ohio, unless return is required by security considerations, contractual obligations, or notice on a specific document.

400 - December 1964 - 448-17-419

Reproduced From
Best Available Copy

FOREWORD

This report was prepared by the Northrop Corporation, Ventura Division, On Air Force Contract No. AF 33(657)-10646, under Project No. 6065, Task No. 606502, "Investigation of Various Textile Parachutes and Control Systems to Achieve Steerability." The work was administered under the direction of the Air Force Flight Dynamics Laboratory Research and Technology Division, with Mr. R. H. Walker, Jr. of the Recovery and Crew Station Branch as project engineer.

This document is prepared in accordance with Exhibit A, Paragraph 3.5.6, of the contract and is submitted to fulfill the contractual obligation specified in Part I, Paragraph A-3, Item II, of the contract. All work on this research program has been conducted by the Aeronautical Engineering Section, Paradynamics Projects Group, under Northrop Ventura Project Number 0779.

The authors wish to acknowledge the contributions of Mr. W. Cook, Mr. P. Yaggy and Mr. J. Weiberg of NASA, Ames Research Center, for their aid and accommodation in providing their facility for the large model wind tunnel tests; and Mr. R. H. Puddycomb of the 6511th Test Group (Parachute) at El Centro, for his cooperation and support in conducting the free flight deployment tests.

This report covers the Phase I research conducted from June 1963 through March 1964; and was prepared by V. F. Riley, Project Engineer, and E. M. Linhart, Project Aerodynamicist.

Reproduced From Best Available Copy

ABSTRACT

This research program covers the detailed investigation of gliding parachutes and their necessary guidance and control systems to achieve a controlled approach to an touchdown at a pre-selected site. Theoretical and analytical investigations have been conducted to determine system feasibility and performance limits; and to establish the configuration of a flexible, self-inflating canopy capable of meeting the program objectives.

A series of exploratory wind tunnel tests with small model steerable parachutes has been conducted to substantiate the findings of the analytical investigation and further define the detail design of the most promising configurations. Additional tests with large scale models in the form of tow tests, wind tunnel tests, and free-flight deployment tests, have been conducted to demonstrate aerodynamic characteristics; and to obtain essential data for use as design criteria for an integrated steerable parachute system.

The results of this research program, reported herein, has culminated in the design of a flexible, self-inflating, steerable parachute canopy which has demonstrated in wind tunnel tests a maximum lift-to-drag ratio of 2:1; has been deployed in free-flight tests at velocities up to 150 knots; and has demonstrated a turn rate of approximately thirty (30) degrees-per-second.

CONTENTS

SECTION		PAGE
1	INTRODUCTION.	1
2	SUMMARY	5
3	ANALYTICAL INVESTIGATION.	9
4	EXPLORATORY INVESTIGATION	23
5	ANALYSIS.	35
6	CONCLUSIONS	77
7	RECOMMENDATIONS	79
8	REFERENCES.	81

APPENDIX		
I	DESCRIPTION OF MODELS TESTED.	83
II	WIND TUNNEL TEST PROGRAM FOR THE SMALL MODEL TESTS	99
III	TRUCK TOW TESTS	111
IV	AMES WIND TUNNEL TESTS.	141

ILLUSTRATIONS

FIGURE		PAGE
1	L/D Max as a Function of Porosity	12
2	L/D Max as a Function of Parachute Diameter.	13
3	C_l vs C_d for Naca 2415 Air Foil Section .	14
4	L/D Max as a Function of Velocity	17
5	L/D vs Aspect Ratio	20
6	Maximum L/D Values Obtained from Small Model Tests	27
7	Model 301 Flying Vertically in the Wind Tunnel.	36
8	Model 301 Flying Vertically in the Wind Tunnel.	37
9	Model 217, 3-ft D_W Version of Model 301 .	38
10	Cross Section of Canopy's Leading Edge. .	40
11	Cross Section of Canopy's Leading Edge. .	40
12	L/D vs Flap Extension-Ames Wind Tunnel Tests	42
13	Cross Section of Model 301 Showing Flow Field	43
14	C_L vs C_D-Ames Wind Tunnel Tests	45
15	Lift Coefficient vs Flap Extension. . . .	47
16	Drag Coefficient vs Flap Extension. . . .	48
17	L/D vs Extension of Interior Lines. . . .	50
18	C_L vs C_D as a Function of Velocity. . . .	52
19	C_L vs C_D as a Function of Velocity. . . .	53
20	C_L vs C_D as a Function of Velocity. . . .	54

ILLUSTRATIONS (CONT)

FIGURE		PAGE
21	L/D Max vs Velocity as a Function of D_w . .	56
22	System C_L and C_D at Max L/D	57
23	C_D vs Percent Reefing-Ames Wind Tunnel Tests	58
24	Weight vs Velocity at Max L/D	63
25	Weight vs Velocity at Max L/D	64
26	Weight vs Velocity at Max L/D	65
27	Turning Torque vs Steering Displacement . .	67
28	Turning Torque vs Steering Displacement . .	68
29	Turning Rate vs Time	71
30	Turning Rate vs Time	72
31	Glide Ratio Control	74
32	Sketches of Models Tested	86
33	Steerable Parachute - Model 301 and 301A . .	92
34	Steerable Parachute - Model 301-16	93
35	Steerable Parachute - Model 302	94
36	Steerable Parachute - Model 303	95
37	Steerable Parachute - Model 304	96
38	Steerable Parachute - Model 402	97
39	Support Installation - Vertical Wind Tunnel	101
40	L/D vs Flap Extension	104
41	C_M vs Strut Angle	105

ILLUSTRATIONS (CONT)

FIGURE		PAGE
42	L/D vs Flap Extension, Model 301A	112
43	L/D vs Center Group Extension, Model 301A	113
44	L/D vs Flap Extension, Model 302.	114
45	L/D vs Flap Extension, Model 303.	115
46	L/D vs Flap Extension, Model 304.	116
47	L/D vs Flap Extension, Model 402.	117
48	L/D vs Flap Extension, Model 101.	118
49	Force Coefficient vs Flap Extension, Model 301A.	119
50	Force Coefficient vs Riser Extension, Model 301A.	120
51	Force Coefficient vs Flap Extension, Model 302	121
52	Force Coefficient vs Flap Extension, Model 303	122
53	Force Coefficient vs Flap Extension, Model 304	123
54	Force Coefficient vs Flap Extension, Model 402	124
55	Force Coefficient vs Flap Extension, Model 101	125
56	Model 301A.	126
57	Model 302	127
58	Model 303	128
59	Model 402	129
60	Model 101	130
61	Boom Assembly Mounted on Truck.	131

ILLUSTRATIONS (CONT)

FIGURE		PAGE
62	Control Mechanism Mounted on Boom	132
63	Instrumentation on the Truck.	133
64	L/D vs Flap Extension-Ames Wind Tunnel Tests	143
65	L/D vs Flap Extension, Model 301.	144
66	L/D vs Flap Extension, Model 301A	145
67	L/D vs Extension of Interior Lines. . . .	146
68	Flap Riser Force vs Flap Extension, Model 301	147
69	Flap Riser Force vs Flap Extension, Model 301A.	148
70	Flap Riser Force vs Flap Extension, Model 301	149
71	Reefing Line Force vs Percent Reefing . .	150
72	Reefing Line Force vs Percent Reefing . .	151
73	L/D vs Flap Extension, Model 302.	152
74	C_D vs Percent Reefing, Model 302.	153
75	L/D vs Flap Extension, Model 303.	154
76	L/D vs Flap Extension, Model 304.	155
77	L/D vs Flap Extension, Model 402.	156
78	L/D vs Flap Extension, Cluster 302's. . .	157
79	L/D vs Flap Extension, Model 101.	158
80	L/D vs Flap Extension, Model 105.	159
81	L/D vs Flap Extension, Model 113.	160
82	L/D vs Flap Extension, Model 113.	161

ILLUSTRATIONS (CONT)

FIGURE		PAGE
83	Model 302 Flying Vertically in the Wind Tunnel.	162
84	Model 302 Flying Vertically in the Wind Tunnel.	163
85	Model 101 Flying Horizontally in Wind Tunnel.	164
86	Model 101 Flying Vertically in the Wind Tunnel.	165

TABLES

TABLE		PAGE
1	Summary of Gliding Parachutes	10
2	Small Model Wind Tunnel Test Data Summary	25
3	Models Selected for Testing	28
4	Results of Tow Truck Test Program	29
5	Models Tested	30
6	Results of Ames Tests	31
7	Results of Deployment Tests	33
8	Opening Force Data	60
9	Weights for Descent Velocities	62
10	Summary of Configurations Tested	84
11	Cluster Configurations	85
12	Small Model Wind Tunnel Results	103

SYMBOLS

A.C.	Aerodynamic Center
C_L	lift coefficient
C_D	drag coefficient
C_R	total parachute force coefficient
C_M	parachute pitching moment coefficient
C_Y	side force coefficient
C_N	yawing moment coefficient
C_{LR}	rolling moment coefficient
C_T	tangential force coefficient
C.P.	Center of Pressure
D_o	nominal parachute diameter (ft)
D_p	inflated parachute diameter (ft)
D	drag force parallel to free stream (lbs)
D_{o_c}	cluster equivalent nominal diameter (ft)
D_V	vent diameter (ft)
D_S	suspension line diameter (ft)
D_W	parachute diameter based on S_W (ft)
E_{CG}	Control line extension for interior lines
E_{CGI}	Control line extension for inner group of interior lines
E_{CGO}	Control line extension for outer group of interior lines
E_F	length of flap control line extension (ft)
E_{LE}	leading edge extension (ft)

F_{CG}	Control Line force for interior lines (lbs)
F_{CGI}	Control line force for inner groups of interior lines (lbs)
F_{CGO}	Control line force for outer group of interior lines (lbs)
F_F	force in flap riser (lbs)
F_R	total or resultant aerodynamic parachute force (lbs)
F_{RL}	tension in reefing line (lbs)
F_T	tangential force (lbs) (measured along geometric axis of parachute)
H_F	control flap depth (ft)
H_S	steering slot depth (ft)
l	lift force normal to free stream (lbs)
lR	rolling moment (ft-lbs)
l/D	lift to drag ratio
L_E	effective suspension line length (ft)
L_S	length of suspension line (ft)
L_R	length of riser (ft)
M	pitching moment (ft-lbs)
N	yawing moment (ft-lbs)
n	number of canopies
q	dynamic pressure (lbs/ft^2)
S_o	nominal parachute area (ft^2)
S_p	projected parachute area (ft^2)
S_w	upper canopy surface wetted area (ft^2)
T	thrust (lbs)
V_T	free stream velocity (ft/sec) (ref. velocity for coefficients)

V_H	horizontal velocity (ft/sec)
V_V	vertical velocity (ft/sec)
W_D	descent weight (lbs)
W_S	suspended weight (lbs)
Y	side force (lbs)
Z	total number of gores in canopy
Z_F	number of gores in flap
α	angle of attack of parachute canopy (deg) (measured between plane of canopy skirt and free stream)
α_r	incremental change in canopy angle of attack
β	$90 - \gamma$
γ	glide angle from horizontal (deg)
λ	total porosity (%)
δ	angle between geometric axis of parachute and relative wind
ϵ	angle between parachute axis and C.P/C.G. axis (deg)
ψ	angle of yaw (deg)

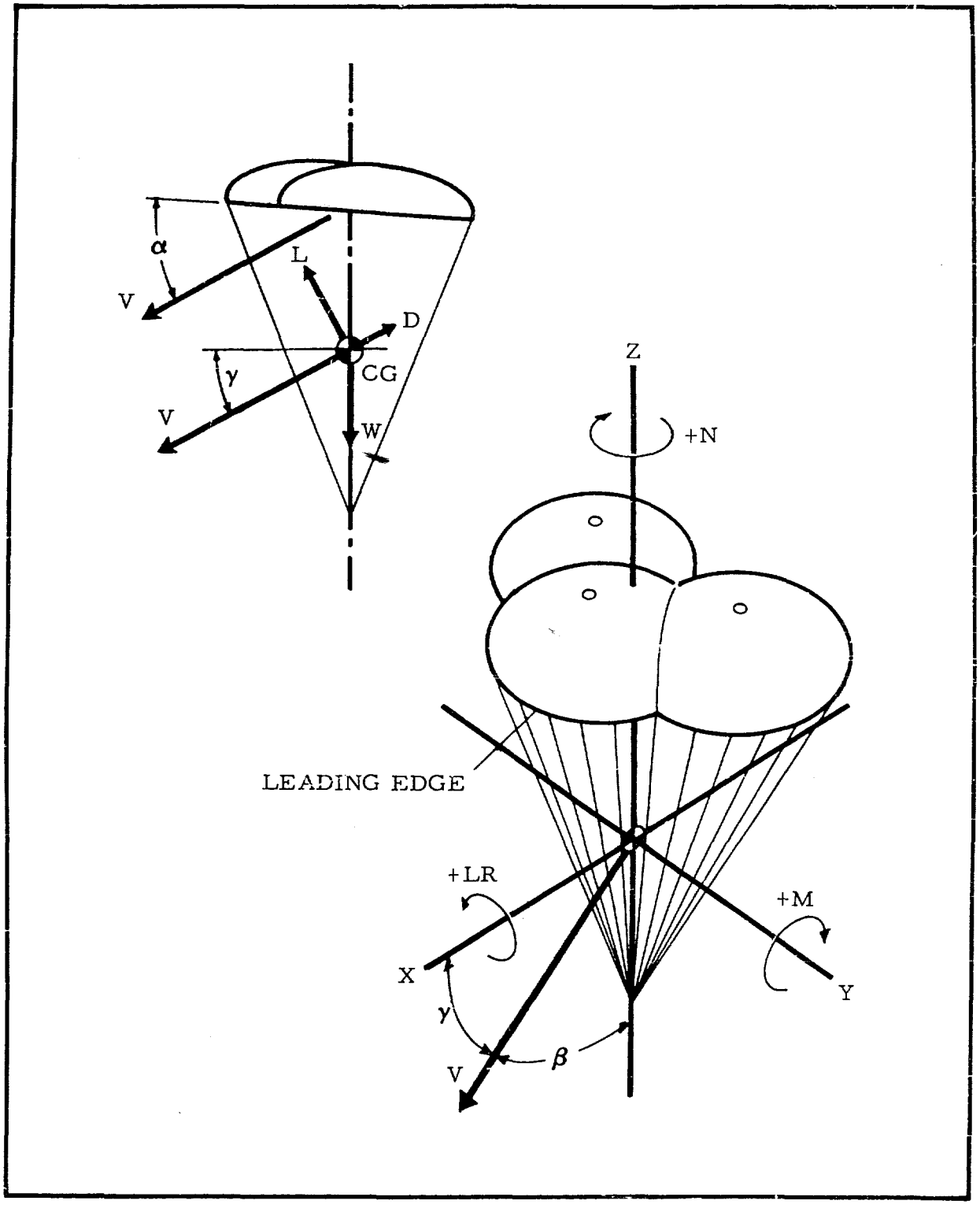

Force & Coordinate System

Preceding Page Blank

SECTION 1

INTRODUCTION

In extending its original research in controllable parachutes, Northrop Ventura was awarded Air Force Contract No. AF 33(657)-10646 on 20 May 1963. The scope of this applied research program involves the detailed investigation of various textile parachute canopy configurations and control systems to achieve steerability and to directionally control the final descent trajectory of parachute decelerated manned or unmanned vehicles. The investigation was to be confined to parachutes capable of fulfilling specific minimum performance criteria, primarily a lift to drag ratio of 2.0.

Prior to awarding this contract, Northrop Ventura conducted research programs in the area of steerable parachutes. These investigations were restricted to the determination of the performance of conventional solid cloth-type or ringsail parachute canopies with a gore removed, slots, or slot-flap combinations, but still retaining the basic inflated shape of conventional parachutes. These canopies, at best, produced a lift-to-drag ratio of approximately 1.5, while current and future requirements for parachute deceleration and recovery applications require significantly increased controlled gliding capabilities.

Manuscript released by authors May 1964 for publication as an FDL Technical Documentary Report.

Phase I of this program embodied a feasibility investigation, including both analytical and laboratory tests, to determine the feasibility of the self-inflatable steerable parachute within specific performance parameters. Analytical and theoretical investigations have been conducted to establish the preliminary canopy configurations, the performance of the proposed configurations, and the limitations imposed by the requirements for a self-inflating shape. Initial efforts in this investigation consisted of a technical literature search of both rigid and flexible canopy shapes and the systematic compiling and analysis of available data. The objective of this initial effort was to appraise the performance contribution of a specific design feature or combination of design features which appeared feasible for incorporation into a self-inflating, flexible parachute canopy; and thereby establish trends which may be used to predict the performance of a specific parachute configuration. The results of this investigation, supported by a theoretical analysis of the aerodynamic principles involved, created the preliminary models for further evaluation in the initial series of small model wind tunnel tests. This test series was conducted to substantiate the findings of the analytical investigations and demonstrate and/or determine the inflation, stability, and aerodynamic characteristics of these configurations. A selection of the most promising of these preliminary models was made for further evaluation as large scale models in a series of tow tests, additional wind tunnel tests, and free flight deployment tests. In addition to demonstrating their aerodynamic characteristics, the large scale tests were conducted to obtain design criteria for determining the requirements for a free-flight program of larger diameter parachutes to be conducted in later phases. The requirements for the free flight program derived from these tests include flap extension and actuation forces, control mechanism actuation and response time, instrumentation, test load configuration, guidance system, and test vehicle on-board electrical system.

This document reports the accomplishments of the Phase I feasibility investigation, including the results of the analytical and theoretical investigations, wind tunnel tests, tow tests, free-flight deployment tests; and presents the requirements and recommendations for conducting subsequent free-flight controlled glide tests.

SECTION 2

SUMMARY

2.1 GENERAL

The primary objective of this program was to develop a non-rigidized, self-inflating, gliding parachute with the capability of gliding at an L/D of 2.0 or better. The program proceeded in the following sequence.

A literature survey of the available data on gliding parachutes was conducted and an analysis of the data was made. Based on the results of this analysis, a series of small models (D_o of approximately 3 ft) were designed and tested to determine the design with the best potentional of meeting the performance requirement. During the small model test series, a total of 19 single model configurations and 3 cluster configurations were tested. As a result of the data obtained from these tests, four basic configurations were selected to be tested as larger models (D_o of approximately 12 ft). The tests were conducted both with a truck tow rig and by testing in a wind tunnel. The model which had the best L/D capability and one other model were then drop tested to check the feasibility of deploying the unconventional canopy which was developed and to obtain information on the deployment characteristics of low porosity canopies. The following paragraphs give a brief summary of the work accomplished during each investigational program during Phase I.

Preceding Page Blank

2.2 ANALYTICAL INVESTIGATION

The analytical investigation consisted of a literature survey, an analysis of the data resulting from this survey, and a theoretical analysis of canopy aerodynamics. The analysis showed that three primary factors, independent of canopy design, affected performance and that certain canopy design features should be included in a canopy design capable of high L/D performance. The factors independent of canopy configuration are: (1) canopy porosity, (2) canopy size and (3) glide path velocity. The canopy configuration design features found to improve L/D performance were: (1) leading edge extensions supported by cloth ribs which shape the leading edge to an airfoil shape (2) controllable flaps at the rear of the canopy, (3) a forward compartment or interior canopy web, and (4) increasing the canopy aspect ratio.

2.3 EXPLORATORY INVESTIGATION

2.3.1 Small Model Tests

The small model tests conducted at the Wright Field vertical wind tunnel showed that the type of configuration which had the best potential for meeting the program objective was a three lobe type of design. This design was in affect a low aspect modified triangular wing made of cloth and depends only on the pressure distribution induced by the airflow around it to maintain its shape.

2.3.2 Tow Tests of Large Models

The tow tests resulted in confirmation of the results of the small model tests. The three lobe design (Model 301) achieved an L/D of just under 2.0 and showed itself as being much superior to the other designs tested. During these tests a significant increase in L/D performance for an increase in size from D_o = 12 ft to D_o = 16 ft was noted. As a secondary result

of these tests, it was shown that a truck tow rig was an economical and practical method of quickly evaluating the performance of gliding parachutes.

2.3.3 Wind Tunnel Tests of Large Models

During tests conducted at the Ames wind tunnel the three lobe design (Model 301) achieved an L/D of 2.1 and was clearly superior to the other designs tested. During this test program, data on L/D performance as a function of flap settings, the affect of interior line rigging on L/D, flap riser forces, reefed drag coefficients, and the affect of velocity on performance were obtained. Also, many of the models from the Aerosail test program were retested (See Reference 1 for previous results).

2.3.4 Deployment Tests of Large Models

Nine aerial drop tests were conducted at the El Centro Test Facility to get data on the deployment characteristics of the three lobe design (Model 301) and the affect of low canopy porosity on opening shock. These tests were conducted for a range of drop velocities and canopy reefing. The three lobe design showed excellent opening characteristics. It was very stable in the reefed condition and the data obtained on opening indicates that deployment of larger canopies of the three lobe design will be possible.

SECTION 3

ANALYTICAL INVESTIGATION

3.1 GENERAL

The initial task of Phase I was an analysis of the data available from previous gliding parachute research programs. The programs from which data were available were, Northrop Ventura in-house research programs, the Northrop Ventura conducted Glide Sail Program, the Northrop Ventura conducted Aerosail Program, the University of Minnesota Gliding Parachute Program and the Pioneer Parasail Development Program. A summary of the more successful designs evolved by these research programs and the performance of these designs is shown in Table 1.

NOTE: During the Ames wind tunnel tests conducted during the latter part of Phase I, it was discovered that the published data from the Aerosail test program was in error. Therefore, to prevent confusion by presenting data which is known to be in error, corrected data is used throughout this report when referring to the Aerosail research program. An explanation for the original erroneous data along with a summary of the uncorrected and corrected L/D max data is presented in Appendix D.

During the investigation of available data it was found that three major parameters have a significant influence on the L/D performance of gliding parachutes and are relatively independent of the canopy configuration. These three parameters and their affect on performance are listed below.

Preceding Page Blank

This document contains blank pages that were not filmed

TABLE 1

SUMMARY OF GLIDING PARACHUTES

Origin and Model Designation	Basic Design	L/D Max.	Model Size	Where Tested	Notes on Performance
Northrop Ventura, (Aerosail Model 101)	Circular flat with extended leading edge, and rear flaps.	1.54	12-ft D_o	Ames	High L/D, leading edge cave-in, stable in pitch, unstable in yaw.
Northrop Ventura, (Cluster 2)	Cluster of Aerosail Models 105 and 101 (105 leading).	1.51	12-ft D_o	Ames	High L/D, leading edge cave-in, stable in pitch, unstable in yaw.
Univ. of Minnesota (Parafoil)	Airfoil shaped canopy, rib supported	1.19 1.10	10-ft D_o 2-ft D_o	U.of M. U.of M.	Very stable about all axis. Leading edge very stable.
Pioneer, (Para-Sail)	Conical louvered canopy	1.06 .84 (Prototype) 1.07 (Modified)	23-ft D_o 32-in. D_o 32-in. D_o	Ames U.of M. U.cf M.	Very stable about all axis. Has been drop-tested.
Northrop Ventura, (Aerosail Model 114)	Same as 101 but with an inflated tube around the skirt of the canopy.	1.94	12-ft D_o	Ames	
Northrop Ventura, (Aerosail Model 113)	Circular flat with flaps (no leading edge extension.	1.11	12-ft D_o	Ames	

(1) Canopy Porosity; increasing canopy porosity results in a decrease in L/D capability.

(2) Parachute Size; increasing canopy diameter results in an increase in L/D capability.

(3) Operational Velocity; increasing operational velocity results in a decreased L/D capability.

The preceding statements are made as a result of the data presented in Figures 1, 2, and 3. These figures are summary plots of data taken from the previously mentioned research programs.

As shown in Figure 1, an increase in canopy porosity decreases the L/D capability of all known gliding parachute configurations. This affect may be due to more than one phenomenon. Any increase in canopy porosity results in an increase in mass flow through the canopy, with a resulting loss of internal canopy pressure and a decrease in pressure differential across the canopy. This in turn results in a loss in lift and canopy rigidity. Also, flow through the fabric of a solid cloth canopy could cause the flow over the upper surface to detach at a point further forward than for a nonporous canopy. This also results in a loss in lift. A large portion of the drag on a gliding parachute at high values of L/D is caused by form drag and suspension line drag, which do not decrease with an increase in mass flow through the canopy surface. Since with the loss in lift due to porosity there is not a proportional decrease in drag, there is a loss in L/D capability.

The effect of parachute size on (L/D) maximum is shown in Figure 2. This increase of L/D with increasing parachute diameter, while holding altitude, velocity and configuration constant, is the same type of trend shown by airfoil sections. Under the conditions given, an increase in parachute diameter corresponds to an increase in Reynolds Number. A characteristic

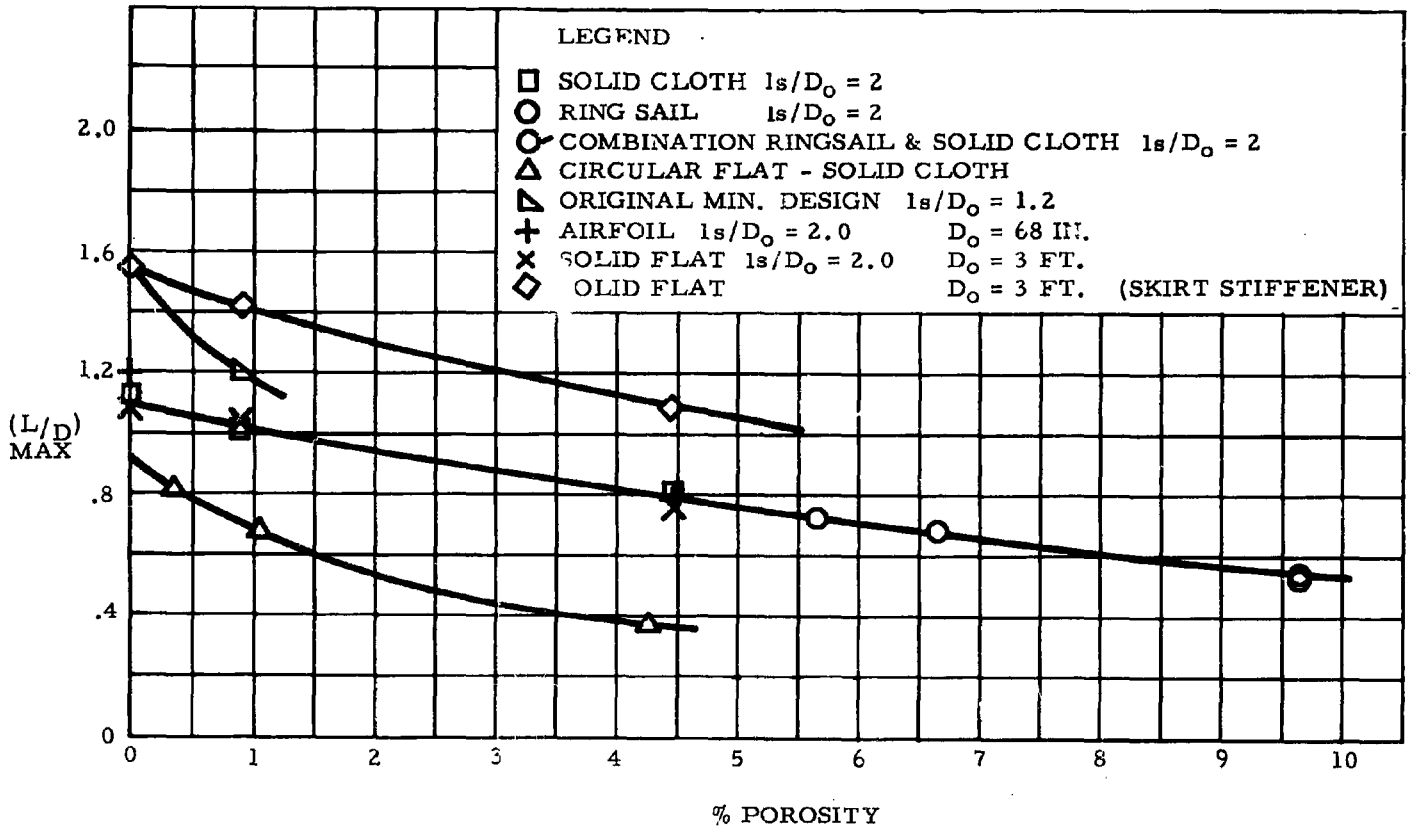

Figure 1. L/D Max as a Function of Porosity

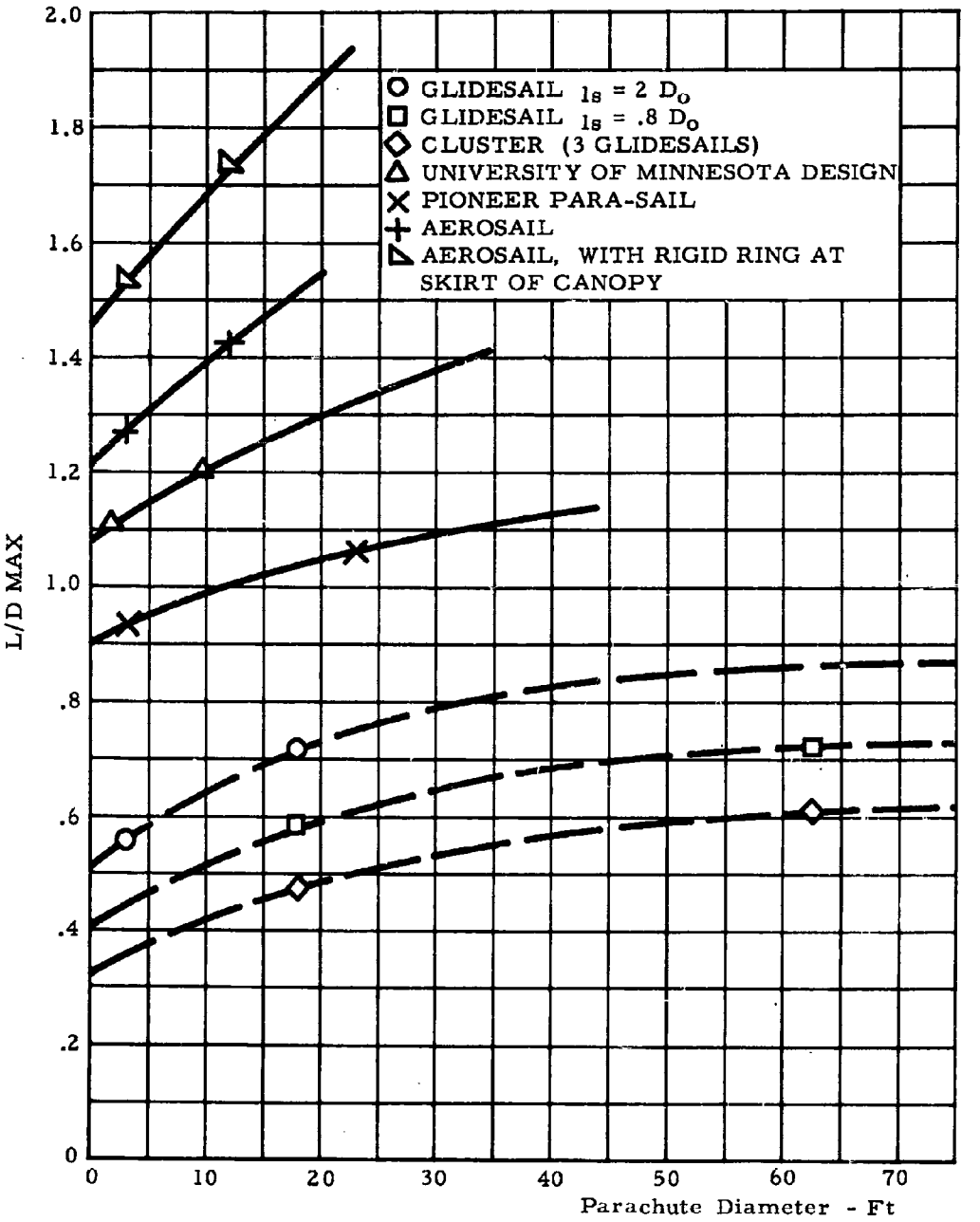

Figure 2. L/D Max as a Function of Parachute Diameter

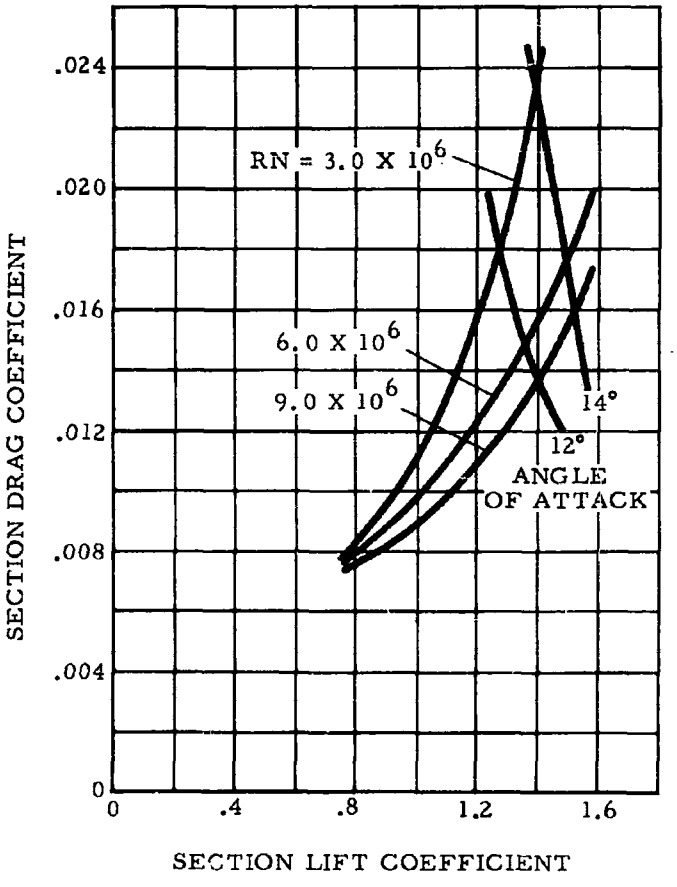

Figure 3. C_l Vs C_d for Naca 2415 Air Foil Section

of high lift airfoil sections is that the maximum C_L that can be obtained increases with increasing Reynolds Number, without a proportionate increase in drag. This is the same as saying that for a wing flying at a constant angle of attack near its stall point an increase in Reynolds number will result in an increase in L/D. It should be noted that this phenomenon is most pronounced at angles of attack near the stall point of the wing. This condition corresponds to a gliding parachute operating at its maximum L/D. In other words, the parachute is acting as a thick airfoil operating close to its stall point. Figure 3 is a replot of section drag coefficient versus section lift coefficient for the NACA 2415 airfoil section. This plot was taken from Reference 2. The data presented in Figure 3 shows the influence of Reynolds Number on the characteristics of a typical airfoil section. It is evident from this data that for a constant angle of attack a large increase in L/D occurs with increasing Reynolds Number. For the airfoil data shown this increase in L/D is 60 percent for an angle of attack of 14 degrees and an increase in Reynolds Number from 3.0×10^6 to 9.0×10^6. Figure 2 shows data from two basic parachute designs. The Glidesail and Para-Sail designs are basically slotted canopy designs, which implies a good deal of canopy porosity, while the Aerosail and University of Minnesota design are solid cloth configurations. As shown by Figure 2 the effect of canopy size is more pronounced for the solid cloth canopies, which are more comparable to a wing, than for the slotted canopy design. The range of Reynolds Numbers covered by the data shown in Figure 2 is 0.6×10^6 to 12×10^6. Although it is not expected that data from a thin airfoil section can be applied directly to a gliding parachute, it is felt that the trend as shown in Figure 2 can be explained as a scale effect such as displayed by airfoils. The generally accepted rule that vertically descending parachutes are not affected by Reynolds Number in the subsonic range is not made invalid by this analysis. Vertically descending parachutes have detached flow over the

entire canopy while gliding parachutes depend on attached flow over a portion of the canopy and are therefore subject to Reynolds Number effects.

The effect of increasing operational velocity as shown in Figure 4 is a loss in L/D capability. This result seems to be in contrast to the results shown in Figure 3, since an increase in velocity, with other conditions not changing, is an increase in Reynolds Number.

However, it must be remembered that a self-inflating parachute is not a rigid structure, and its shape is determined by a balance of aerodynamic forces and strain in the canopy material and suspension lines. This in turn leads to the possibility of canopy distortion with increasing aerodynamic forces. What probably happens is that the drag of the suspension lines and the form drag of the canopy increase with velocity while the canopy distorts with the result that lift does not increase proportionately with drag. This in turn results in a net loss in L/D.

3.2 CANOPY CONFIGURATION DESIGN

When designing a self-inflating gliding parachute one is faced with the obvious fact that the canopy can only be made to hold a shape that can be supported by the pressure distribution on the canopy. In previous research programs three basic designs were used. These were slotted canopies such as the Para-Sail, solid cloth designs such as the University of Minnesota design which uses ribs to support the roof of the canopy and thus attain an improved airfoil shape and the Aerosail design which employs ribs to obtain a shaped leading edge and has an extendible rear flap to get a better airfoil profile. The maximum L/D which can be obtained with these three designs seems to be limited in each case by the canopy angle of attack at which the leading edge caves in. Tests at the University of Minnesota indicate that the

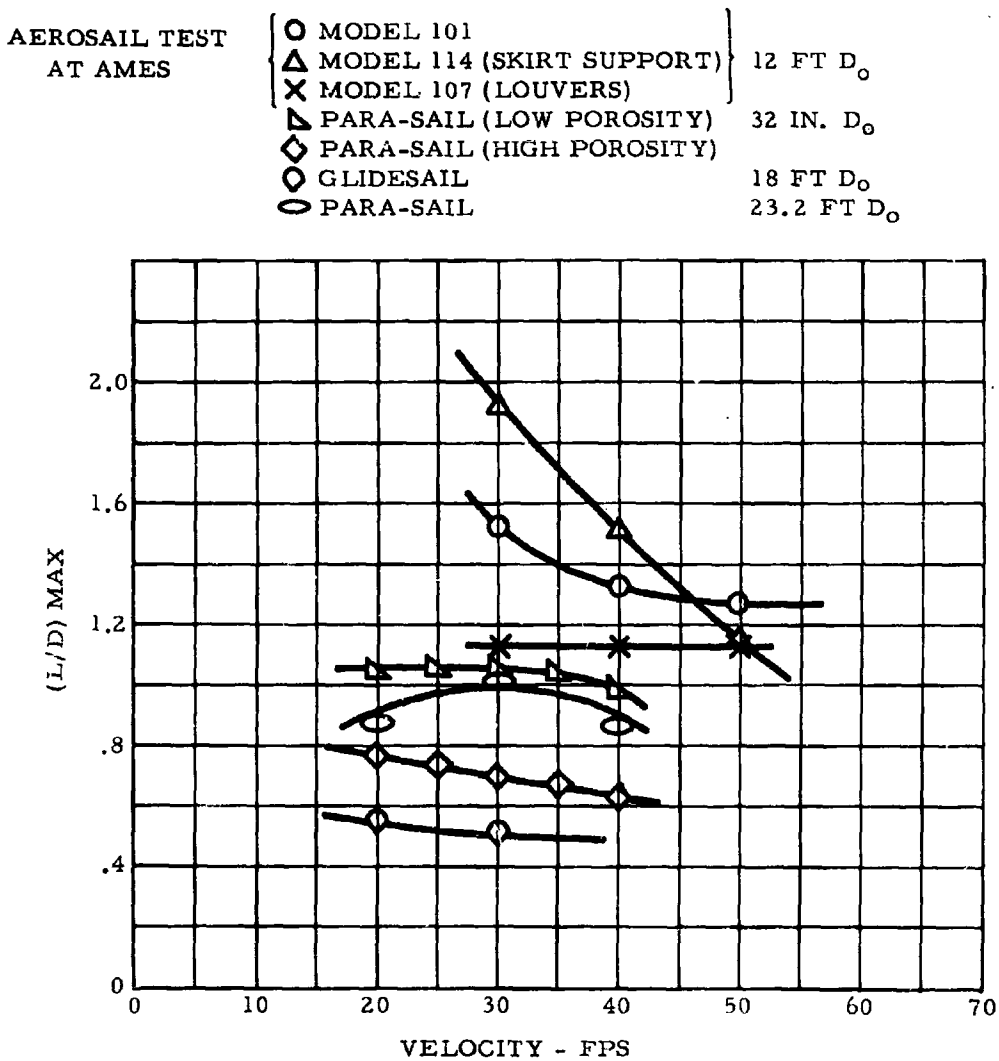

Figure 4. L/D Max as a Function of Velocity

maximum L/D for the Para-Sail design is about 1.07 and for the University of Minnesota design 1.19. The Aerosail design achieved an L/D of 1.54 while a 3-chute cluster of Aerosails reached an L/D of 1.51. Again the L/D capability of all these configurations is limited by leading edge collapse. These three test programs indicate that in order to get values of L/D = 2 or better, some way must be found to design a canopy which will hold its shape at lower canopy angles or attack, or to increase lift, decrease drag or both for the angle of attack the canopy will maintain without collapsing.

Three methods of getting improved results are indicated by the results of previous research programs and by wing theory.

The first approach is to extend the leading edge of the canopy by using ribs and thus increase the angle of attack of the leading edge of the canopy. This is the approach used in the Minnesota design and the Aerosail design and has resulted in appreciable increases in L/D over the basic parachute design without the leading edge extensions.

The second approach is one suggested by the results attained by a three chute cluster in the Aerosail test program. The cluster in this case achieved an L/D appreciably higher than the lead parachute attained while flying alone. What was done in this test was to take a circular flat parachute with an extended and rolled-under leading edge and use it for the front parachute in the cluster. The two rear chutes were basically the same except that they had rear flaps that were extended and did not have the rolled-under leading edge. The reason that this configuration reached comparatively high values of L/D may have been due to the front parachute having an increased internal pressure. This higher internal pressure could have been caused by the influence of the canopies behind it and the fact that it was basically a solid flat canopy without vents or flaps to reduce internal pressure.

Another possibility suggested by the three chute cluster and also by wing theory is the reduction of induced drag by increasing aspect ratio. For a wing with an elliptical lift distribution the difference in drag, for a constant C_L or angle of attack, and aspect ratios of AR_1 and AR_2 is

$$C_{D1} - C_{D2} = \frac{C_L^2}{\pi}\left(\frac{1}{AR_1} - \frac{1}{AR_2}\right).$$

Figure 5 shows a curve which gives the increase in L/D performance which would be obtained by applying this equation to a typical gliding parachute. As an example of what could theoretically be gained in L/D performance let us take the case of changing a parachute configuration from a circular parachute to a chute with an elliptical planform with a major to minor axis ratio of 1:5. Aspect ratio is defined as b^2/S

b = span

S = planform area.

For a circle

AR = 1.273

For an ellipse with major to minor axis ratio of 1.5:1

AR = 1.9.

As shown in Figure 5 an increase in AR from 1.27 to 1.9 corresponds to an increase in L/D from 1.72 to 2.0. It must be noted that this increase in L/D is based on theory which has proved to be accurate for rigid wings but which may not apply accurately to an airfoil section as thick as a parachute profile. However, the increase in L/D with AR for small values of AR, does indicate a significant increase in L/D should occur even with parachute profiles. It should further be noted, that when C_L is held constant and drag reduced, what effectively is happening is that L/D is increased, while holding angle of attack constant. This is a very important characteristic for increasing the maximum L/D of a gliding parachute. In most cases, the maximum L/D is limited by leading edge collapse, and the affect of

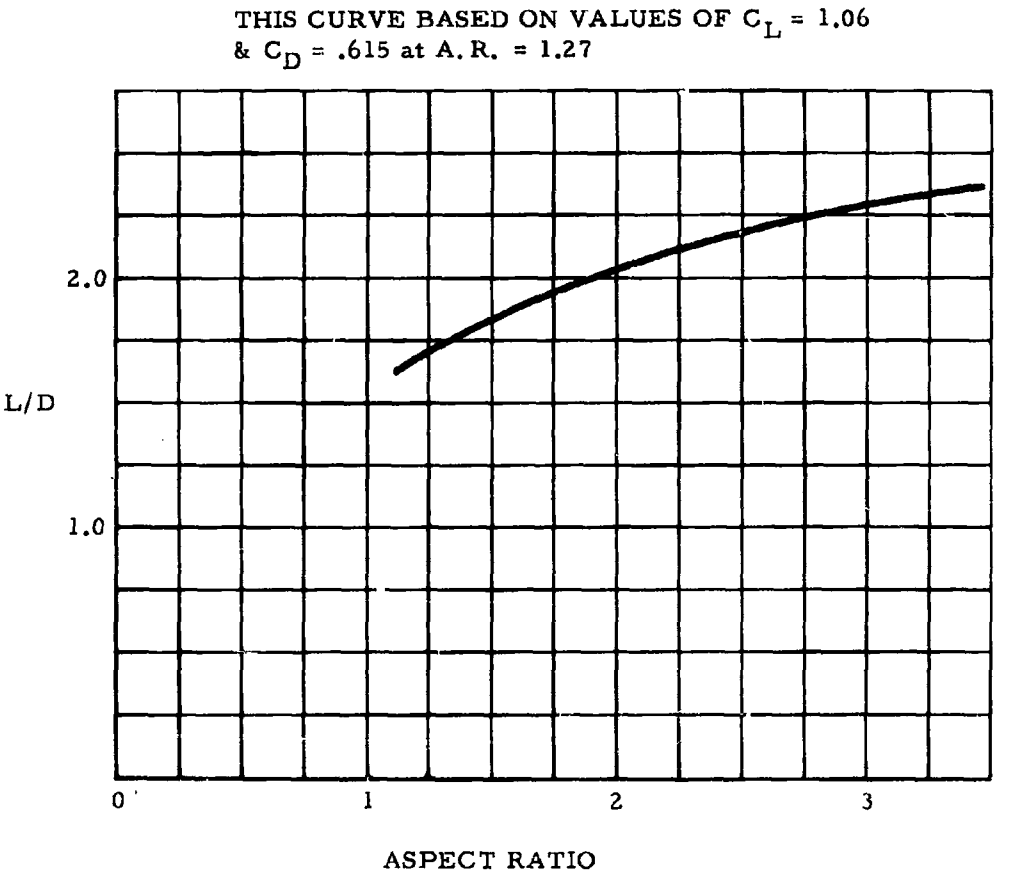

Figure 5. L/D Vs Aspect Ratio

increasing AR is to give a higher L/D without decreasing canopy angle of attack. As indicated by the preceding discussion, the following list of design features is considered desirable in a high performance gliding parachute.

(1) Canopy leading edge shaping to maintain the aerodynamic stagnation point below the canopy skirt while gliding.

(2) Addition of a forward pocket to the parachute canopy to maintain a higher internal pressure in the forward canopy area and thereby delay leading edge collapse while gliding at high lift to drag ratios.

(3) Increasing the parachute Aspect Ratio to reduce the parachute drag coefficient and thereby increase the L/D ratio for a given angle of attack.

(4) Controllable flaps at the rear of the canopy to provide a flatter canopy profile and turn control.

SECTION 4

EXPLORATORY INVESTIGATION

4.1 GENERAL

Based on the concepts evolved during the analytical investigation, a series of canopy configurations were designed. Small models of these designs (D_o of approximately 3 ft) were then tested in the Wright Field vertical wind tunnel. After evaluating the results of the small model tests, five configurations were selected to be tested with larger models. Tests with the larger Models (12- and 16-ft diameter) were then conducted by towing them with a truck equipped with test equipment, and by flying them in the Ames 40 x 80 Wind Tunnel. The two designs which showed the best performance during the tow tests and Ames wind tunnel tests were then aerial drop tested at the El Centro Drop Test Facility. A summary of the results of these test programs is presented in the following paragraphs. During the various tests conducted, data such as L/D vs flap extension, flap riser forces, reefed drag coefficients, and stability coefficients were taken. Since the primary objective of this research program was to develop a self inflating gliding parachute with an L/D capability of 2.0 or greater, the data presented in this section outlines the design evolution resulting in a configuration which meets this objective.

For complete detailed test procedures and test results refer to Appendices I, II, III, and IV. Also included in these

This document contains
blank pages that were
not filmed

Preceding Page Blank

Appendices are detailed descriptions and photographs of the models tested.

4.2 SMALL MODEL TESTS

In order to determine the validity of the conclusions reached as a result of the analytical investigation, a series of models were designed. These models, approximately 3-ft D_o, incorporated the design features suggested in Paragraph 3.2, and can be classified into three types of configurations as follows:

(1) Single canopies without internal lines, webs or stiffening.

(2) Single canopies with inflated structure or mechanical stiffening.

(3) Single canopies with internal webs and lines but no inflated or mechanical rigidizing structure.

Group (1) consists primarily of the Aerosail Model 101 design, the University of Minnesota design, variations and modifications of these two basic designs, and several other original designs.. Group (2) consists of an Aerosail Model 101 with inflated stiffening tubes and a circular flat canopy with a V boom structure for stiffening. Group (3) are designs attempting to incorporate a compartmented-type of structure. This is done either by building the model in three lobes or by using interior lines to distort the canopy to the desired shape. Several variations on these basic ideas were tried. Sketches and descriptions of all the small models are given in Appendix I.

These models were tested in the Wright Field vertical wind tunnel. Because the models were small (D_o approximately 3 ft), the data obtained from these tests was basically qualitative in nature. The results of these tests were evaluated on a comparative basis, that is, a model's performance was evaluated as compared to the rest of the models being tested. A summary of the configurations tested and results of the tests are presented in Table 2.

TABLE 2

SMALL MODEL WIND TUNNEL

Model No.	Description	Rigging for Best L/D	L/D	Remarks
201	Basic Minnesota Design	Run as rigged	1.28	Model was unstable in roll.
202	University of Minnesota Design with two flaps added to the rear of the canopy	As rigged	1.4	Moderate instability in yaw, stable in pitch. Leading edge pushed in.
203	University of Minnesota Design front half with Aerosail rear half.	Front risers extended 5.25 inches.	1.375	Moderate instability. Leading edge pushed in.
204	Basic Aerosail with extended leading edge. (Same design as Model 101 tested at Ames.)	Flaps extended 3.6 inches.	1.28	Fairly unstable pitch and yaw.
205	Model 204 with the addition of two rear ribs.	Flaps extended 2.5 inches.	1.28	Fairly unstable pitch and yaw.
206	Square design with side control panels.	Flaps extended 1.75 inches.	No data	Poor inflation, very unstable.
207	Single design incorporating features of a three chute cluster.	As rigged.	1.25	Fair stability all axis, has tendency to fly yawed.
208	Variation of Model 207.	Flaps extended 1.75 inches.	1.35	Instable unless restrained. Front lobe of chute buckled near intersection with rear lobes.
209	Variation of Model 207.	Flaps extended 1.125 inches.	1.57	Very stable all axis, slight buckling of leading edges of rear lobes.
210	Modification of Model 204(1st modification of leading edge).	Rear center gore pulled in 2.5 inches. Front risers extended 1.75 inches. Flaps extended 2.5 inches.	1.19	Fair stability, bottom of leading edge folded in.
211	Modification of Model 204(2nd modification of leading edge.)	Rear center gore pulled in 6.4 inches. Front risers extended 1.75 inches. Flaps extended 7.1 inches.	1.26	Stable in pitch, yaws to about 45 degrees.
212	Model 204 with addition of leading edge flaps.	Front risers extended 4.7 inches. Flaps extended 4.7 inches.		Object of testing this model was to try for lowest stable L/D. Model oscillated ± 20 degrees in yaw and ± 10 degrees in pitch.

Reproduced From
Best Available Copy

TABLE 2

WIND TUNNEL TEST DATA SUMMARY

	[illegible] of leading edge.)	[illegible] inches. Front risers extended 1.75 inches. Flaps extended 7.1 inches.		
212	Model 204 with addition of leading edge flaps.	Front risers extended 4.7 inches. Flaps extended 4.7 inches.		Object of testing this model was to try for lowest stable L/D. Model oscillated ± 20 degrees in yaw and ± 10 degrees in pitch.
213	Triangular arrangement of six circular flap canopies.	Flaps extended 1.75 inches.	.885	Leading edge of rear canopies collapsed.
214	Circular flat canopy with V arrangement of booms.	Side flaps extended 1.75 inches. Rear boom lines pulled in 1.75 inches.	1.65	Flew yawed with this rigging. Appeared to be capable of doing better if time could be taken to optimize rigging.
215	Model 204 with inflated tubes in leading edge and forward portion of canopy.	Rear center gore pulled in 6 inches. Front risers extended 1.75 inches. Flap extended 7.1 inches.	1.43	Stable about all axis. Leading edge held shape well.
216	Modification of Model 209. Leading edge of rear lobes have gussets.	Flaps extended 1.25 inches. Lines on front to be rigged 36" from bottom of gusset.	1.60	Good inflation, very stable.
217	Further modification of Model 209. Rolled under leading edge all three lobes. Front lobe shorted longitudinally.	Flaps extended 2.75-3.5 inches. All leading edge lines rigged 36" from bottom of gussets.	1.67	Good inflation, very stable, with fairing on top did about L/D = 1.73. At V = 30 fps L/D = 1.73. At V = 90 fps L/D = 1.55.
218	Circular flat chute with lines attached to interior of chute.	Flaps extended 1.25-[illegible] inches. All lines 36 inches except line 14 & 16 = 32.5, 43 & 45 = 39.0, and 44 = 38.5 inches.	1.38 - 1.43	Idea of getting desired canopy shape by pulling internal lines appears feasible but different line arrangement is needed.
219	Circular flat chute with forward pocket and longitudinal rib.	Flaps extended 1.75. Rear center lines pulled in 6.5 inches.	1.25	Unstable for all rigging combinations tried.
C-1	Three chute cluster 211 lead chutes 204 rear chutes.	Flaps extended 3.6 inches. All risers lengthened to make total line lengths of 48 inches.	1.35	Fair stability about all axis.
C-2	Three chute cluster 201 lead chutes 204 rear chutes.	All risers lengthened to make total line lengths of 48 inches. Flaps extended 4.70 inches.	1.32	Stable in pitch, had tendency to fly yawed.
C-3	Three chute cluster 215 lead chutes 204 rear chutes.	Flaps extended 3.6 inches. All risers lengthened to make total line lengths of 48 inches.	1.57	Pressure in inflated tubes too low with result they buckled.

Reproduced From
Best Available Copy

2

Figure 6 is a summary, in graphical form, of the maximum L/D performance of the models tested. As shown by Table 2 and Figure 6, Model 217 gave the highest value of L/D maximum. Model 217 also displayed desirable stability characteristics. In particular this model had excellent roll and yaw stability as compared to most of the other models tested during this program. The significant results of the Wright Field wind tunnel tests were:

(1) It appeared feasible to develop a nonrigid, self-inflating, parachute with an L/D capability of 2.0.

(2) The three lobe design, of which Model 217 gave the best results, had the best potential of being able to get L/D values of 2.0.

4.3 LARGE MODEL TESTS

As a result of the Wright Field wind tunnel test, several models were selected to be tested as larger models. These larger models were approximately 12-ft D_o. The configurations chosen were Models 217, 218, and 202 from the Wright Field series of small model tests and Model 101 from the Aerosail test program at Ames. Model 217 showed the best performance during the Wright Field tests.

However, it was decided that it would also be desirable to test larger versions of Models 218 and 202. Model 101 was included for testing as a reference to which the performance of the other Models could be compared. Table 3 lists the Model numbers and a brief description of the Models selected for testing during the large model tests.

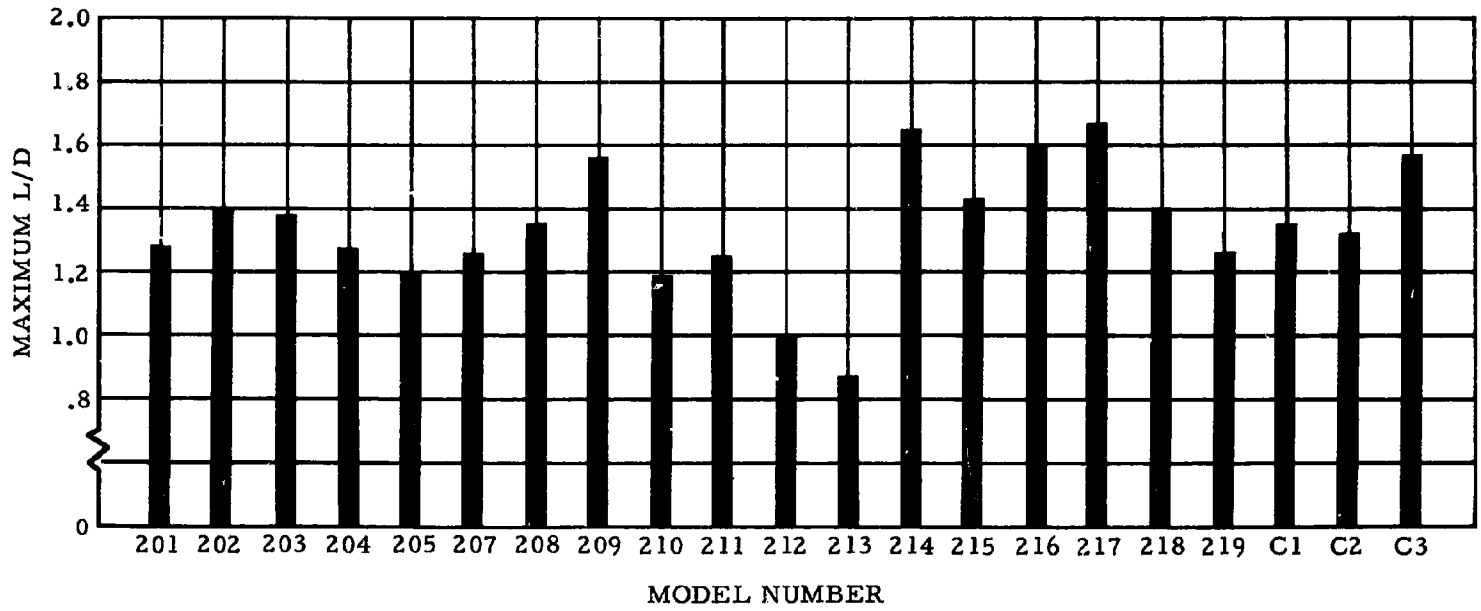

Figure 6. Maximum L/D Values Obtained From Small Model Tests

TABLE 3

MODELS SELECTED FOR TESTING

Model Number	Model Description
301A	Model 217 with fairing.
301	Model 217 without fairing.
302	Model 218, with modified L.E., from 3-ft D_o tests.
303	Model 203 from 3-ft D_o tests.
304	Modified version of Model 218 from 3-ft D_o tests.
101	Model 101 from 12-ft D_o Aerosail tests.
402	Model 302 in 16-ft D_o size.

4.3.1 Truck Tow Tests

Due to delays in the availability of the Ames 40 x 80 wind tunnel, a truck tow test rig was constructed to expedite the testing of larger models. The models selected for testing on the tow truck were 301A, 302, 303, 304, 402 and 101. The results of the tow truck test program briefly summarized are in Table 4. For a description of the tow truck test rig and a complete summary of the data obtained during the truck tests refer to Appendix III.

TABLE 4

RESULTS OF TOW TRUCK TEST PROGRAM

Model Number	Maximum L/D	Comments
301A	1.95	Had the best stability and best indicated performance of the models tested.
302	1.48	Good stability and canopy shape.
303	1.46	Excellent stability and canopy shape.
304	1.24	Rigged with interior lines cross connected to flaps. Control forces very light. Fair stability.
402	1.72	Very good stability and canopy shape. This model is identical to 302 except D_o = 16 ft.
101	1.19	This is the model which gave best results in Aerosail test program.

The significance of the results from the tow tests are summarized by the following statements.

(1) Model 301A gave the best L/D performance and had excellent yaw stability. This model showed the best potential of achieving an L/D of 2.0.

(2) A definite improvement in Max. L/D performance was noted between Model 302 and Model 402 which seems to indicate an increase of L/D capability with increasing size.

(3) None of the models tested appear to have the potential of matching the performance of the three lobe type of design.

(4) Relatively small flap riser extensions are necessary to achieve Max. L/D performance. This results in low control line extension capability being required to operate the parachute.

4.3.2 Ames Wind Tunnel Tests

The test program at the Ames 40 x 80 wind tunnel was conducted in two parts. During the first part of the test program, the models listed in Table 3 were tested. The results of these tests indicated that the instrumentation used had given erroneous data and also that the published data for the Aerosail test program was in error. Therefore, a second series of tests were conducted at Ames and most of the models were retested. Also, many of the models from the Aerosail test program were retested. Table 5 lists the models tested during both parts of the test program.

TABLE 5
MODELS TESTED

Models For Ames Test Program	Model Description
301	Model 217 from Small Model tests.
301A	Model 217 with fairing.
302	Model 218, with modified L.E., from Small Model tests.
303	Model 202 from Small Model tests.
304	Model 218 from Small Model tests.
101	Model 101 from 12-ft D_o Aerosail tests.
402	Model 302 in 16-ft D_o size.
Cluster No. 4	Cluster of three model 302's.
105	From Aerosail Test Program
107	From Aerosail Test Program
113	From Aerosail Test Program

The results of the Ames tunnel tests in general substantiated the data obtained both from the small model tests at Wright Field and the tow tests. The following table is a

brief summary of the results of Ames tests. For a complete summary of test results and description of the test procedure, refer to Appendix IV.

TABLE 6

RESULTS OF AMES TESTS

Model	Maximum L/D	Comments
301A	1.41 (v=60 fps)	Model flying horizontal
301	2.10 (v=30 fps)	Model flying vertical
	1.82 (v=45 fps)	
	1.72 (v=60 fps)	
	1.34 (v=30 fps)	Flying horizontal, rigged with 2 D_o lines
	1.53 (v=45 fps)	
	1.69 (v=60 fps)	
302	1.53 (v=30 fps)	Flying vertical
303	1.31 (v=30 fps)	Flying vertical
304	1.25 (v=30 fps)	Flying horizontal
402	1.41 (v=30 fps)	Flying horizontal
	1.35 (v=30 fps)	Flying vertical - May not have been best rigging.
101	1.32 (v=30 fps)	Flying vertical
105	1.20 (v=30 fps)	Flying vertical
107	1.16 (v=30 fps)	Flying vertical
113	1.05 (v=30 fps)	Flying vertical
Cluster 3-302	1.21 (v=30 fps)	Flying vertical

As shown by Table 6 Model 301 was the only configuration tested which achieved an L/D of 2.0. The single most important result of this test series was that of the design approaches tried, only the three lobe design (Model 301) showed the capability of performing with an L/D value as high as 2.0.

4.5 DEPLOYMENT DROP TESTS

In order to test the feasibility of deploying Model 301, and to get information on the deployment characteristics and opening loads for very low porosity canopies, drop tests were conducted at the El Centro parachute drop test facility. The two configurations tested were Models 301 and 302. Model 301 was tested in both 12-ft D_W and 16-ft D_W versions and Model 302 had a D_o of 12 ft.

Table 7 is a summary of the results of the deployment tests. The primary objective of these drop tests was to investigate the feasibility of deploying the Model 301 type of configuration. The results of this drop test program were quite encouraging. Model 301 displayed excellent stability during the reefed stage and did not display any adverse inflation characteristics. As far as can be determined by the results obtained with the relatively small (12-ft diameter) drop test models deployment of the 301 design should not be a major problem.

TABLE 7

RESULTS OF DEPLOYMENT TESTS

Test No.	Model	Drop Speed KEAS	Altitude Ft	Percent* Reefing	Average Descent Velocity	System Descent Weight	Opening Force	Disreef Force	Comments
1	301 (D_W=12 ft)	93	5050	20	55 fps	70 lbs	NA	NA	Reefing cutters did not fire. Parachute descended
2	302 (D_o=12 ft)	100	3000	20	19 fps	68 lbs	NA	NA	Oscillated during reefed stage 45 degrees. Made a stable gliding descent after full opening.
3	301 (D_W=12 ft)	100	3000	20	17 fps	70 lbs	690 lbs	692 lbs	Very stable during reefed stage. Made a spiral descent to left after full opening.
4	302 (D_o=12 ft)	125	3000	15	19 fps	68 lbs	530	460	Mild oscillation during reefed stage. Made a stable gliding descent after full opening.
5	301 (D_W=12 ft)	125	3000	15	57 fps	70 lbs	NA	NA	Reefing cutters did not fire, descended reefed.
6	301 (D_W=12 ft)	150	3000	12.5	17 fps	70 lbs	380	720	Reefed descent stable. Stable glide descent with a slow spiral turn.
7	302 (D_o=12 ft)	150	3000	12.5	19 fps	68 lbs			Some oscillation during reefed stage. Stable gliding descent after full opening.
8	301 (D_W=12 ft)	150	3000	15	18 fps	70 lbs	655	565	Model rigged with 6 inch flap differential. Had 30 deg. per sec turn rate after full opening.
9	301 (D_W=16 ft)	125	3000	20	30 fps	224 lbs	NA	NA	Reefing line broke during deployment with resulting canopy damage.

NOTE: All 12-ft diameter models were dropped with 6-in. flap extension.
The 16-ft D_W model 301 was dropped with 8-in. flap extension.

* Percent reefing is ratio of reefed diameter to nominal diameter (D_o) for Model 302.
For Model 301, percent reefing is ratio of reefing line length for each lobe to lobe circumference.

SECTION 5

ANALYSIS

5.1 GENERAL

As shown by the summary of results from the experimental test programs presented in Section 4 of this report it is apparent that the three lobe design (Model 301) gave the best performance. It proved itself superior to all other designs tested in L/D capability, stability while gliding, and stability during reefed descent. Therefore at this point in the research program all other configurations were dropped from consideration and an analysis of the characteristics and performance of Model 301 was made. An analysis of the requirements of a drop test vehicle with which to conduct the drop tests specified in Reference 3 is also included in this section. The previously mentioned analysis are presented in the following paragraphs.

5.2 DESCRIPTION OF MODEL 301 CANOPY CONSTRUCTION, AND CANOPY PROFILE IN FLIGHT

As stated in the previous paragraphs, Model 301 evolved as the configuration with the highest performance. A description of its canopy configuration is as follows. Referring to Figures 7, 8 and 9, it can be seen that the configuration basically consists of three lobes. The side lobes are circular in planform as is the rear half of the front lobe. The planform of the forward half of the front lobe is obtained by laying out a circle and then removing a triangular portion as shown in the following sketch.

This document contains
blank pages that were
not filmed

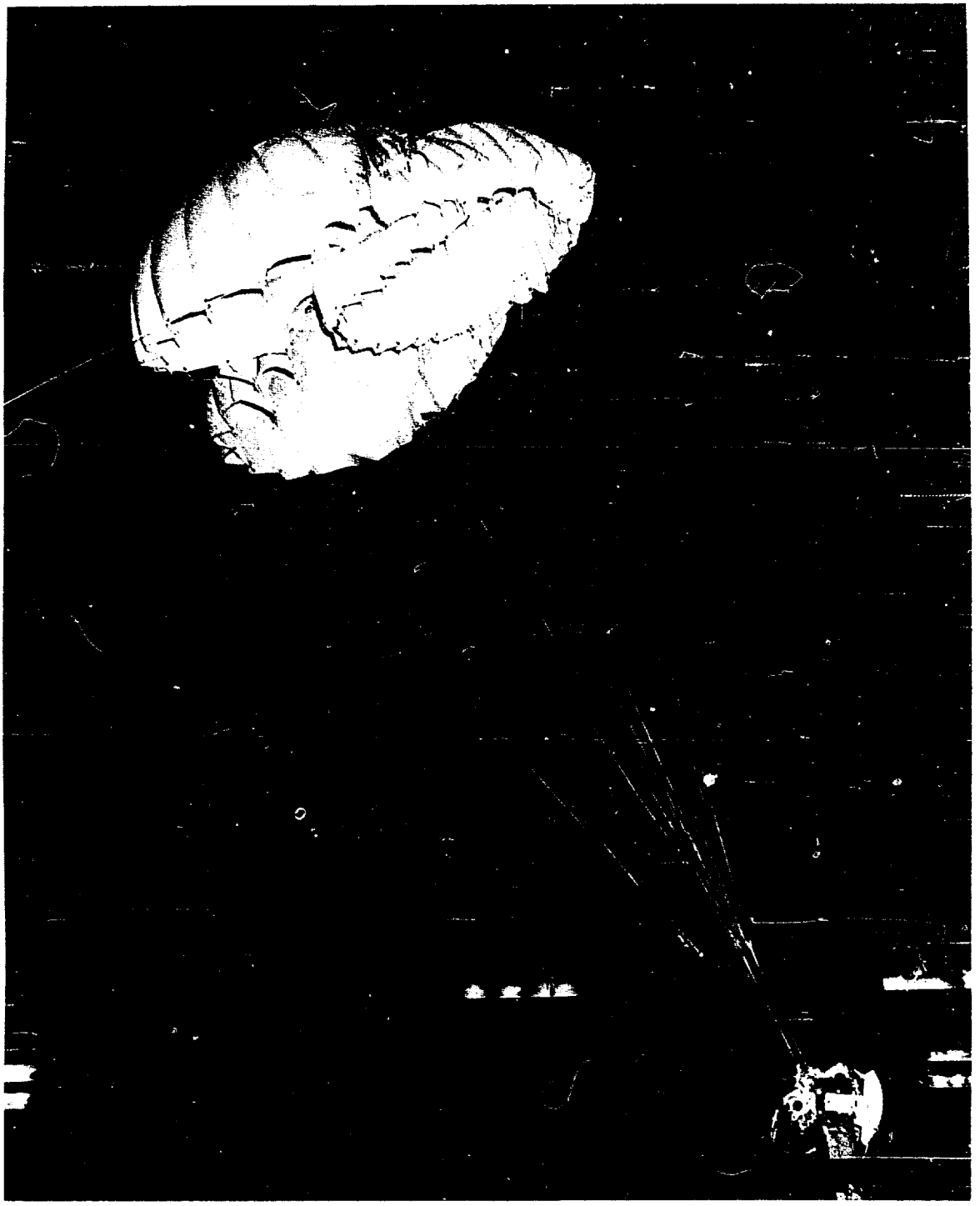

Figure 7. Model 301 Flying Vertically in the Wind Tunnel

Reproduced From
Best Available Copy

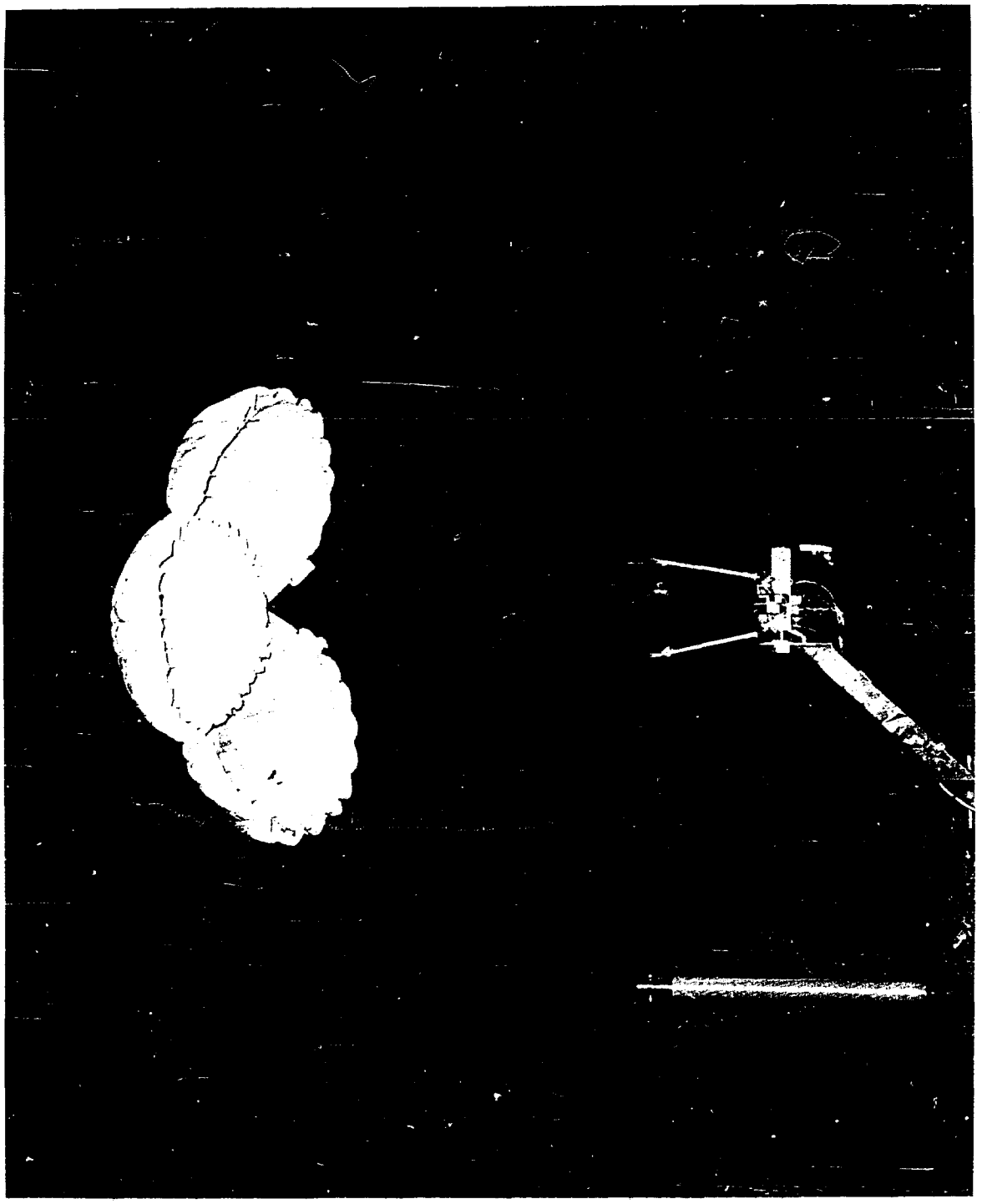

NV26

Figure 8. Model 301 Flying Vertically in the Wind Tunnel

Reproduced From
Best Available Copy

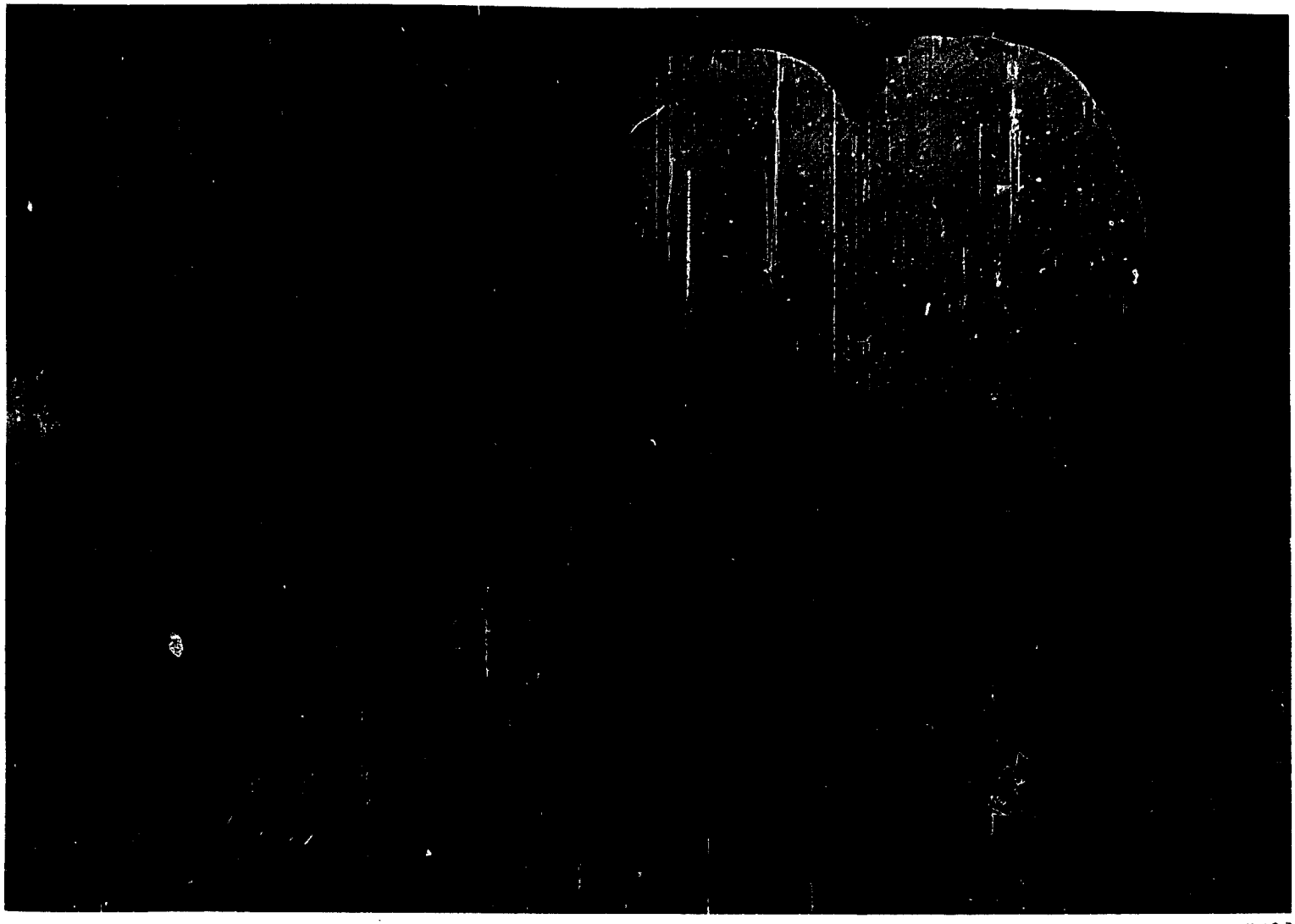

NV27

Figure 9. Model 217, 3 - Ft D_W - Version of Model 301

Reproduced From
Best Available Copy

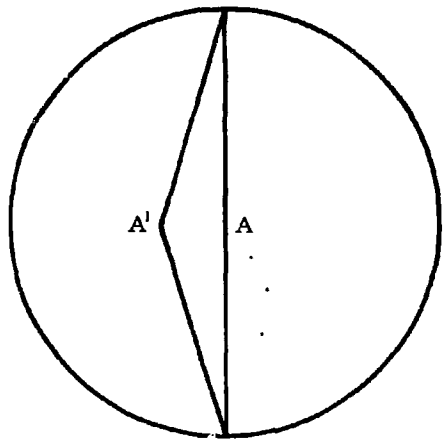

Point A' is then brought back to point A. This has the affect of increasing the aspect ratio and putting in what would be twist for a rigid wing. This type of construction results in an increasing angle of attack from the lobe intersection points on the canopy leading edge to the centerline of the canopy.

The leading edges of the three lobes are shaped through the use of flexible ribs and the canopy surface is rolled under to approximate the leading edge of a rigid airfoil. The following sketches illustrate typical leading edge sections. Figures 10 and 11 are cross sections of the leading edge of the canopy when it is inflated. The cross sections are taken at a rib and at a station midway between two ribs. Aerodynamic forces shape the canopy leading edge as shown by these two figures. At the rib station the leading edge conforms to the shape of the rib; however at a station midway between two ribs the rolled under portion of the leading edge is pushed up.

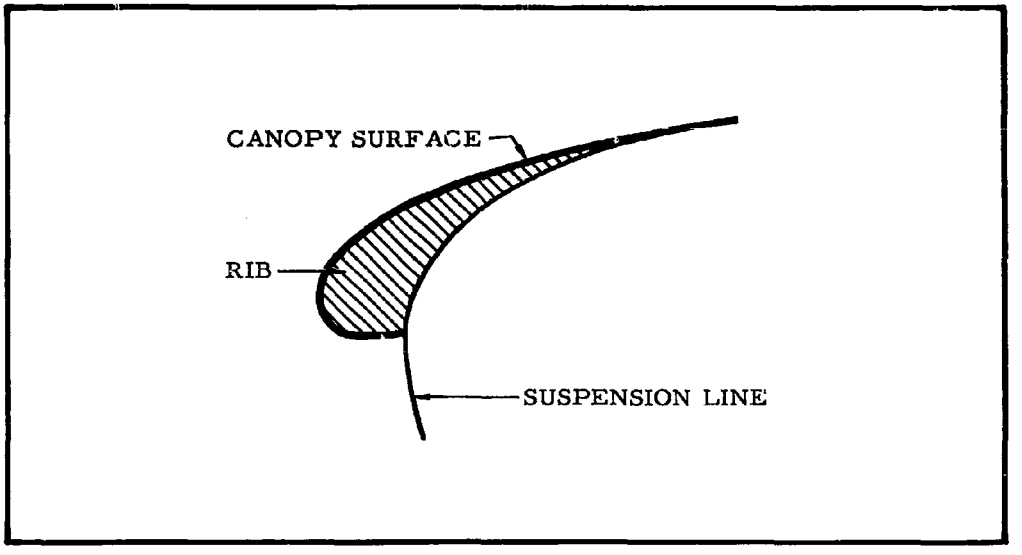

Figure 10. Cross Section of Canopy's Leading Edge

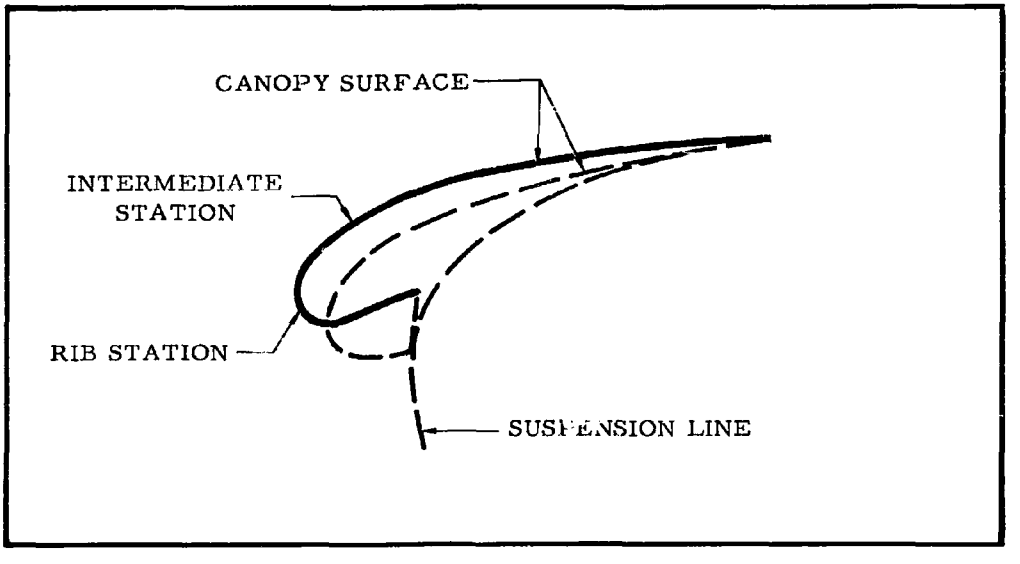

Figure 11. Cross Section of Canopy's Leading Edge

Figure 11 compares the leading edge shape at this station to the shape at a rib as shown by the dotted outline.

All suspension lines are equal length. At canopy stations that have leading edge ribs, the length of the suspension line is measured from the rear edge of the rolled under leading edge surface. This also results in an effectively higher canopy angle of attack at the lobe centerlines. The rear portion of each side lobe is constructed in such a manner that it can be extended above the nominal canopy skirt plane. This is accomplished by cutting flaps into the rear edge of the canopy.

The slots between the flaps and main canopy are then closed by adding triangular gussets to seal the slot and provide load continuity. Figure 9 shows also the rear portion of the front lobe which forms an interior load carrying web and provides the necessary internal canopy pressure distribution to support the canopy leading edge at low angles of attack. Figures 33 and 34, Appendix I give construction details of 12-ft D_W and 16-ft D_W versions of the three lobe design.

5.3 AERODYNAMIC CHARACTERISTICS

5.3.1 Affect of Flap Extension on L/D Performance

Figure 12 shows the affect of flap extension on L/D. There are three curves shown on Figure 12 corresponding to three velocities. The shape of these three curves are similar though shifted down and to the left as velocity increases. It should be noted that the range of flap extension for each velocity is limited to a rather narrow range. The range of flap extension is governed by two limitations corresponding to a maximum and a minimum flap extension. The maximum flap extension is limited by leading edge deformation and finally by canopy deflation. As the flaps are extended L/D increases until a point is reached

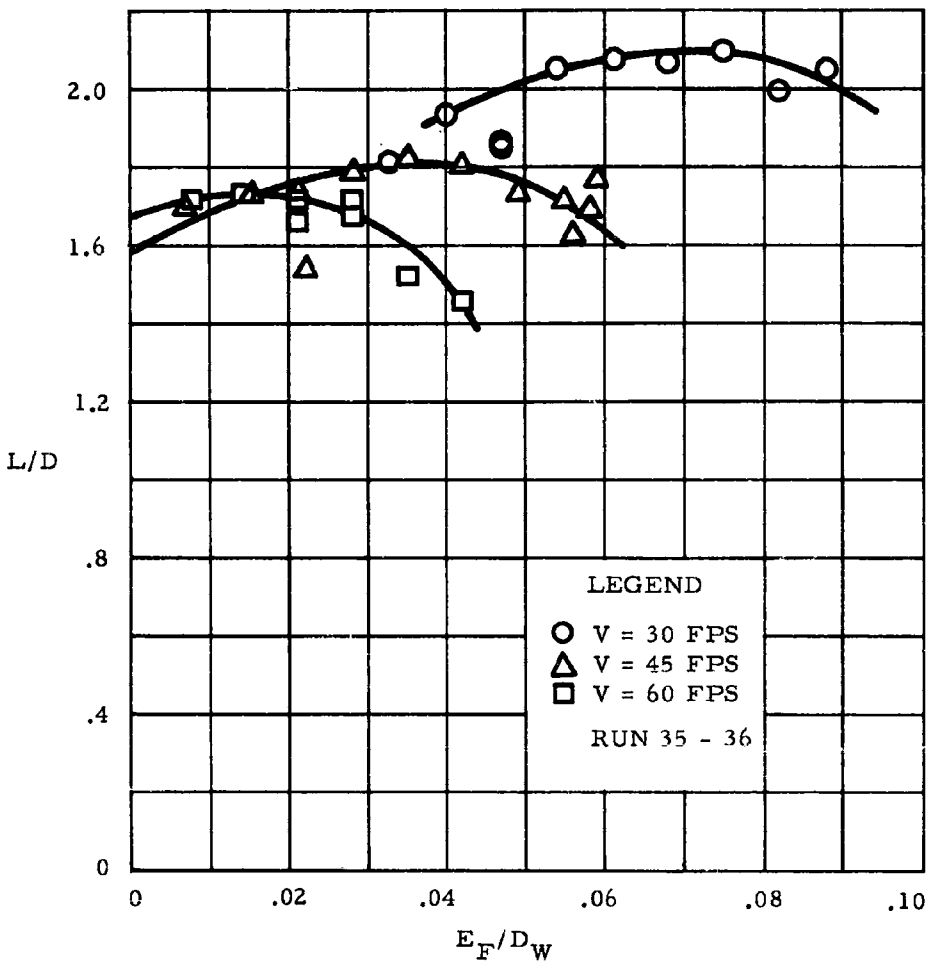

Figure 12. L/D Vs Flap Extension Ames Wind Tunnel Tests

when the leading begins to be pushed back. If flap extension is continued, a point is reached where the internal pressure in the canopy is reduced to such a degree that the front of the canopy is pushed in and the canopy collapses. After the canopy collapse a cyclic process of inflation and collapse occurs until flap extension is reduced. This type of behavior was characteristic of all the configurations tested during this program. The apparent reason Model 301 can go to a lower angle of attack and not collapse the leading edge is the combination of the interior canopy web, which is the rear portion of the front lobe, and the rolled under leading edge. As shown in Figure 13, what probably happens is that the rear web causes forward circulation inside the canopy which provides pressure inside the leading edge sufficiently high to maintain the inflated leading edge shape.

Figure 13. Cross Section of Model 301 Showing Flow Field

The minimum flap extension limitation is a result of instability of the canopy in pitch. At flap extensions below the minimum for stability, the parachute begins to oscillate in pitch. This behavior is also a characteristic of low-porosity, conventional-parachute canopies. If the flaps are retracted

sufficiently, Model 301 will assume a stable glide in the reverse direction. A better understanding of what occurs when the flaps are varied can be obtained from Figure 14. Figure 14 is a plot of C_L vs C_D for Model 301. As with Figure 12, three curves corresponding to three test velocities are shown. The three curves are similar in shape, shifting downward with increasing velocity. The data presented in this figure is representative of the portion of a C_L vs C_D plot for a conventional airfoil near its stall point. The dashed curve is an extrapolation of what the 30-ft/sec curve would look like if it were not for the previously mentioned limitations on the angle of attack range of the canopy. This curve is presented to impress upon the reader that the parachute is functioning like an airfoil and to provide a basis for explaining its behavior as the flaps are varied. If Model 301 were stable at L/D = 0, this would correspond to a $C_L = 0$ and $C_D = 1.0$ as shown by the dashed curve. Then, as the flaps were extended, the trim point would move up the curve and to the left and then back down the left side of the curve. This is equivalent to an airfoil starting from stall at a 90-degree angle of attack and reducing the angle of attack until the flow attaches to the upper surface. The important points to be noted here are that extending the flaps reduces both lift and drag and is equivalent to reducing the canopy angle of attack, while retracting the flaps increases lift, drag, and canopy angle of attack. The stall point, equivalent to the stall which occurs with an airfoil, occurs at minimum flap extension.

5.3.2 Affect of Velocity on L/D Performance

As was noted in Section 3, velocity or more correctly dynamic pressure (q) has a significant effect on the L/D capability of gliding parachutes. The affect is clearly shown by Figures 12 and 14. As can be seen from these figures there

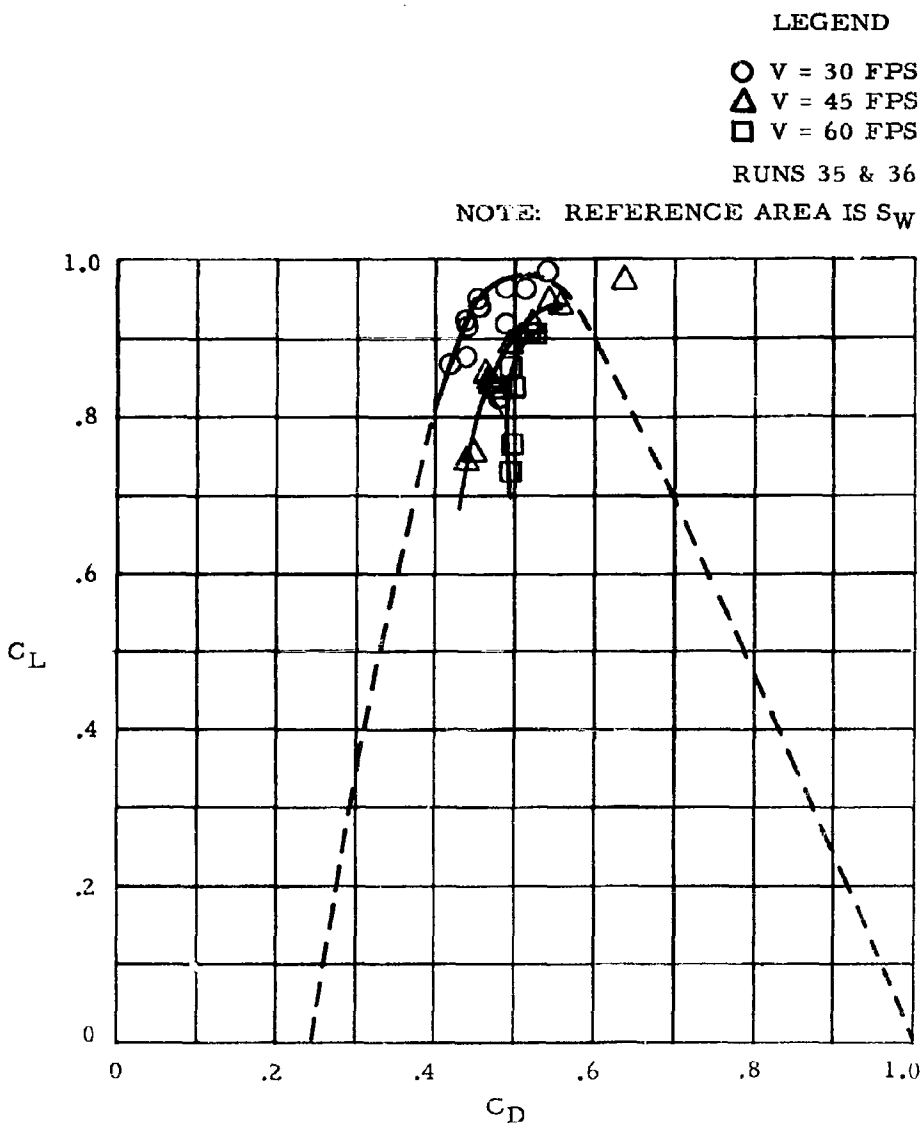

Figure 14. C_L Vs C_D - Ames Wind Tunnel Tests

is a pronounced reduction in L/D maximum as velocity is increased. An insight to what causes this decrease in performance can be gained by analyzing Figures 15 and 16. These figures are plots of C_L versus flap extension and C_D versus flap extension for the three velocities tested. As shown by Figure 15, there is a large reduction in C_L, for a constant flap setting, as velocity increases. Figure 16 shows a trend which has the opposite affect on L/D. As velocity increases, there is a slight reduction in drag. The result of these two trends is that even though drag decreases with velocity the loss in lift capability is much larger and a net loss in L/D capability occurs. The reduction of drag with increasing velocity is not unusual as this is a characteristic of most airfoils as Reynolds Number is increased. However, the large reduction of lift coefficient is in variance to what is usually experienced with airfoils. A logical reason for this behavior can be obtained if one takes into account the elasticity and flexibility inherent in a nylon cloth canopy. Even if it is assumed that the shape of the canopy pressure distribution remains constant and that the canopy loads increase in proportion to q, the elasticity of the canopy and suspension lines will allow the canopy to distort. The canopy will deform the most in the areas of highest loading and in doing so adjusts itself to a shape which is compatible with the air load distribution and the stress distribution in the canopy material and suspension lines. As a result, the canopy adjusts itself to a less efficient airfoil shape. This canopy distortion would not necessarily increase drag because the skin friction and suspension line drag coefficients would remain the same or decrease as Reynolds Number increased and the induced drag coefficient due to lift would decrease. This is just the type of trend shown by Figure 16. The loss of lift and slight decrease in drag with increasing q is also the reason for the smaller flap deflections needed to

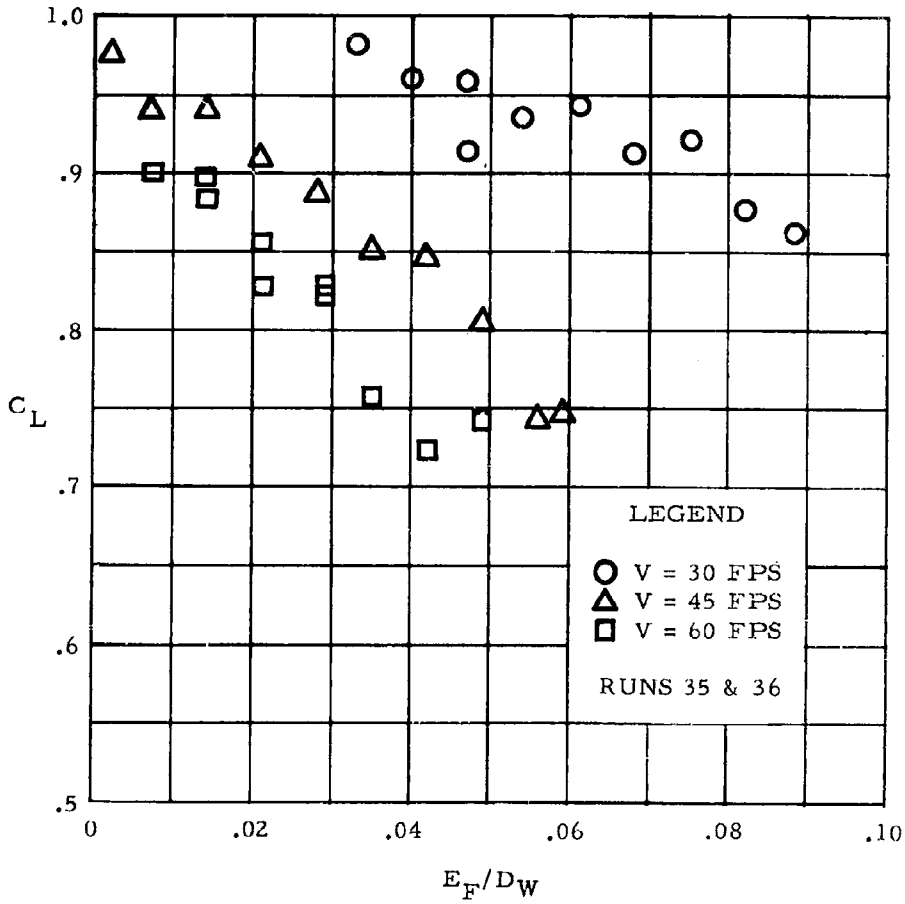

NOTE: C_L BASED ON S_W

Figure 15. Lift Coefficient Vs Flap Extension

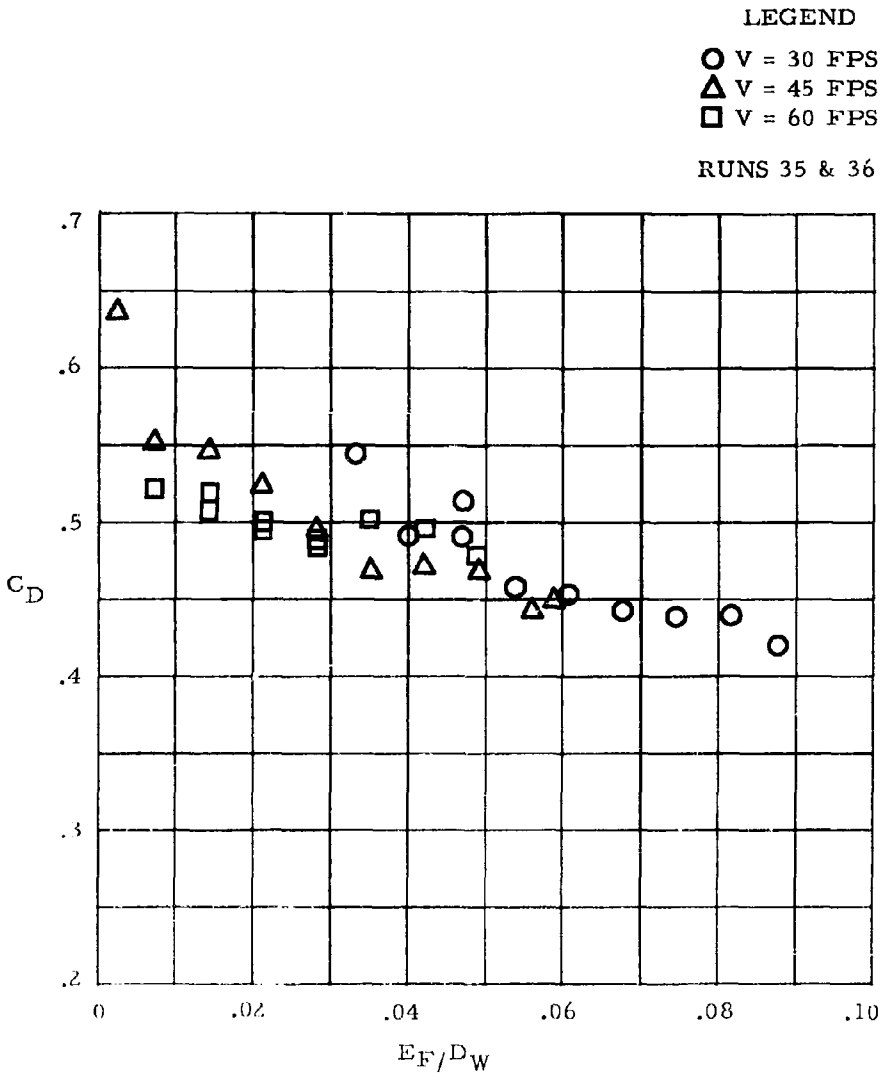

Figure 16. Drag Coefficient Vs Flap Extension

obtain L/D maximum as shown by Figure 12. Inspection of Figure 14 shows that L/D maximum occurs at approximately the same C_L but at succeedingly higher values of C_D as velocity increases. As shown by Figure 15, holding a constant C_L as velocity increases results in reducing the flap extension and therefore causes the shift in L/D maximum to the left shown by Figure 12.

5.3.3 Affect on L/D of Rigging of Interior Web

In an attempt to find an optimum setting for the interior canopy web in Model 301, a series of settings were run while holding flap setting and q constant. The result of these tests are presented in Figure 17. As can be seen from this figure, the optimum setting occurred at zero extension. This result becomes important when packing a parachute of this type for deployment. Because all suspension lines are equal in length, it is possible to pack the canopy as if it were a three-parachute cluster with no loose lines or lines packed inside the canopy.

5.3.4 Corrected Data for Performance Calculations

In order to determine the performance of Model 301 for free flight conditions with an attached test vehicle it is necessary to correct the raw wind tunnel data (see Figure 14). These corrections are made to compensate for the affects of the parachute weight, line drag and vehicle drag. The correction to the wind tunnel data for parachute weight is necessary because the wind tunnel tests were conducted with the parachute flying vertically from the floor of the tunnel. This resulted in the parachute having to lift its own weight and thus introduced an error resulting in the indicated C_L values being low. A correction for line drag is necessary to compensate for the fact that line lengths increase directly as the change in D_o but the canopy area increases as the diameter ratio squared. Vehicle drag coefficient, based on canopy reference

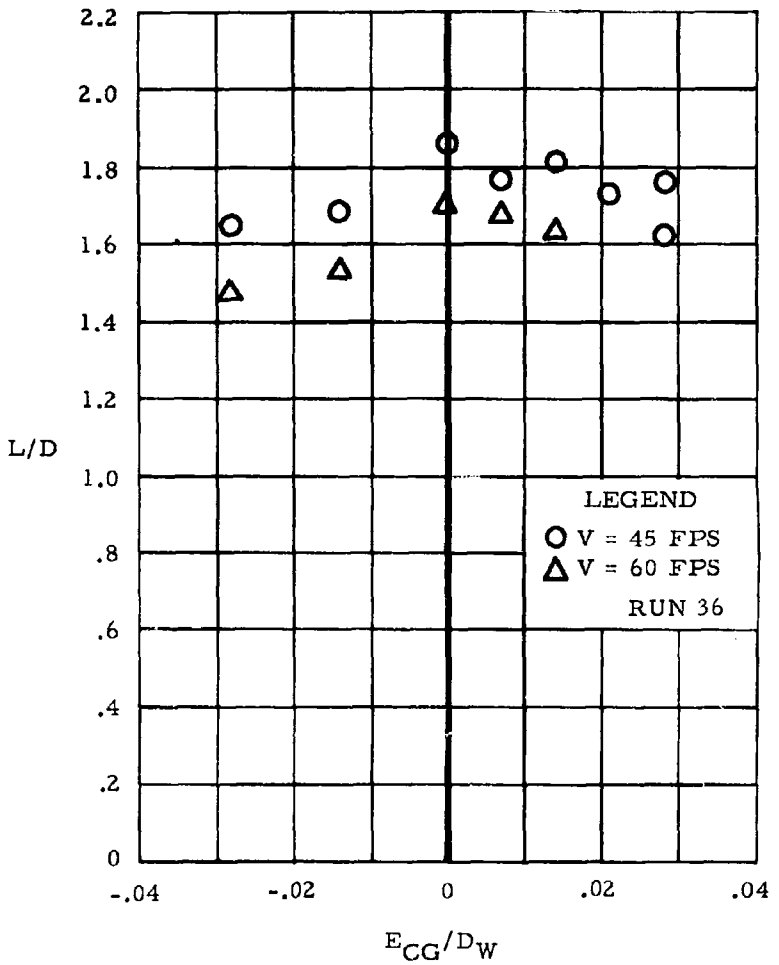

Figure 17. L/D Vs Extension of Interior Lines

area, is added directly. The results of these corrections are presented in Figures 18, 19 and 20. The curves presented in these figures are C_L versus C_D for 16, 28 and 40-ft versions of Model 301 attached to a test vehicle with a C_DS of 4.5 ft^2 (based on vehicle frontal area).

The equations used to give corrected values of C_L and C_D were as follows:

C_L = C_L (wind tunnel test) + ΔC_L (due to weight of the parachute).

$$\Delta C_L = \frac{\text{Weight of Parachute}}{q\ S_W}.$$

C_D = C_D (Wind Tunnel Test) - ΔC_D (Suspension lines on 301-12) + ΔC_D (Suspension lines on 301 - D_W) + ΔC_D (Test Vehicle)

$$\Delta C_D \text{ (Suspension lines)} = \frac{C_DS \text{ (Suspension Lines)}}{S_W}$$

$$\Delta C_D \text{ (Test Vehicle)} = \frac{C_DS \text{ (Test Vehicle)}}{S_W}$$

The following values were used for C_D corrections:

*Model	ΔC_D (Suspension Line Drag)	ΔC_D (Test Vehicle)
301-12	.0501	.040
301-16	.0498	.025
301-28	.0257	.007
301-40	.01975	.004

*NOTE: Number following 301 indicates canopy diameter.

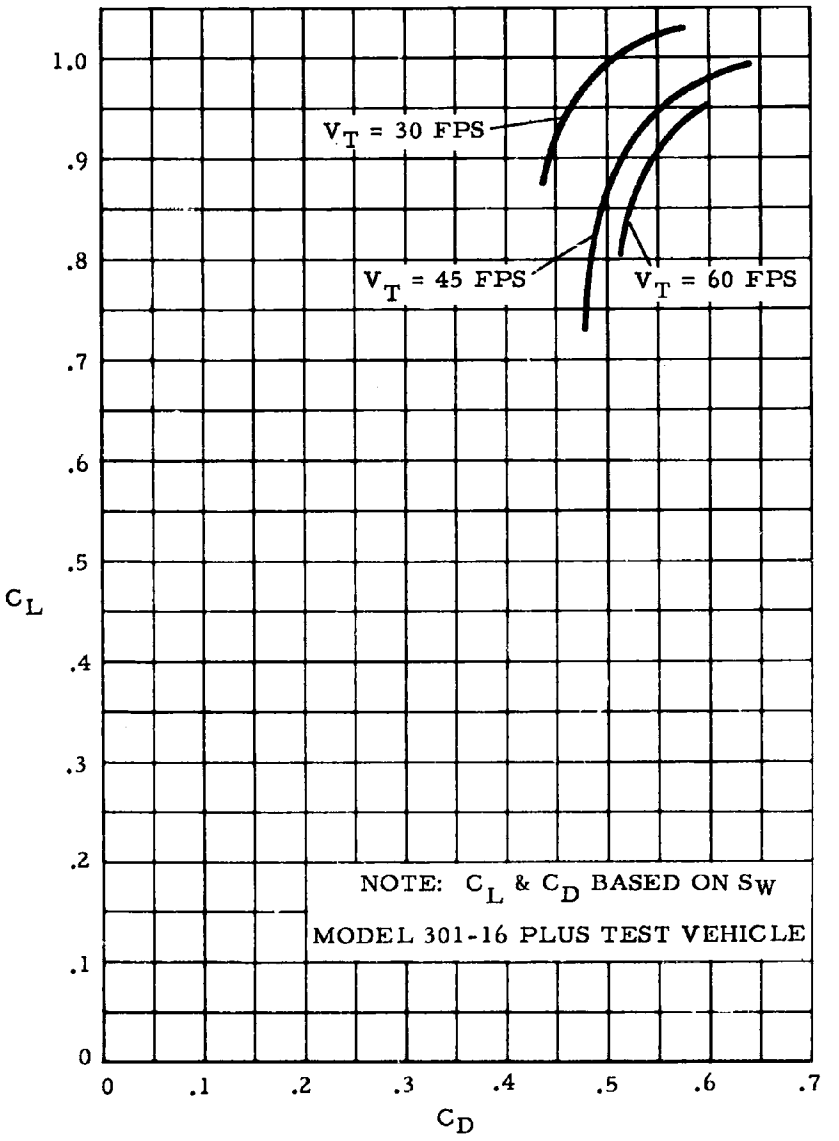

Figure 18. C_L Vs C_D as a Function of Velocity

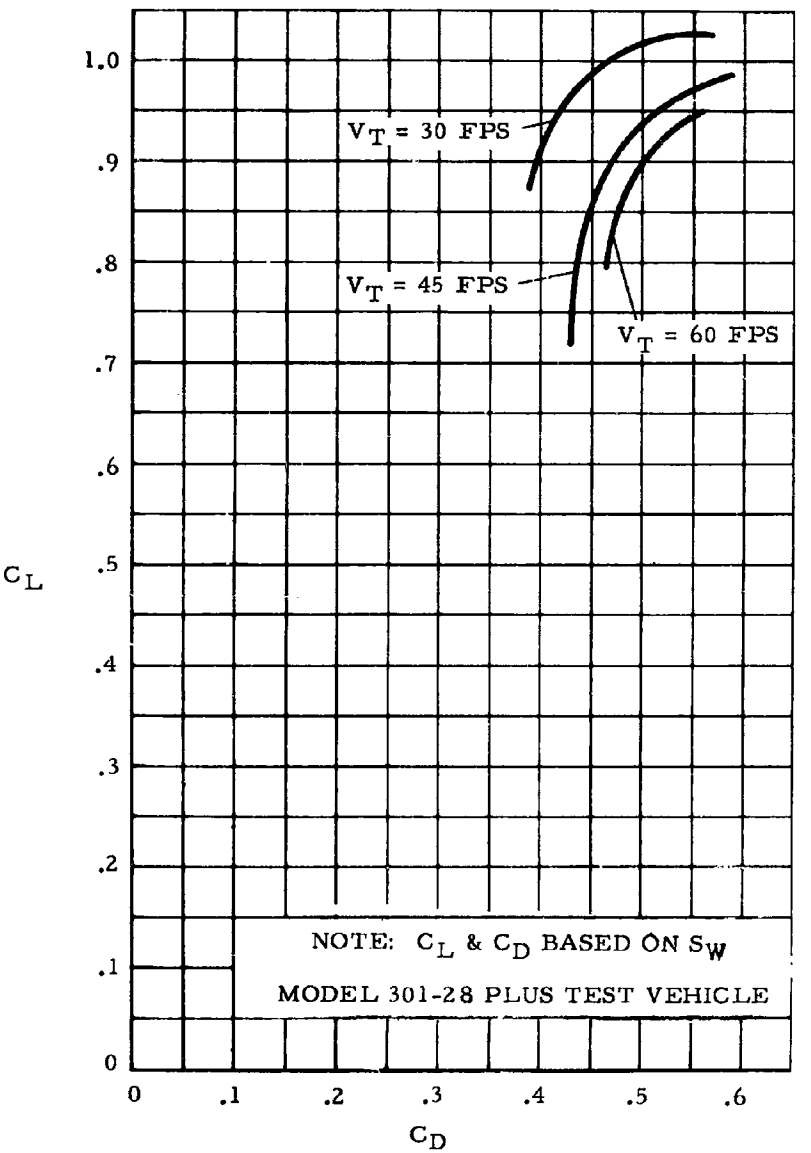

Figure 19. C_L Vs C_D as a Function of Velocity

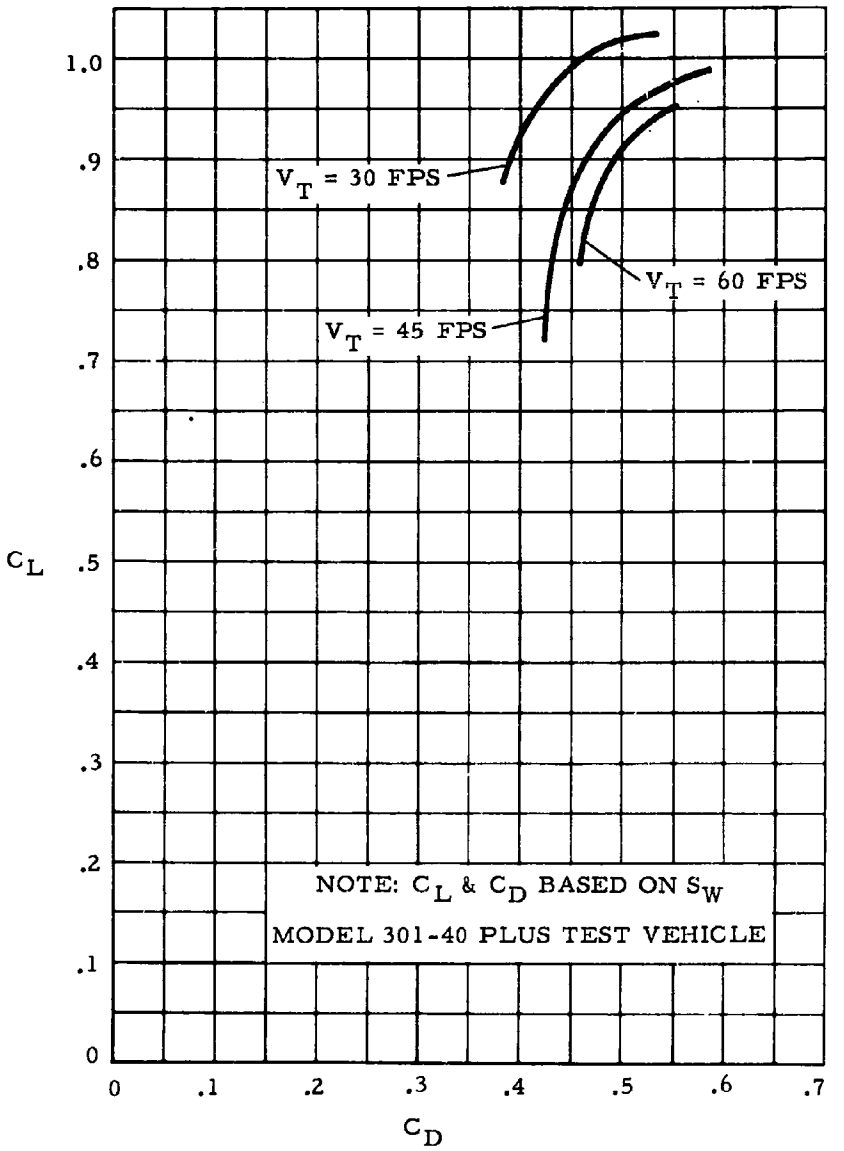

Figure 20. C_L Vs C_D as a Function of Velocity

C_L corrections were as follows:

Velocity	ΔC_L
30 fps	.04
45 fps	.02
60 fps	.01

It should be noted that there has been no correction applied to compensate for the increased Reynolds Number for the larger canopies. There is not sufficient data available on gliding parachutes to calculate the affect of changing Reynolds Number but an increase in L/D can normally be expected from an increase in Reynolds Number.

Based on the data presented in Figures 18, 19 and 20, L/D maximum as a function of velocity, and values of C_L and C_D at L/D maximum as a function of velocity were plotted. This data is presented in Figures 21 and 22.

5.3.5 Reefed Drag Coefficients and Opening Shock Factors for Model 301

In order to calculate opening shock factors with data obtained from drop tests, it is necessary to have steady state drag coefficients. These drag coefficients were obtained during the Ames Wind Tunnel Tests and are presented in Figure 23 as a plot of C_D versus percent reefing. Percent reefing for Model 301 is defined as the ratio of the length of the reefing line to the nominal skirt circumference for each individual lobe, that is, percent reefing = $\frac{\text{length of reefing line for one lobe}}{\text{circumference of one lobe.}}$

If F_o is used to denote the maximum opening force, F_c the drag force obtained at constant velocity and X is an amplification factor denoting the relationship between maximum opening force, (F_o) and the constant drag force, (F_c), then

$$X = \frac{F_o}{F_c} = \frac{F_o}{C_D \, q \, S}$$

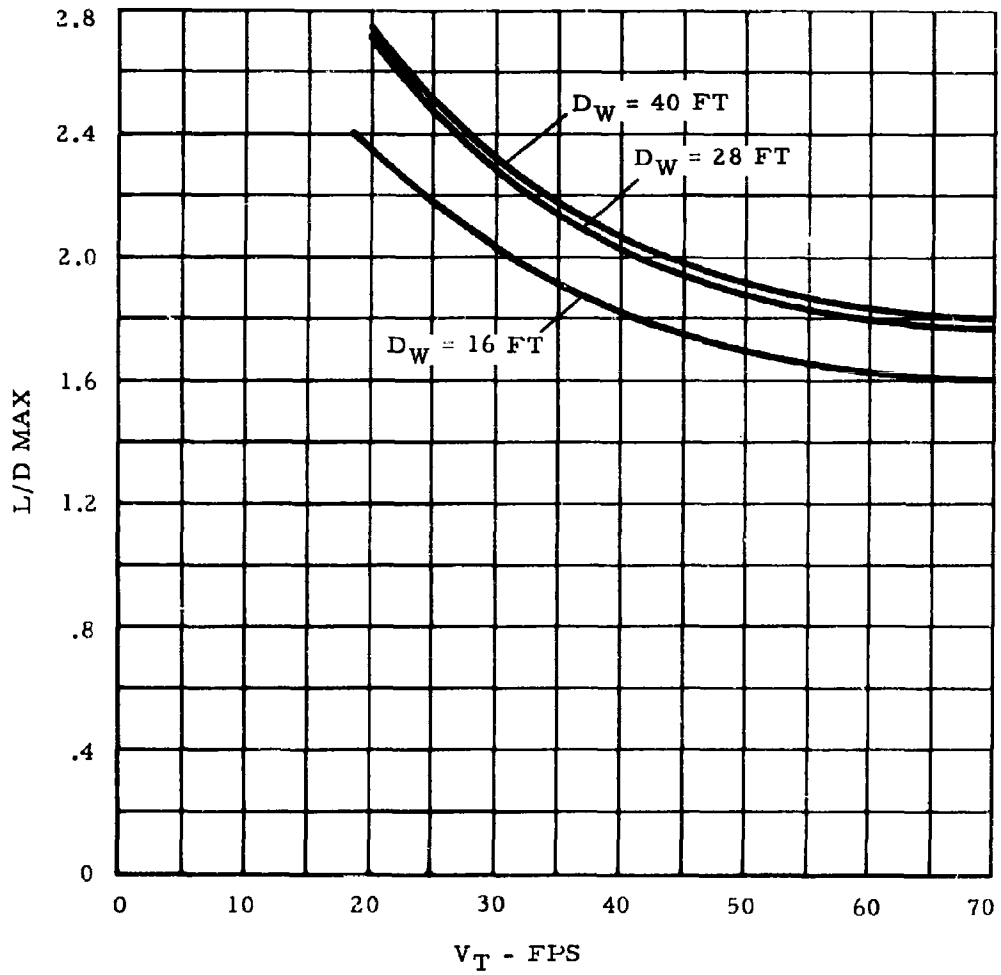

Figure 21. L/D Max Vs Velocity as a Function of D_w

NOTE: C_L & C_D BASED ON S_W

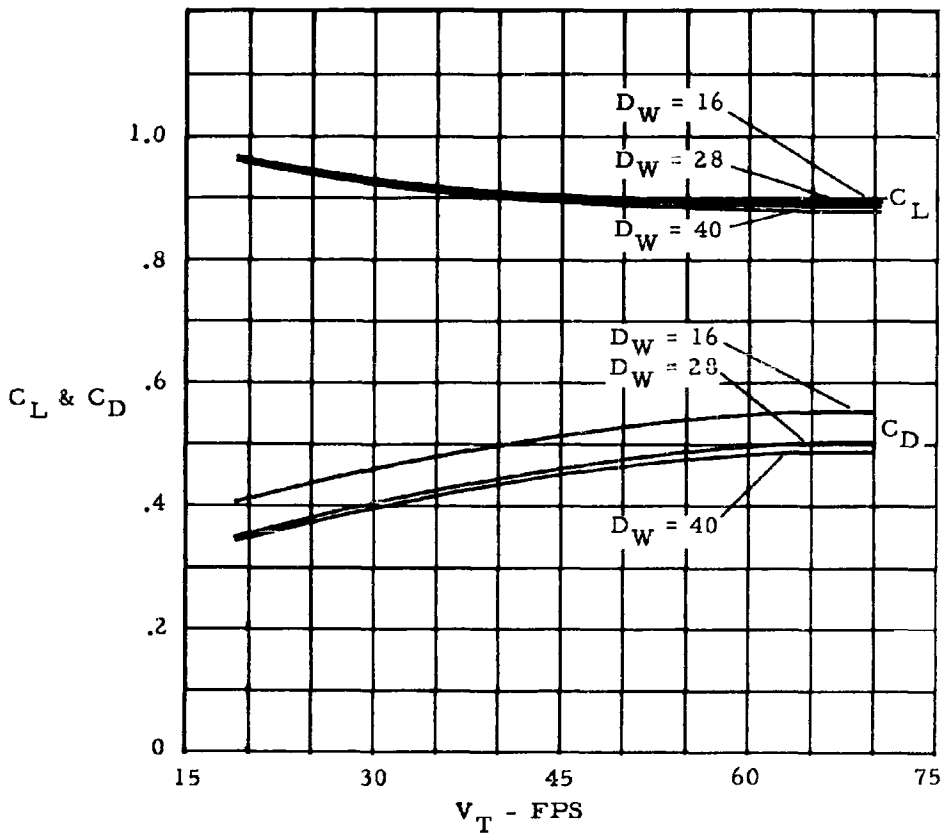

Figure 22. System C_L and C_D at Max L/D

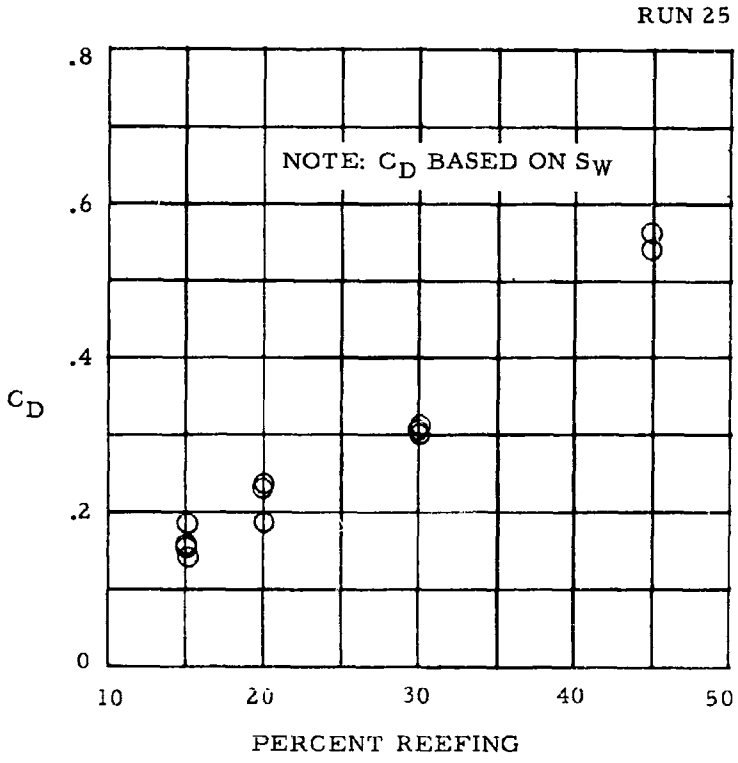

Figure 23. C_D Vs Percent Reefing Ames Wind Tunnel Tests

This value for X is usually considered independent of canopy loading for W/C_DS values greater than 30. However, for the drop tests conducted with Model 301, W/C_DS was less than 5.0 and as a result the X factors computed from this data must be used judiciously when calculating opening loads with higher values of W/C_DS. In order to calculate the X factor when going from reefed to full open, it is necessary to have full open steady state C_D values. Because of the flight characteristics of Model 301 which prevented obtaining C_D values at 90 degree canopy angles of attack it is necessary to assume a steady state C_D value. Table 8 gives the results based on the previous discussion.

5.4 L/D PERFORMANCE

5.4.1 Performance Equations and Parameters for Gliding Flight

The equation which gives the relationship between total velocity (V_T), system weight (W), lift to drag ratio (L/D), drag coefficient (C_D), canopy area (S), and density (ρ) is given by the equation.

$$V_T = \left[\frac{W \sin(\cot^{-1} L/D)}{C_D S \rho/2}\right]^{1/2}$$

This equation can also be written in terms of the lift coefficient (C_L) and in this form is

$$V_T = \left[\frac{W \cos(\cot^{-1} L/D)}{C_L S \rho/2}\right]^{1/2}$$

The relationships between total velocity (V_T), vertical velocity (V_V) and horizontal velocity (V_H) are

$$V_V = V_T \sin(\cot^{-1} L/D)$$

and

$$V_H = V_T \cos(\cot^{-1} L/D)$$

TABLE 8
OPENING FORCE DATA

Percent (%) Reefing	q (Reefed Opening)	C_{D_C} (Reefed)	F_C (Reefed)	F_O (Reefed)	X (Reefed)	$\frac{W}{C_D S}$ (Reefed)
12.5	30 psf	.130	440	380	.864	4.76
15	35 psf	.155	615	655	.939	3.95
20	20 psf	.195	440	690	1.57	3.17
Percent (%) Reefing	**q Disreefed**	**C_D (Full Open)**	**F_C (Full Open)**	**F_O* (Full Open)**	**X* (Full Open)**	**$\frac{W}{C_D S}$ (Full Open)**
12.5	8.1 psf	1.0	915	720	.787	.619
15	4.3 psf	1.0	486	565	1.16	.619
20	3.1 psf	1.0	350	692	1.98	.619

*From percent reefing indicated to full open.

As can be seen from Figures 15, 16, 18, 19, and 20, C_L and C_D are functions of velocity and flap setting. Therefore, in order to calculate performance as a function of weight, for a given size parachute, it is necessary to select a condition such as maximum L/D and plot values of C_L and C_D as a function of velocity for this condition. Using these plots it is possible to compute W as a function of V_T. The results of these computations can be plotted as W versus V_T, V_V, and V_H. These plots allow the determination of weight necessary to give a desired descent velocity.

5.4.2 Performance of Model 301 at L/D Max

The performance characteristics of Models 301-16, 301-28 and 301-40 (D_W = 16-ft, 28-ft and 40-ft versions of Model 301) are presented in the following paragraphs for the maximum L/D condition.

Figures 21 and 22 are plots of L/D max and C_L versus C_D, corresponding to L/D max. They are plotted as a function of V_T for three values of D_W (16-ft, 28-ft, and 40-ft). By making use of these plots and the equations from Paragraph 5.4.1, the results plotted in Figures 24, 25 and 26 were obtained. These figures give W as a function of V_T, V_V and V_H for Models 301-16, 301-28 and 301-40. It should be remembered that the results shown by these plots include the effect of test vehicle drag. Using the results shown in Figures 24, 25 and 26, the necessary weights for descent velocities of 8, 15, 22 and 30 ft/sec and D_W = 16, 28 and 40 are presented in the following table.

TABLE 9
WEIGHTS FOR DESCENT VELOCITIES

Rate of Descent Ft/Sec	Descent Weights (lbs)		
	16 Ft D_W	28 Ft D_W	40 Ft D_W
8	100	375	750
15	275	925	1900
22	500	1650	3450
30	845	2825	5925
h = sea level			

The descent velocities shown in the previous table correspond to the velocities specified in Northrop Ventura Report No. 2689 (Reference 3), that is, rates of descent specified are vertical rates while gliding at L/D max.

5.5 STEERING CONTROL REQUIREMENTS

The utilization of the glide capability of the Steerable Parachute system requires a means of controlling the flight characteristics of the system to permit changing the glide angle and execute steering maneuvers. Control of the glide angle and steering is accomplished by extending or retracting the control flaps, that is, by adjusting the position of the flaps in relation to the main portion of the parachute canopy.

Steering or turning maneuvers can be accomplished by asymmetrically adjusting the control flaps so as to produce a turning or steering moment (N) which will cause the parachute and vehicle to turn about its vertical or yaw axis.

The results of the Ames Research Center wind tunnel tests and information from the truck tow test series were used to augment material from previous programs to provide data for analysis of the control and guidance subsystem requirements.

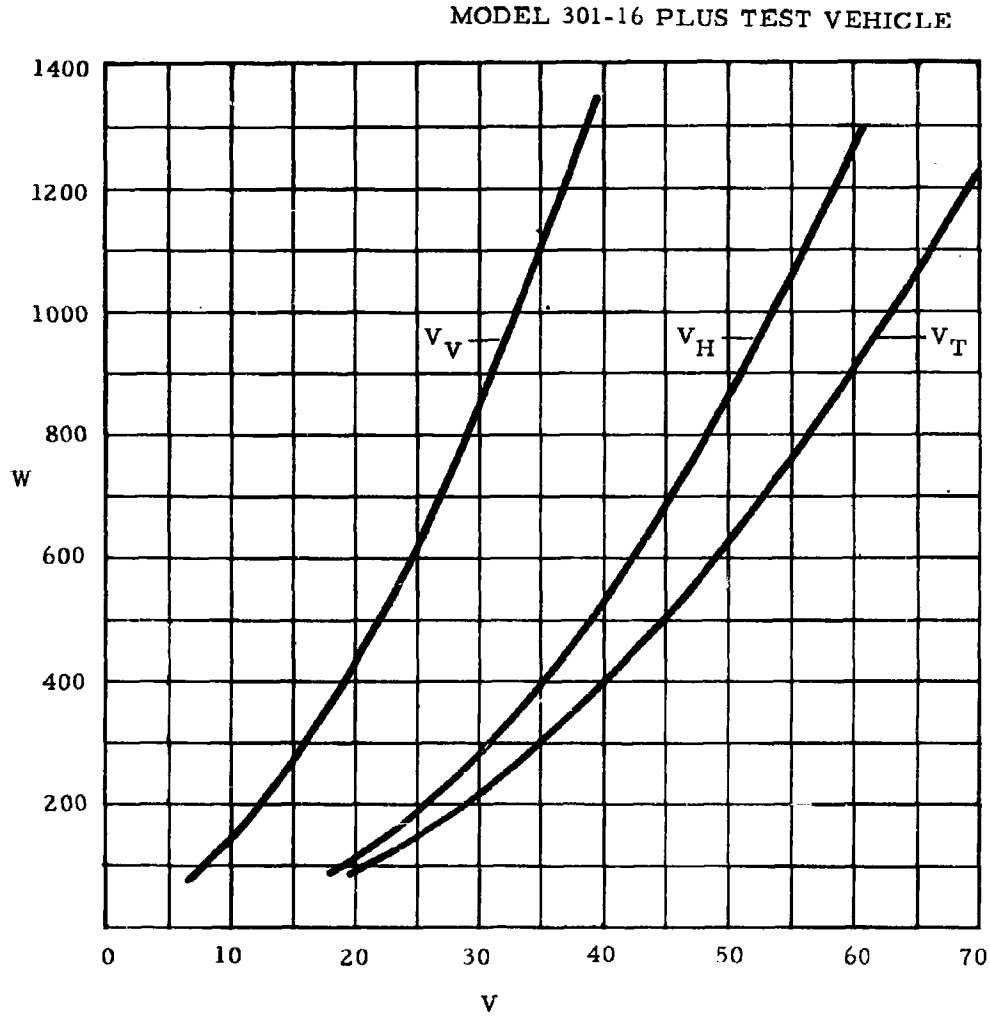

Figure 24. Weight Vs Velocity at Max L/D

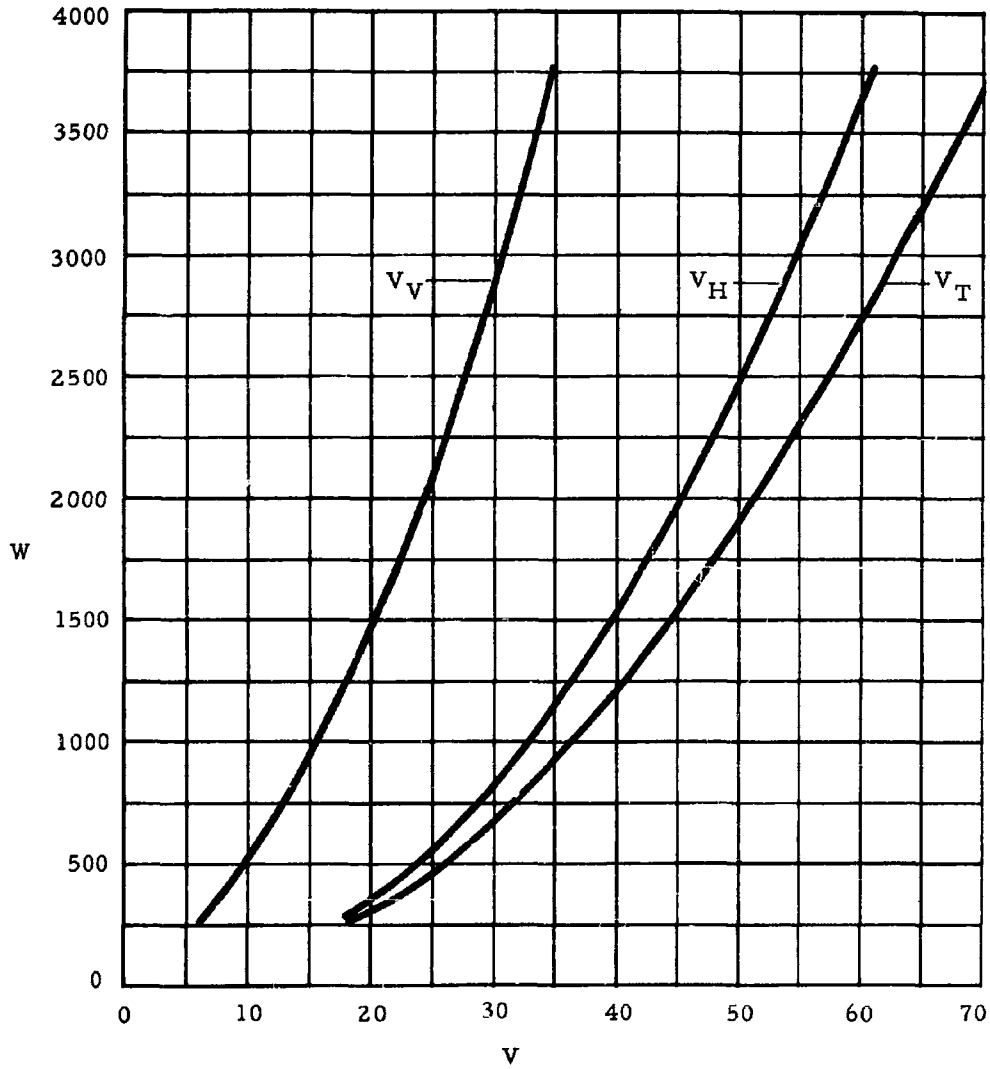

Figure 25. Weight Vs Velocity at Max L/D

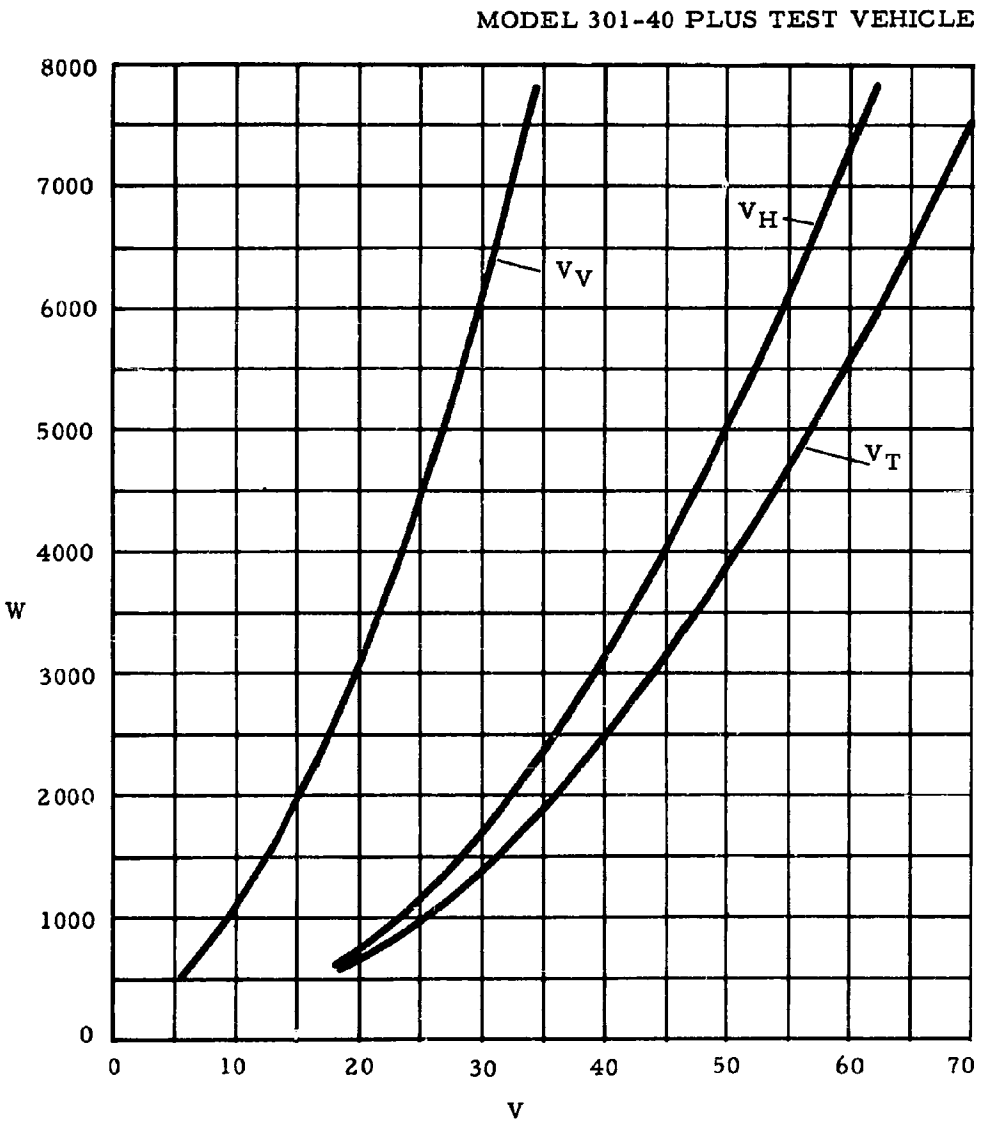

Figure 26. Weight Vs Velocity at Max L/D

Analysis of the results of differentially operating the glide control flaps provide a basis for obtaining estimated turning moments. Using the following assumptions and equations, values of turning torque as a function of differential flap extension were computed.

(1) L/D data obtained for the 12-ft D_W models was considered applicable to larger models. Experience indicates this to be a conservative assumption.

(2) Steering or turning moments were considered to be a result of a difference in the horizontal component of drag caused by variations in flap extension.

(3) The difference in horizontal components of drag were assumed to act on the parachute through a moment arm measured from the centerline of the parachute to the midpoint of the flap.

The turning torque (N) is given by the equation

$$N = r\Delta D_H$$

where D_H = horizontal drag component

ΔD = change in drag due to change in flap setting

$$\Delta D_H = \Delta D \sin \beta$$
$$= \Delta C_D \, S \, q \sin \beta$$

r = effective radius through which ΔD_H acts

The change in drag coefficient (ΔC_D) for a change in flap setting is obtained from Figure 16. The velocity for a given descent weight is computed by the methods of Paragraph 5.4.1.

The results of calculations using the preceding methods are plotted in Figure 27 for a 16-ft parachute and in Figure 28 for a 40-ft parachute.

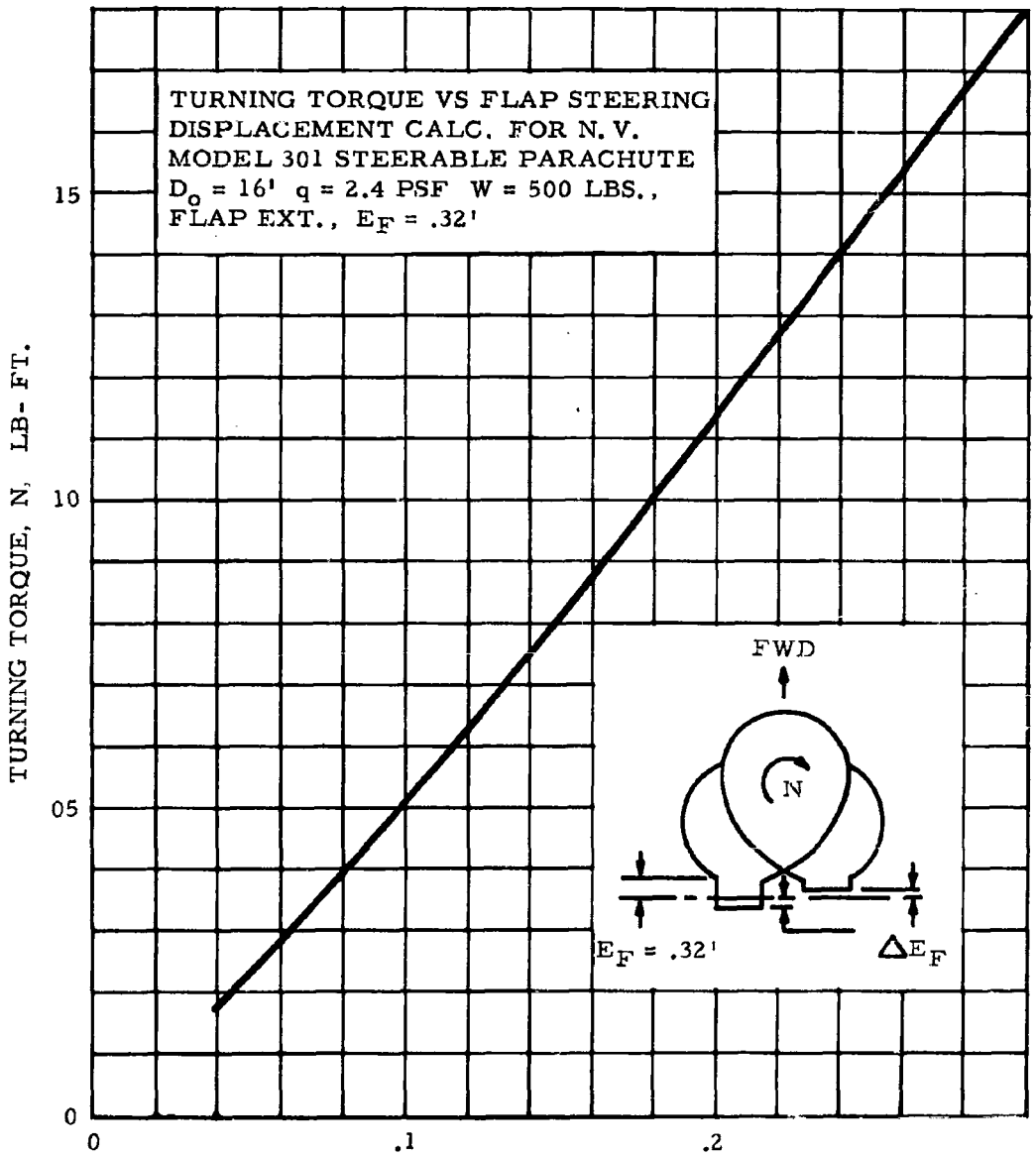

Figure 27. Turning Torque Vs Flap Steering Displacement

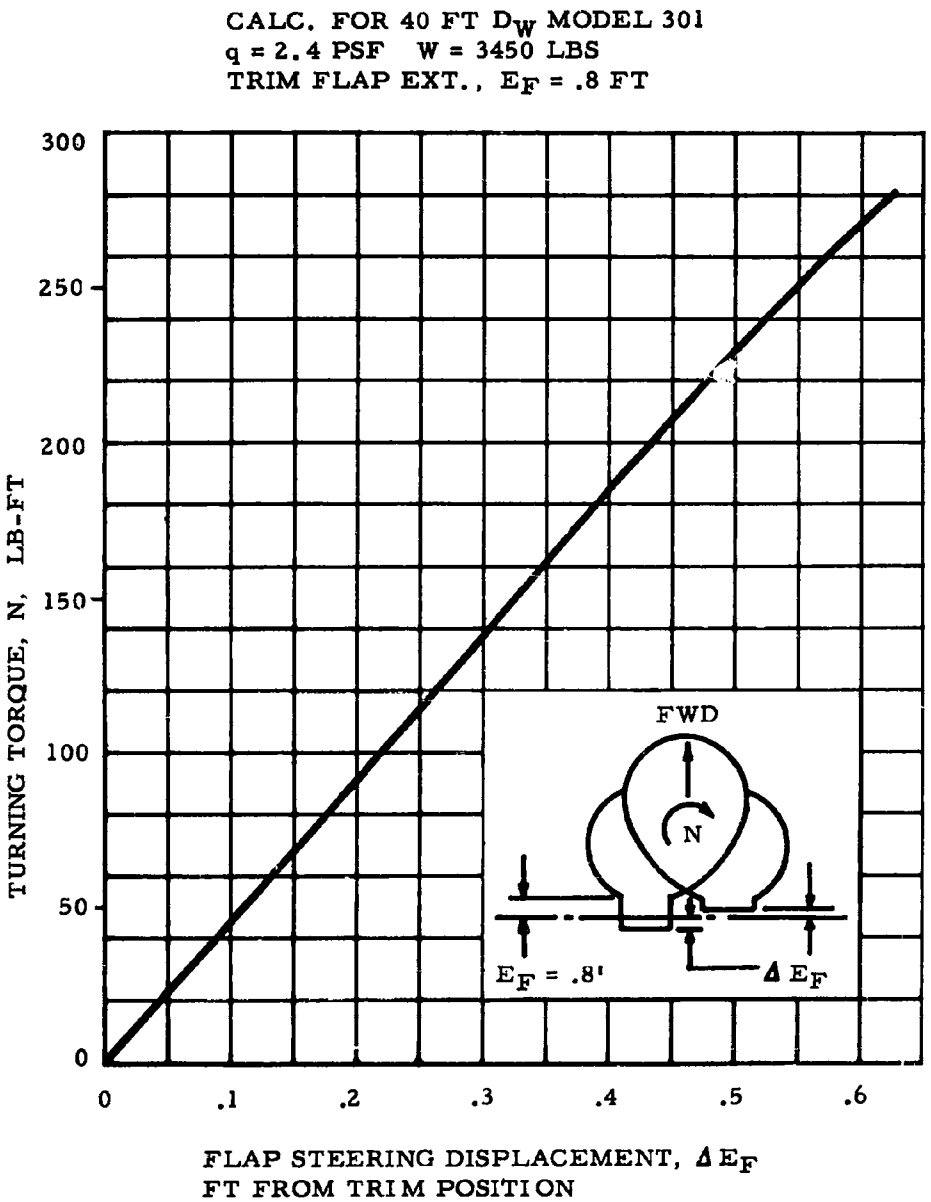

Figure 28. Turning Torque Vs Flap Steering Displacement

If the assumptions are made that the rate of turn is equal to the rate of yaw and that the yawing parachute system is restrained only by inertial and viscous retarding moments, then the equation for the rate of turn ($\dot{\theta}$) is

$$\dot{\theta} = \frac{N}{B}\left(1 - e^{-\left(\frac{Bt}{J}\right)}\right)$$

N = yawing moment
B = damping factor
t = time
J = moment of inertia

In order to check the order of magnitude of the turning response that could be expected with Model 301, the same two cases for which yawing moments were previously calculated were investigated.

Because of the lack of data available to exactly calculate the unknowns in the previous equation it is necessary to use approximations to obtain values for B and J.

Values for B were obtained by extrapolating data contained in Reference 4. The moments of inertia were calculated by using the mass distribution of the proposed drop test vehicle and by making an educated guess at the contribution due to the mass of the canopy and its included air mass. The assumption was also made that the vehicle and canopy act as a rigid unit.

The numbers used are

$B = 21.8 \frac{\text{lb ft sec}}{\text{radian}}$ for the 16-ft 500-lb system.

$B = 856.7 \frac{\text{lb ft sec}}{\text{radian}}$ for the 40-ft 3450-lb system.

$J = 38.8$ slug ft^2 for the 16-ft 500-lb system.

$J = 669.6$ slug ft^2 for the 40-ft 3450-lb system.

Using the preceding numbers and data from Figures 27 and 28, the results presented in Figure 29 and 30 were calculated. Drop tests conducted by Northrop Ventura during an in-house program with a 16-ft version of Model 301 have shown that the results shown in Figure 29 are of the right order of magnitude.

5.6 DROP TEST VEHICLE CONTROL REQUIREMENTS

The requirements of the control system of the drop test vehicle are that the vehicle be able to provide the necessary flap deflections to the parachute for all anticipated flight conditions. Table 9 tabulates the anticipated drop conditions. The modes of flap deflections required are differential for turn control and collective for glide control. In order to provide as versatile a control system as possible, the two control modes should be operable simultaneously and independently. The control system should be so designed as to prevent steering and glide control flap deflections from adding to values that exceed maximum deflections.

5.6.1 Turn Control

The maximum differential flap travel requirement is set by the flap travel needed to test the 40-ft parachute. As a reasonable requirement, it was assumed that full differential control should be available at neutral collective flaps. Sufficient differential flap travel should be available to extend the flap on the outside of the turn to the point where the side lobe on the outside of the turn begins to collapse. Figure 12 shows the limits for collective flap extension. For test vehicle design purposes, it was felt that differential flap travel sufficient to extend one flap to the maximum for collective flap extension (see Figure 12) would be adequate. A maximum parachute diameter of 40-ft and a velocity of 30 fps gives the requirement of ± 3.6-ft per flap.

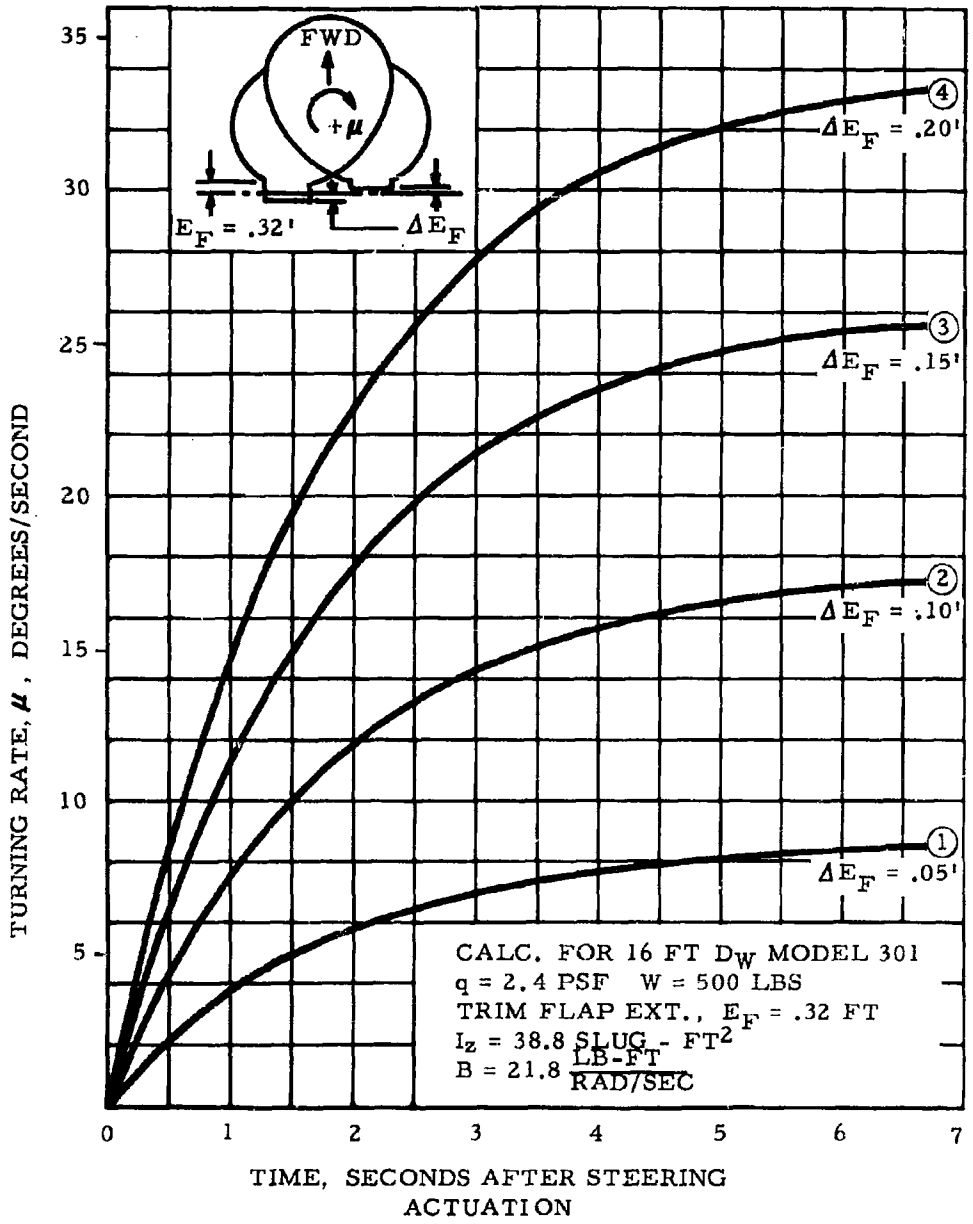

Figure 29. Turning Rate Vs Time

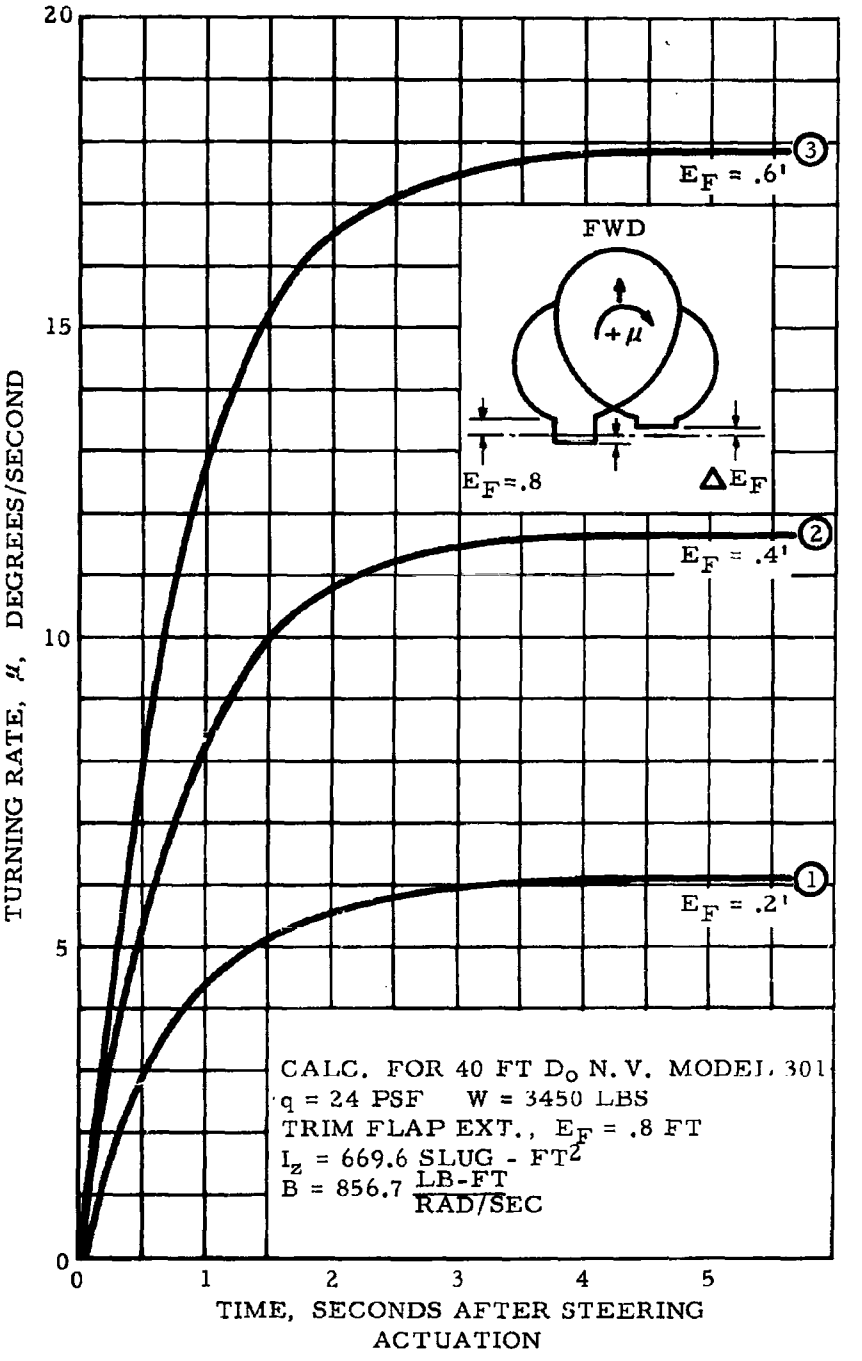

Figure 30. Turning Rate Vs Time

In order to determine flap riser loads, data from Figure 69 was used. A negative deflection of 3.6 ft for one flap is the maximum deflection and highest load condition. A positive deflection (see Figure 69) of $\frac{E_F}{D_W}$ of .09 gives a value of $\frac{\Delta F_F}{qS_W}$ of approximately .09 for one flap. Assuming that the flap being retracted will experience the same change in loading as the flap being extended, the maximum flap loading will be .09 qS_W or 530 lbs for a 40-ft parachute at 60 ft/sec. With the flaps cross-connected to balance out loads, a differential load of 1060 lbs results. It is the authors opinion that a flap rate of travel of 0.5 ft/sec will provide sufficient response time to adequately conduct drop tests.

5.6.2 Glide Ratio Control

The glide ratio or glide path angle can be varied by collectively varying the extension of the control flaps in relation to the main canopy as detailed in Paragraph 5.3.1.

At least three different methods are possible for accomplishing this adjustment. These are shown in Figure 31 and described as follows:

(1) Differentially extend the main canopy and retract the collective control flaps, or vice versa, travel distances being ratioed inversely to loads to minimize power requirements.

(2) Extend or retract main canopy. Extension of the main canopy will result in a relative decrease in control flap extension.

(3) Extend or retract control flaps collectively to directly vary E_F.

While methods B and C require the simplest mechanical configurations, response times may be marginal for full travel actuations for the 40-ft systems due to power requirements caused by unbalanced line loads.

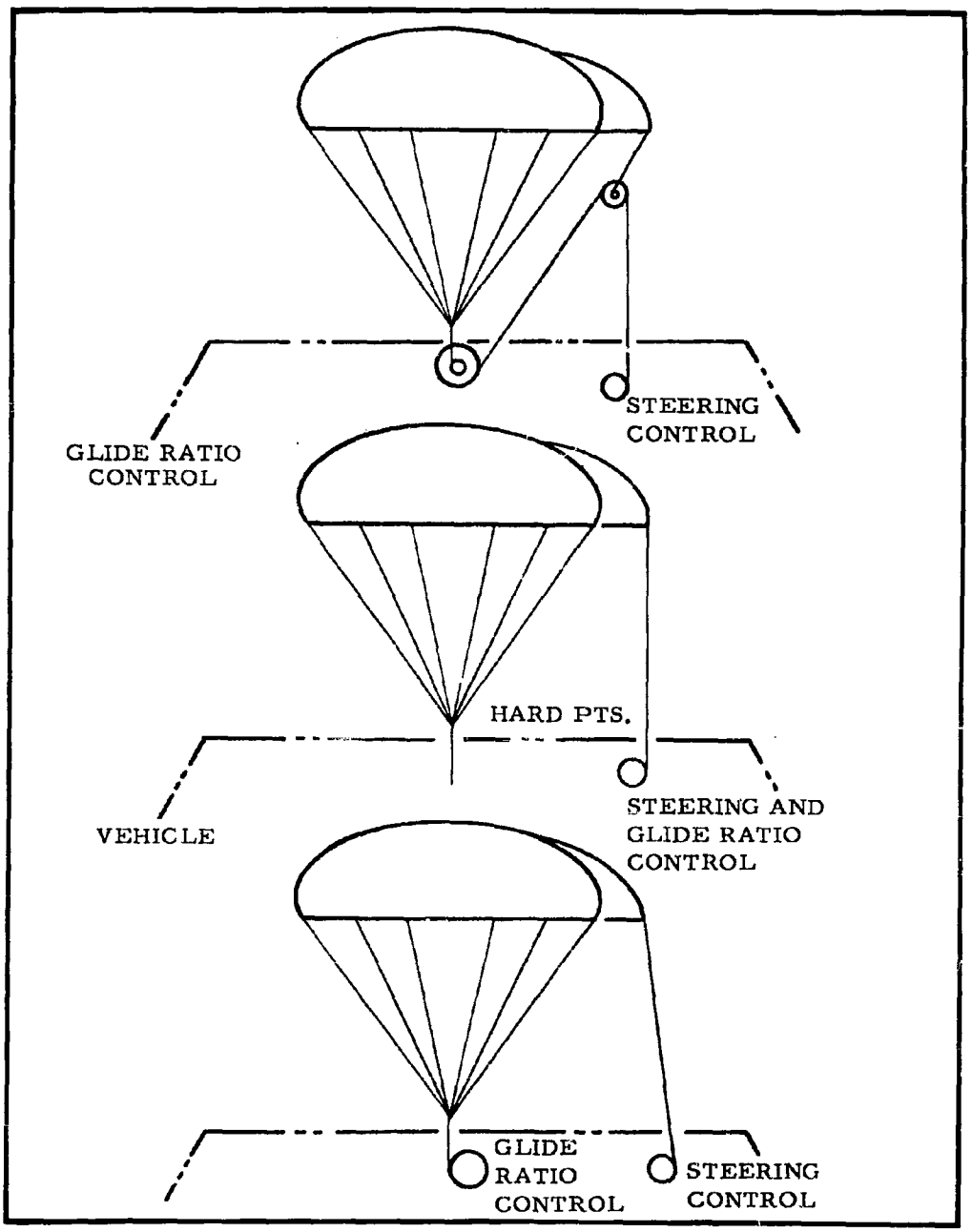

Figure 31. Glide Ratio Control

Method A minimizes these loads, permitting fast actuation at reasonable power inputs by balancing the main canopy load against the control flap loads as schematically shown in Figure 31. This method is therefore contemplated for the Phase II steerable parachute control system.

A collective flap deflection (See Figure 12) of $\frac{E_F}{D_W} = .09$ is sufficient for positive extension. In order to conduct tests to determine parachute performance at L/D values near zero, it is desirable to have a negative flap capability of $E_F/D_W = .09$. Using the assumptions of Paragraph 5.6.1 to obtain flap loads results in a total F_F/qS_W of approximately .23 for fully retracted flap. For a 40 ft parachute at 60 ft/sec this results in a load of 1350 lbs per flap. These loads are based on the assumption that the flap loads increase linearly for negative flap deflections and as such the preceding load may be high. It is the authors' opinion that a flap travel rate of 1 ft/sec will provide adequate glide control.

5.7 GUIDANCE REQUIREMENTS

The results of the study of the steerable parachute control response characteristics described in previous sections of this report indicate that a system landing requirement of 200-ft impact radius accuracy from deployment altitudes of 5,000 to 15,000 ft can be met through the use of a reasonably proficient operator at a ground control station so situated as to provide adequate visual observation of the parachute and the landing site for the duration of the parachute flight.

SECTION 6

CONCLUSIONS

It may be concluded from the research efforts reported herein that only one configuration of the steerable parachutes investigated has demonstrated the capability of meeting the primary objective of this program; that is, a lift-to-drag ratio of 2:1 (L/D = 2.0). In addition, this configuration (Model 301) has exhibited superior aerodynamic characteristics in stability, deployment behavior, and turn-rate capability. Although adequate data is not available at small lift-to-drag values, Model 301 has indicated the best potential of achieving a vertical or near vertical descent with moderate stability as well as maximum glide with excellent stability.

The results of the tests conducted under this research program have clearly shown the direction to be taken in the design of a steerable parachute descent system. Sufficient data from tests of Model 301 have been obtained for use as design criteria in establishing the requirements of mechanical components and assembly of the guidance and control system for use in subsequent phases of the program. Model 301 may be controlled in glide and steering by extension and retraction of the two control flaps and therefore lends itself to a simple control mechanism with a minimum of control functions and actuating forces.

The exploratory tests have also affirmed the following phenomenon of gliding parachutes:

Preceding Page Blank

(1) Maximum lift to drag ratio decreases with an increase in total velocity. It is felt that canopy distortion at higher dynamic pressure is responsible for this change.

(2) Reefed opening shock factors are not appreciably increased with the use of low permeability canopy materials and no unusual deployment problems are in evidence.

(3) Vertical velocities while gliding in the range of maximum lift-to-drag ratio, are reduced to approximately one-half the velocity expected while descending vertically.

SECTION 7

RECOMMENDATIONS

As a general direction in conducting the subsequent phases of this research program, Northrop Ventura makes the following recommendations:

(1) Model 301 alone be used for all further investigations. Three sizes, 16-ft D_w, 28-ft D_w, and 40-ft D_w of this model should be designed and fabricated for further evaluation.

(2) One model of each size should be fabricated from a stronger, low permeability cloth. This recommendation is made to evaluate material strength, and therefore canopy deformation as a cause of lower lift-to-drag ratios at high dynamic pressures. Selection of canopy material should be contingent on the parachute structural analysis being conducted in Phase II.

(3) Initial free-flight tests of the steerable parachute, deployed at velocities of 150 knots, should be made with a rudimentary, bomb-type vehicles. All tests made with the control system test vehicle may then be made from a C-130 drop aircraft at a maximum deployment velocity of 110 knots.

(4) At least one successful free-flight test should be made in Phase III with each of the three sizes of canopies at four vertical velocities (8, 15, 22, and 30 ft/sec) to determine the adequacy of the test equipment and instrumentation and to establish basic performance characteristics.

(5) At least two successful free flight tests should be made in Phase IV with each size canopy and at each of four velocities to determine complete system functional and operational data and investigate landing techniques.

(6) At least two successful flight tests in Phase IV for each size canopy with a bomb ballasted to give a vertical velocity of 30 ft/sec. Deployment to be made at 150 and 225 knots. These drops to be made to obtain information on deployment and inflation at high q.

SECTION 8

REFERENCES

(1)	Kinzy, R. F.	Final Report, Research and Development of Gliding Parachutes (Aerosail) Northrop Ventura Report No. 2818, September 1960
(2)	Abbot, I. Van Doenhoff, A. Stivers, L.	NACA ACR No. 15C05 Summary of Airfoil Data
(3)	Riley, V. F.	Program Plan and Work Description, Steerable Parachute, Northrop Ventura Report No. 2689, 22 February 1963.
(4)	Ewing, E. G.	Rotofoil Performance Evaluation, Radioplane Report No. 705, January, 1953.

APPENDIX I

DESCRIPTION OF MODELS TESTED

1.1 GENERAL

Contained in this section are descriptions, and drawings of the models tested during Phase I.

1.2 SMALL MODELS

Table 10 is a summary of the configurations tested during the 3-ft D_o model tests. Contained in this table are the model identification numbers and a brief description of the type and origin of the canopy design. Table 11 lists the cluster configurations tested. Sketches of the models are presented in Figure 32.

1.3 LARGE MODELS

Figures 33 to 38 are construction drawings of the 12- and 16-ft diameter models designed for this research program. These models were 301, 301A, 302, 303, 304, 402 and 301-16. For details on the models from the Aerosail test program which were tested during this program, refer to Ref. (1).

This document contains
blank pages that were
not filmed

TABLE 10
SUMMARY OF CONFIGURATIONS TESTED

Model No.	Model Description
201	Basic University of Minnesota Gliding Parachute
202	University of Minnesota Gliding Parachute with two flaps added to rear of canopy
203	University of Minnesota Gliding Parachute Configuration as forward half of canopy and N. V. Aerosail configuration as rear half of canopy
204	Basic N. V. Aerosail with extended leading edge (Aerosail Model 101)
205	Basic N. V. Aerosail with extended leading edge (Aerosail Model 101) with addition of two longitudinal ribs in aft portion of canopy
206	Square Parachute Design with side flaps to provide directional control
207	A single parachute designed to incorporate best glide features of a three parachute cluster
208	First variation of Model 207
209	Second variation of Model 207
210	N. V. Aerosail with modified leading edge gussets (1st modification)
211	N. V. Aerosail with modified leading edge gussets (2nd modification)
212	N. V. Aerosail with extended leading edge and with addition of flap on forward edge of canopy
213	Triangular pattern of six N. V. basic Aerosail parachutes with aft three canopies pushing forward three canopies
214	Circular solid flat canopy with two stiffening booms arranged in a "V" configuration with the point at the leading edge
215	N. V. basic Aerosail employing a pneumatically stiffened leading edge
216	Modification of 209. Leading edge of rear side lobes have gussets
217	Modification of Model 209. Leading edge is rolled under on all three lobes. Front lobe shortened longitudinally.
218	Circular flat canopy with lines attached to the interior of the canopy
219	Circular flat canopy with a forward pocket and longitudinal rib.

TABLE 11
CLUSTER CONFIGURATIONS

Cluster No.	Configuration
1	3 Model 204's
2	1 Model 101 leading
	2 Model 204's following
3	1 Model 215 leading
	2 Model 204's following

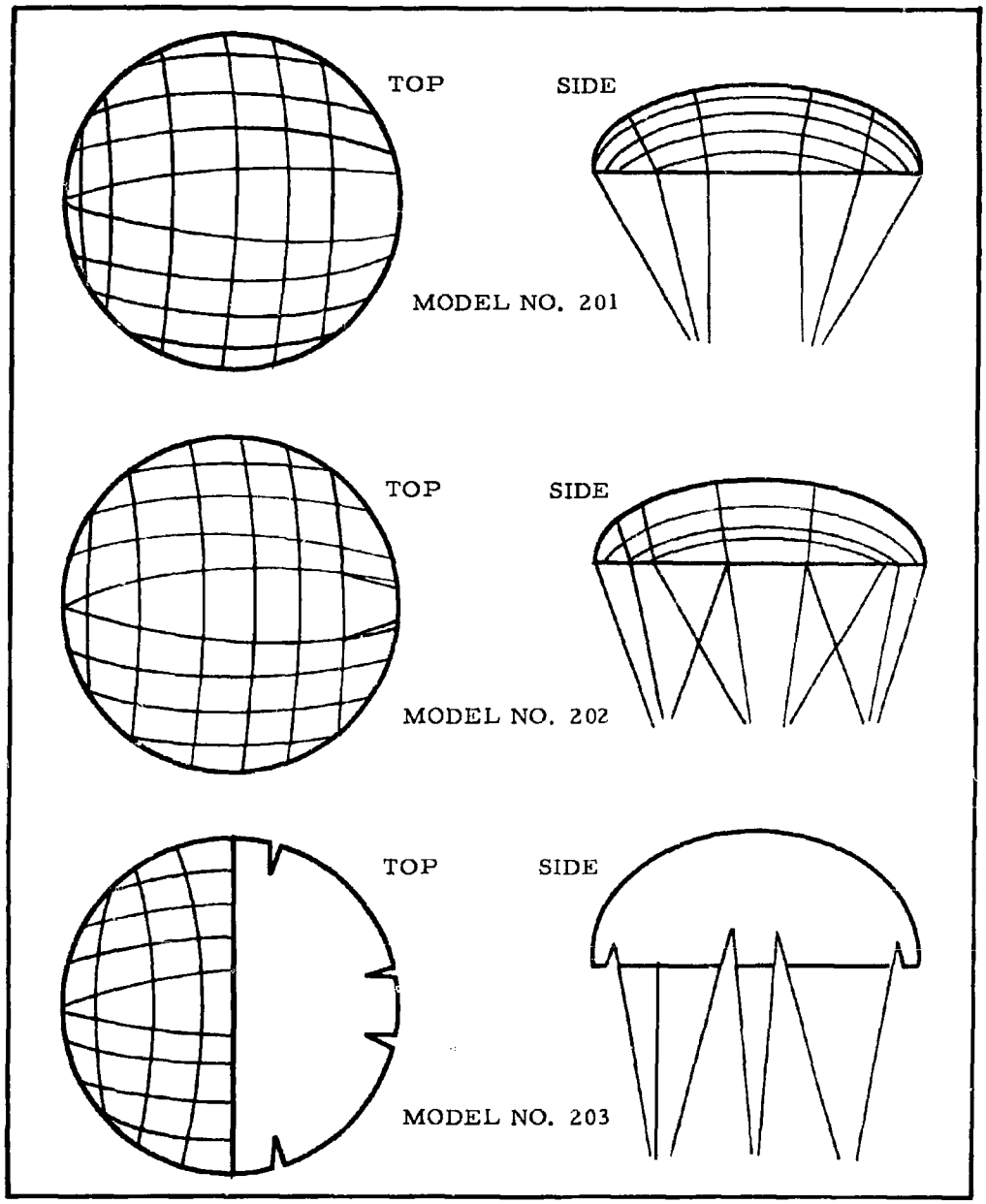

Figure 32. Sketches of Models 201, 202 & 203 Tested

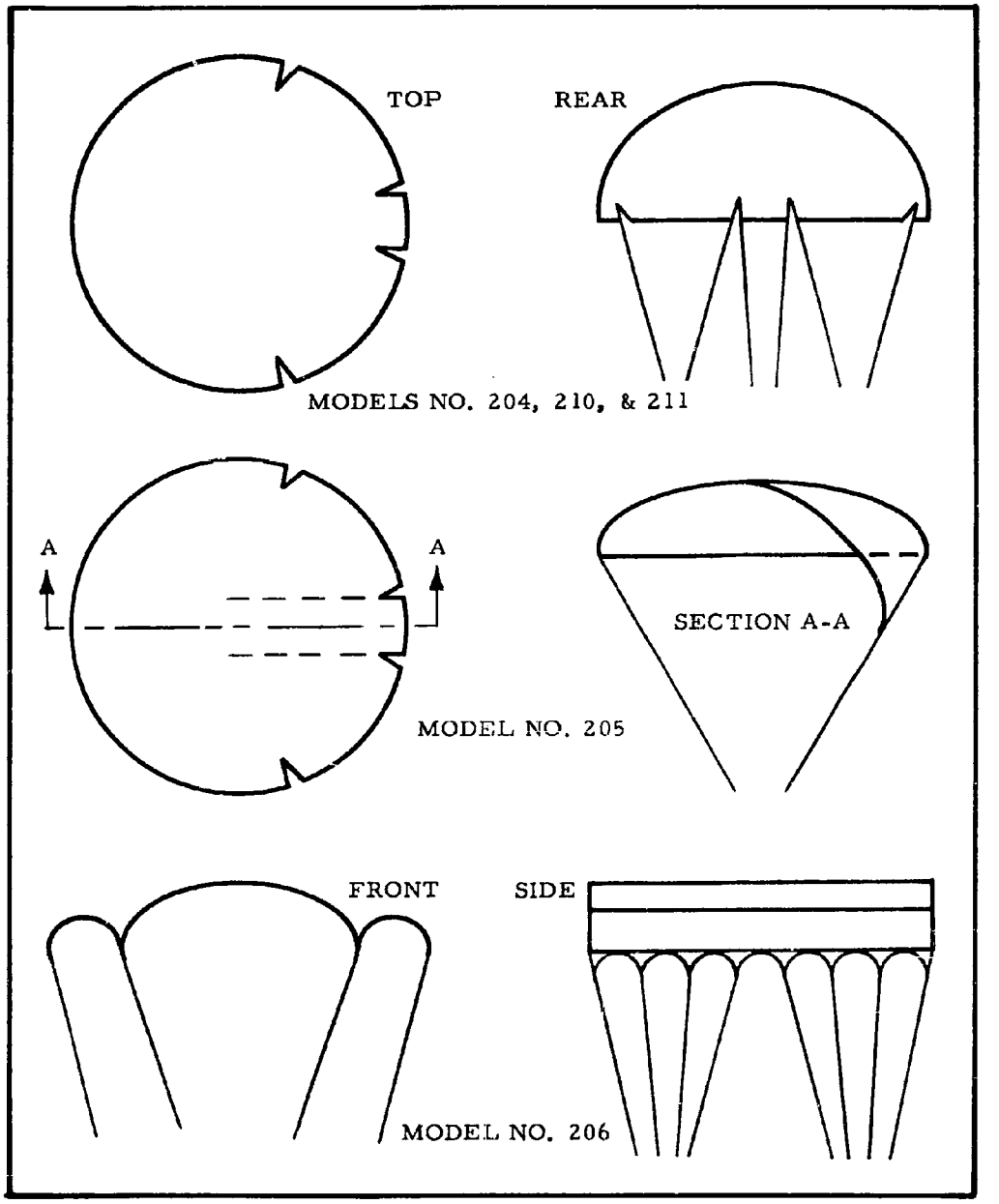

Figure 32a. Sketches of Models 204, 205, 206, 210 & 211 Tested

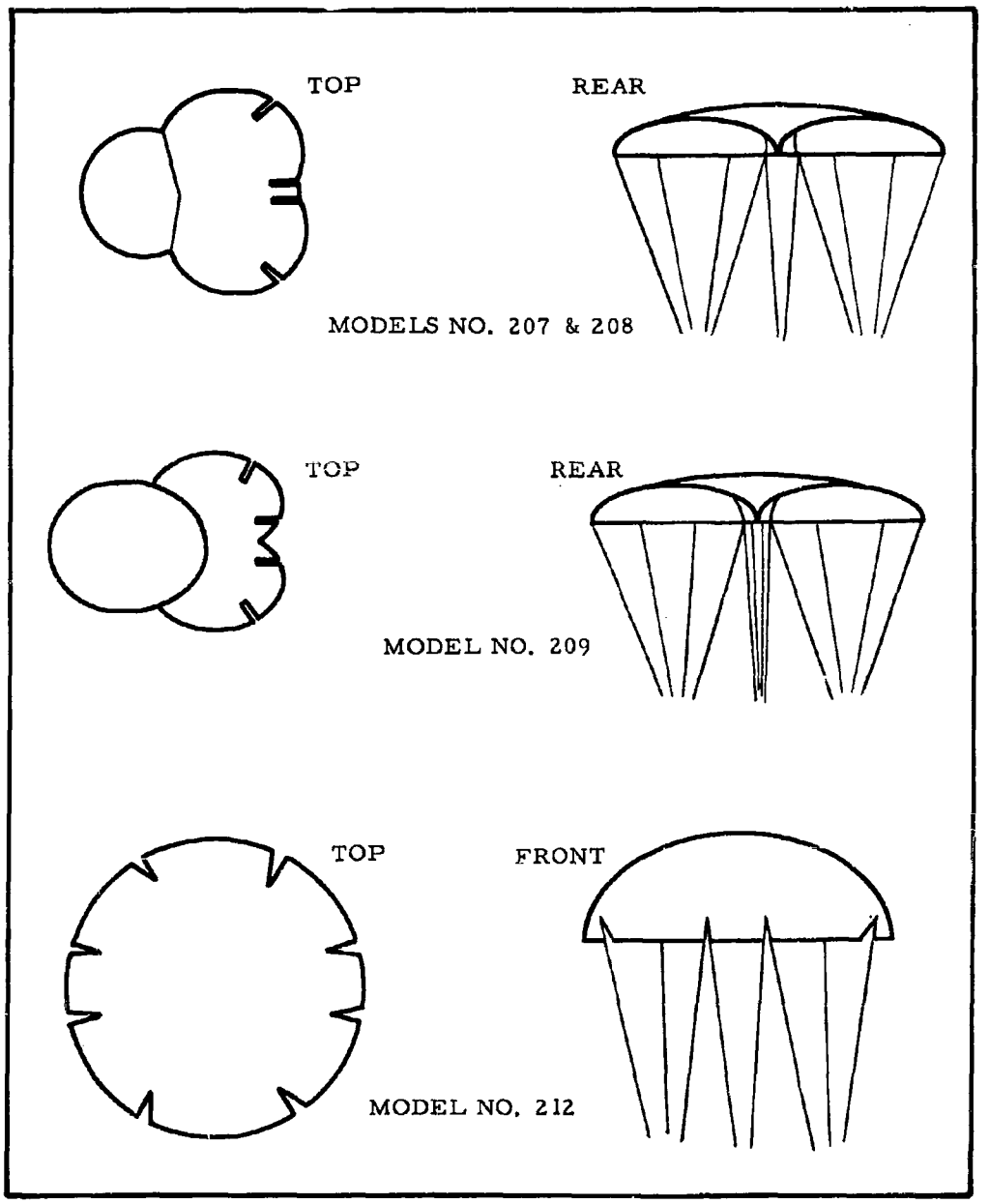

Figure 32b. Sketches of Models 207, 208, 209 & 212 Tested

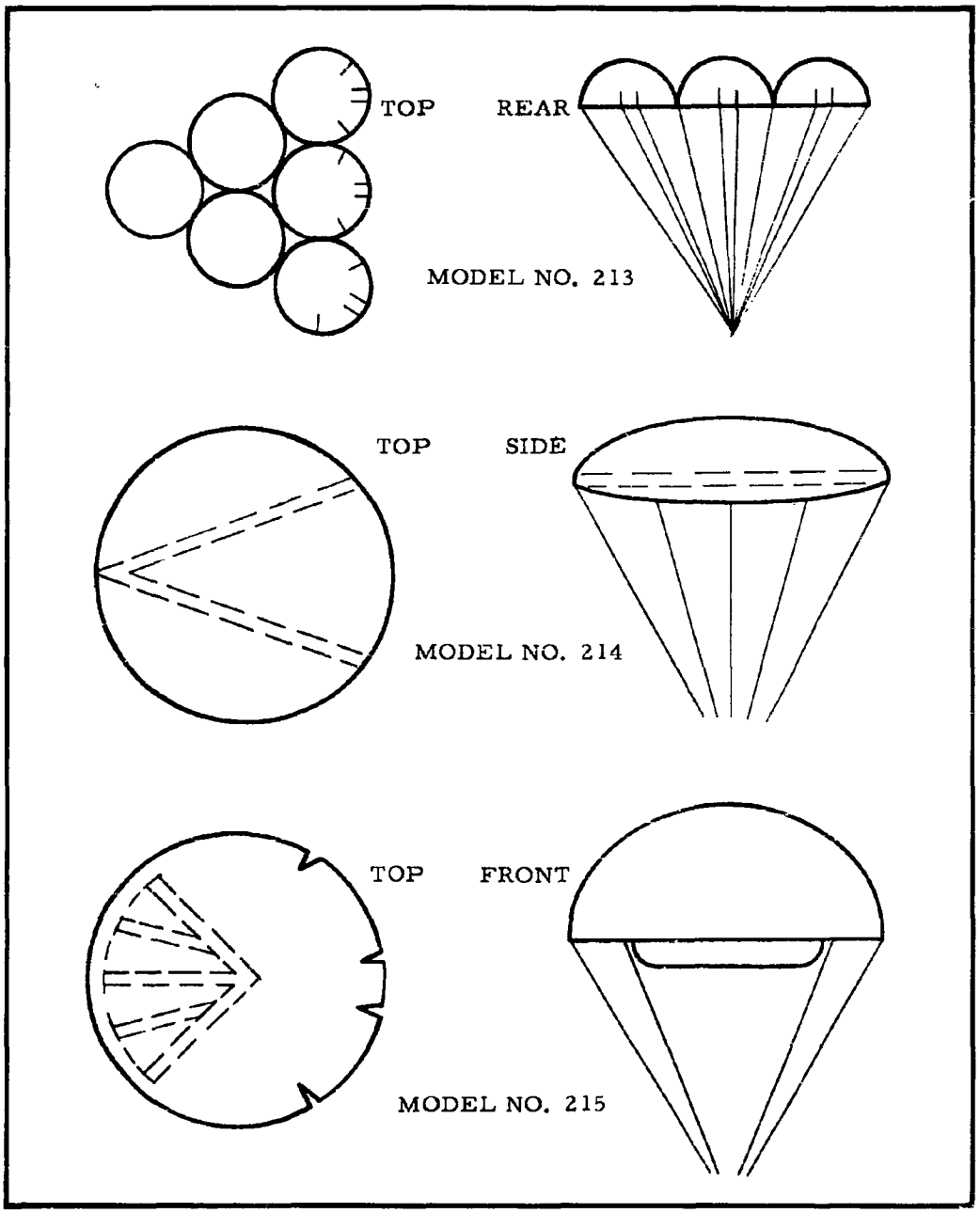

Figure 32c. Sketches of Models 213, 214 & 215 Tested

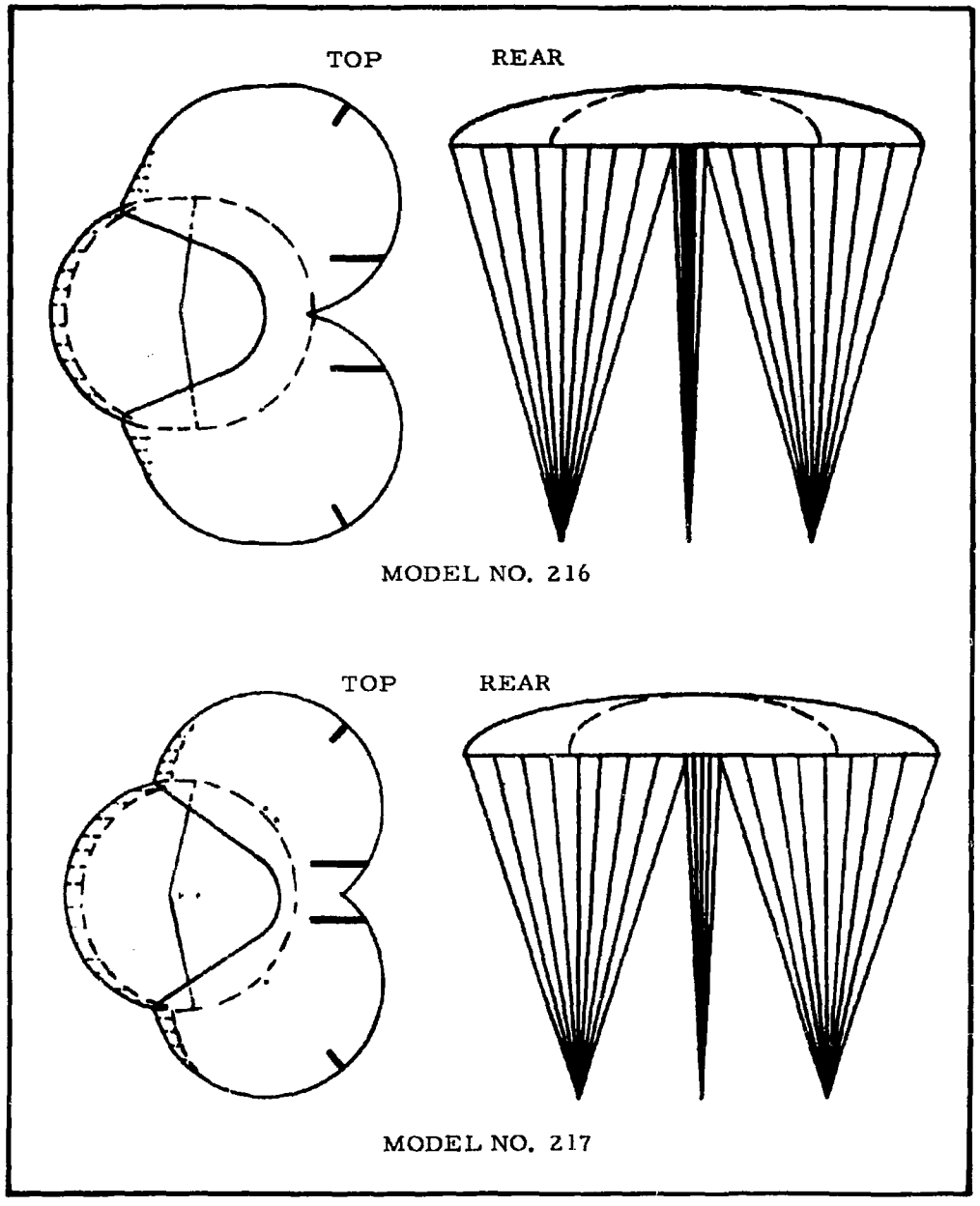

Figure 32d. Sketches of Models 216 & 217 Tested

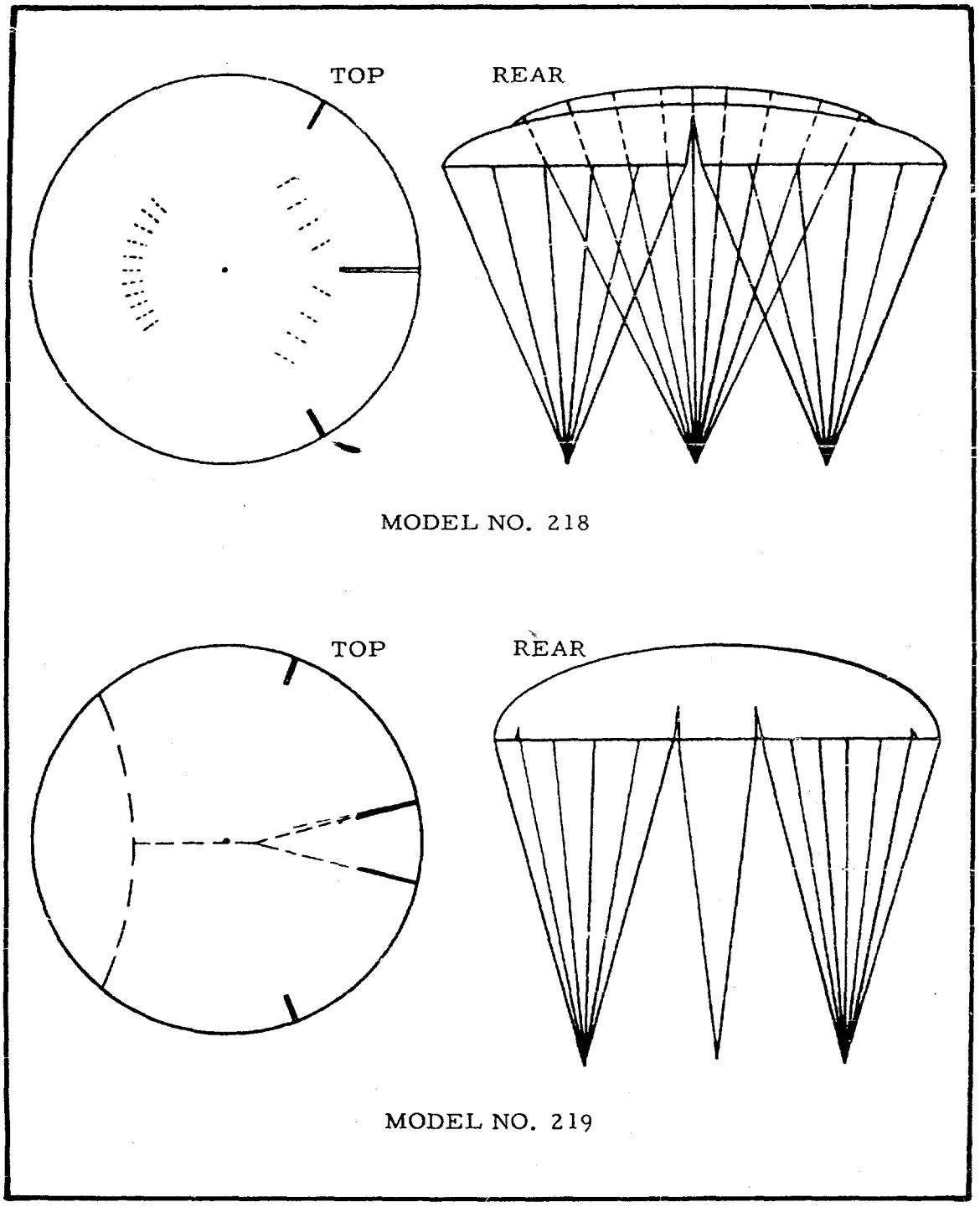

Figure 32e. Sketches of Models 218 & 219 Tested

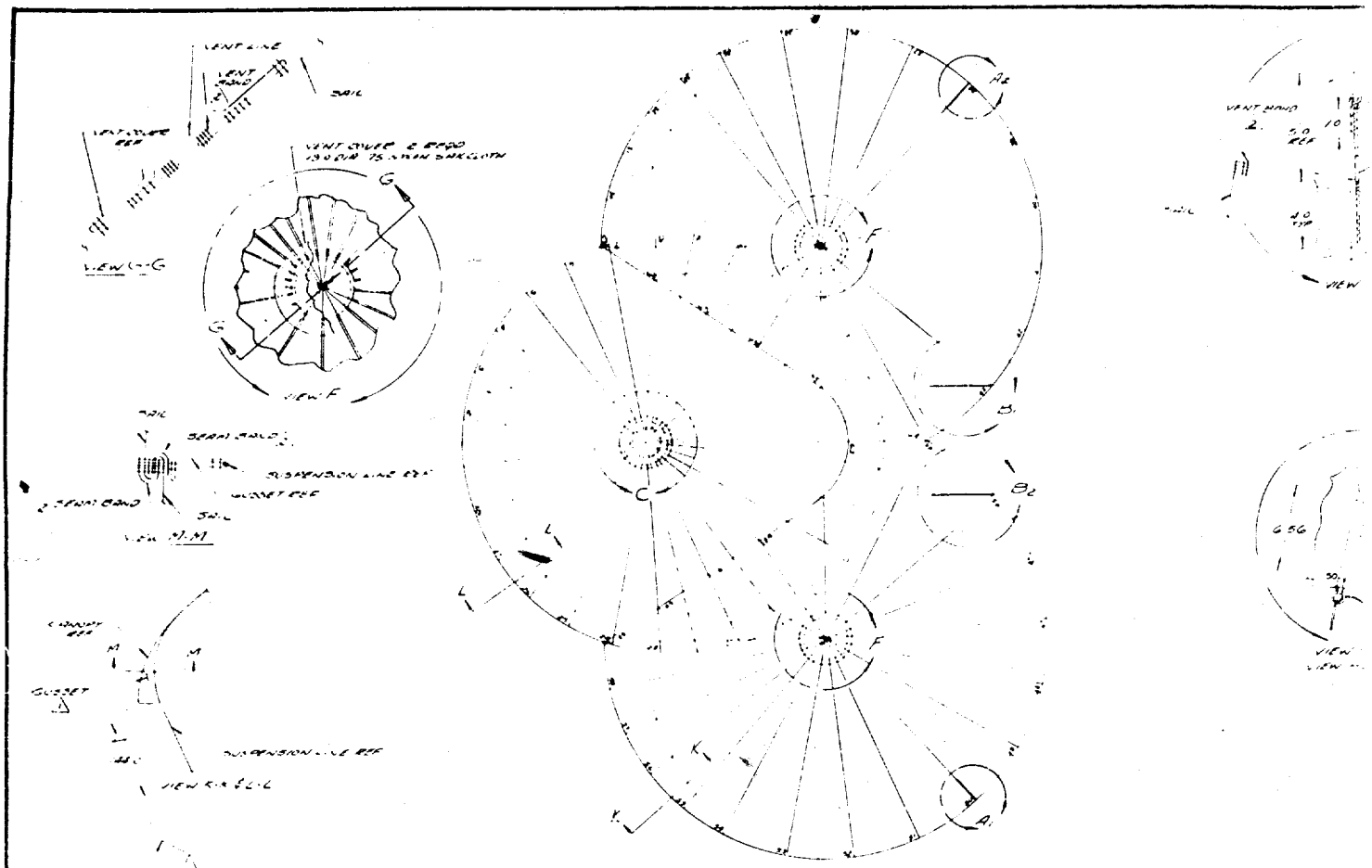

LINE LOCATIONS

LINES 2 THRU 13, 23 THRU 37, 43 & 44 RIGHT HAND RISER
LINES 14 THRU 22, 38 THRU 42, 45 & 46 LEFT HAND RISER
LINES 33 THRU 42 RIGHT FLAP RISER
LINES 46 THRU 49 LEFT FLAP RISER
LINES 30, 48, 45 & 50 END IN SNAPS

GORE NO.	A	B	C	D	E	F	G
1	30.5	30.5	11.20	1.25	1.0	11.0	11.36
2	38.14	30.5	11.20	1.25	9.25	11.0	11.36
3	38.20	38.14	11.0	1.25	7.36	9.25	11.18
4	38.44	38.20	10.82	1.25	5.70	7.35	10.36
5	39.60	38.44	10.80	1.21	3.70	5.70	11.0
6	40.86	39.60	10.80	1.0	1.70	3.70	11.0
7	42.20	40.86	10.80	1.12		1.70	10.36
8A	43.05	43.15	4.20	.49			
8B	43.15	42.20	6.50	.68			
9	42.78	43.05	10.80	1.12			
10	42.62	42.78		1.12			
11	42.52	42.62		1.14			
12	42.41	42.52					
13	42.20	42.41					
14	42.20	42.20					
15	42.20	42.20					
16	42.20	42.20					
17	42.41	42.20					
18	42.52	42.41					
19	42.62	42.52		1.14			
20	42.78	42.62		1.12			
21	43.05	42.78	10.80	1.12			
22A	43.15	43.05	4.20	.49			
22B	42.20	43.15	6.50	.63			
23	40.86	42.20	10.80	1.12	1.70		10.36
24	39.60	40.86	10.80	1.18	3.70	1.70	11.0
25	38.44	39.60	10.80	1.21	5.70	3.70	11.0
26	38.20	38.44	10.82	1.25	7.35	5.70	10.36
27	38.14	38.20	11.0	1.25	9.25	7.36	11.18
28	38.30	38.30	11.20	1.25	11.0	11.0	11.36
29	43.63	44.34	8.82	.94	9.25	11.0	5.34
30	41.73	42.68	8.82	.94	7.35	9.25	9.22
31	42.38	41.73	8.82	.94	5.70	7.35	9.06
32	42.38	42.38	5.82	.94	3.70	5.70	3.04
33	42.38	42.38	5.82	.94	1.70	3.70	9.63
34	42.38	42.38	14.50	1.57		1.70	14.70
35	42.38	42.38	14.50	1.57			

GORE NO.	A
36	42.38
37	
38	
39	
40	
41	
42	42.38
43	42.38
44	42.38
45	42.38
46	
47	
48	
49	
50	
51	
52	
53	42.38
54	42.38
55	42.38
56	41.73
57	43.63
58	44.03
59	30.71
60	43.36
61	41.58
62	43.76
63	42.38
64	42.38
65	41.58
66	43.36
67	30.71
68	42.38

1

#92

Reproduced From
Best Available Copy

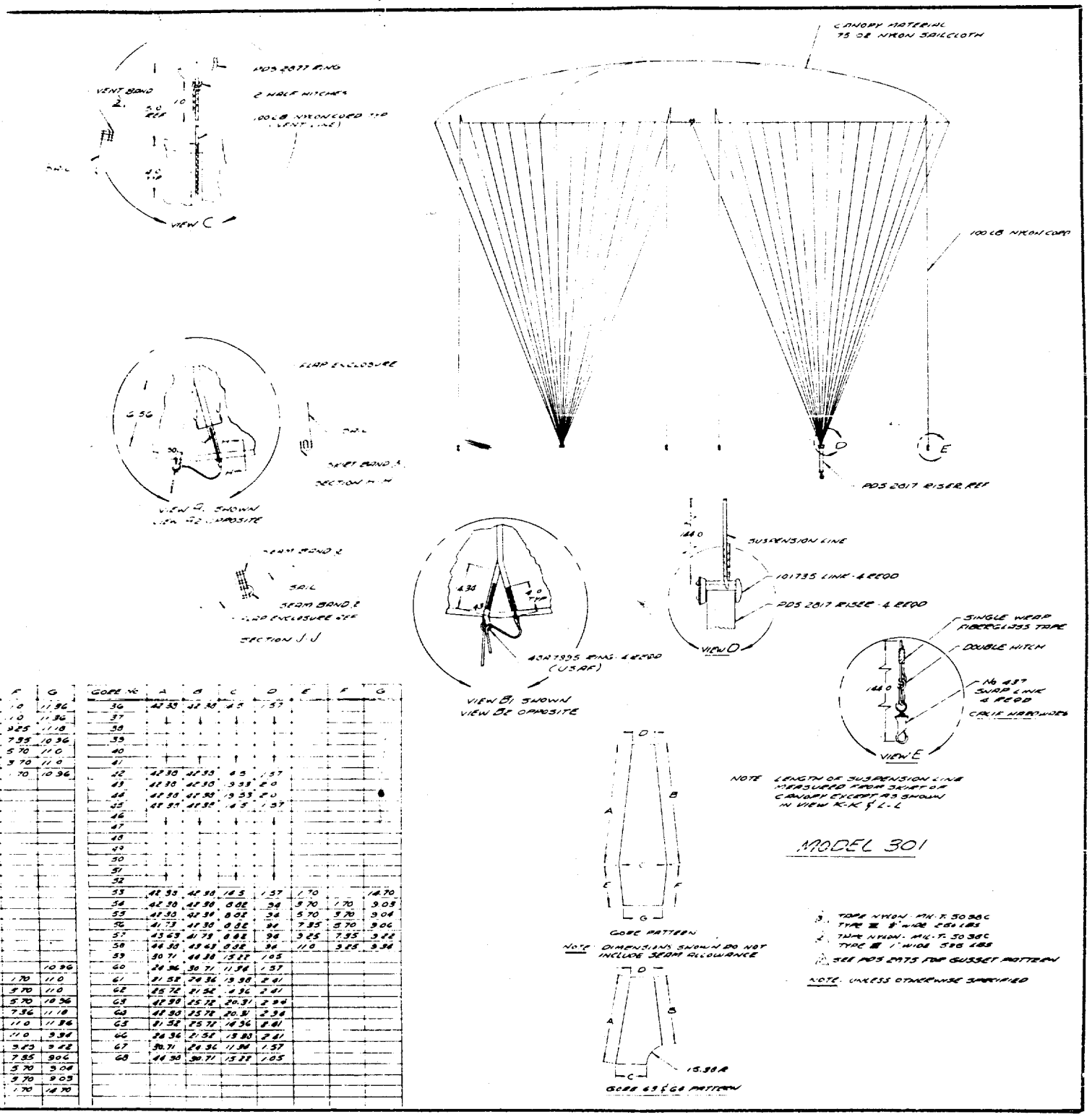

F	G
1.0	11.96
1.0	11.96
3.25	11.18
7.95	10.96
5.70	11.0
5.70	11.0
1.70	10.96

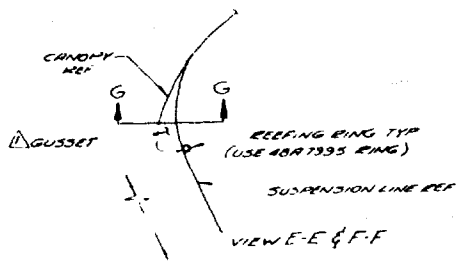

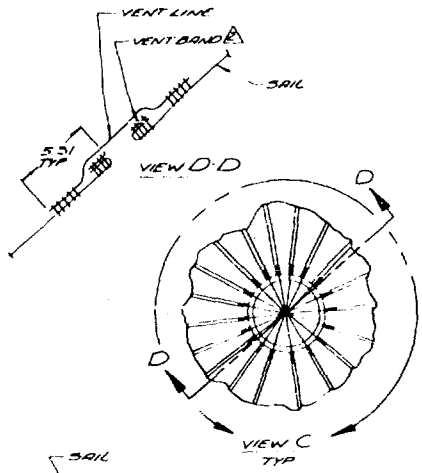

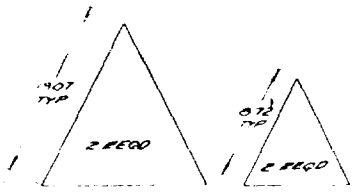

FLAP ENCLOSURES

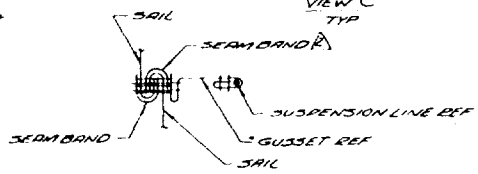

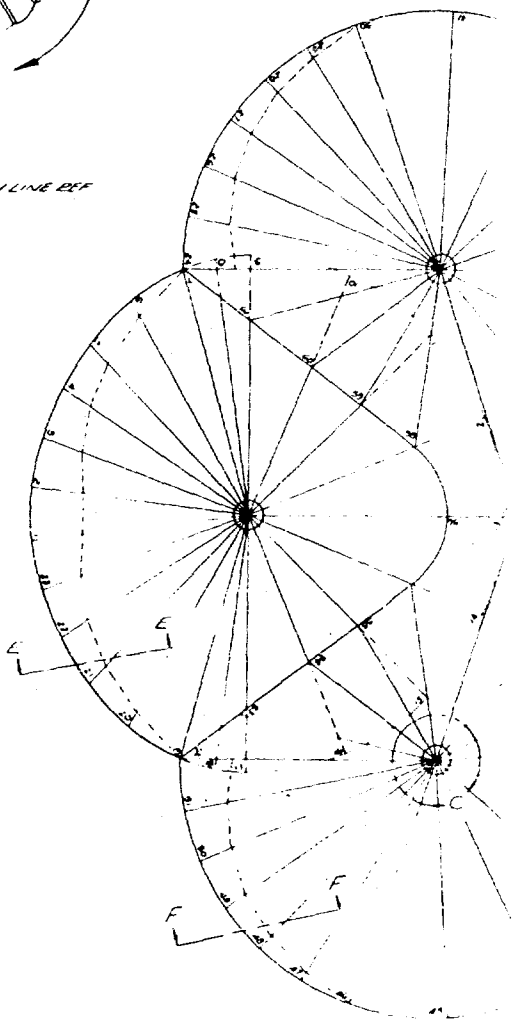

GORE	A	B	C	D	E	F	G
1	50.6	50.6	43	70	4.6	14.6	11.0
2	51.2	50.6			12.3	14.6	11.5
3	52.2	51.2			9.7	12.3	12.4
4	53.7	52.2			7.5	9.7	12.9
5	55.5	53.7			4.9	7.5	13.4
6	57.2	55.5	14.3	70	2.2	4.9	13.8
7	58.4	57.2	11.5	56		2.2	
8	59.6	58.4	10.5	56			
9	59.6	59.6	24.6	14			
10							
11							
12							
13							
14							
15							
16	59.6	59.6	24.6	14			
17	58.4	59.6	10.5	56			
18	57.2	58.4	11.5	56	2.2		
19	55.5	57.2	14.3	70	4.9	2.2	13.8
20	53.7	55.5			7.5	4.9	13.4
21	52.2	53.7			9.7	7.5	12.9
22	51.2	52.2			12.3	9.7	12.4
23	50.6	51.2	14.3	70	14.6	14.6	11.5
24	59.6	59.6	12.8	76	12.8	14.6	10.3
25					9.7	12.3	11.3
26					7.5	9.7	11.5
27					4.9	7.5	12.0
28					2.2	4.9	12.4
29	59.6	59.6	12.8	76		2.2	13.0
30	59.6	59.6	24.6	14			
31	59.6	59.6	24.6	14			

GORE	A	B	C	D	E	F	G
32	59.6	59.6	24.6	14			
33							
34							
35							
36							
37							
38							
39							
40							
41							
42							
43							
44							
45	59.6	59.6	24.6	14			
46	59.6	59.6	12.8	76	2.2		13.0
47					4.9	2.2	12.4
48					7.5	4.9	12.0
49					9.7	7.5	11.5
50					12.3	9.7	11.3
51	59.6	59.6	12.8	76	14.6	12.8	10.8
52	45.0	59.6	20.4	84			
53	36.4	45.0	18.5	12			
54	35.0	36.4	15.0	12			
55	33.3	35.0	16.8	12			
56							
57							
58	35.0	33.3	16.8	12			
59	36.4	35.0	15.0	12			
60	45.0	36.4	18.5	12			
61	59.6	45.0	20.4	84			

1

#93

Reproduced From
Best Available Copy

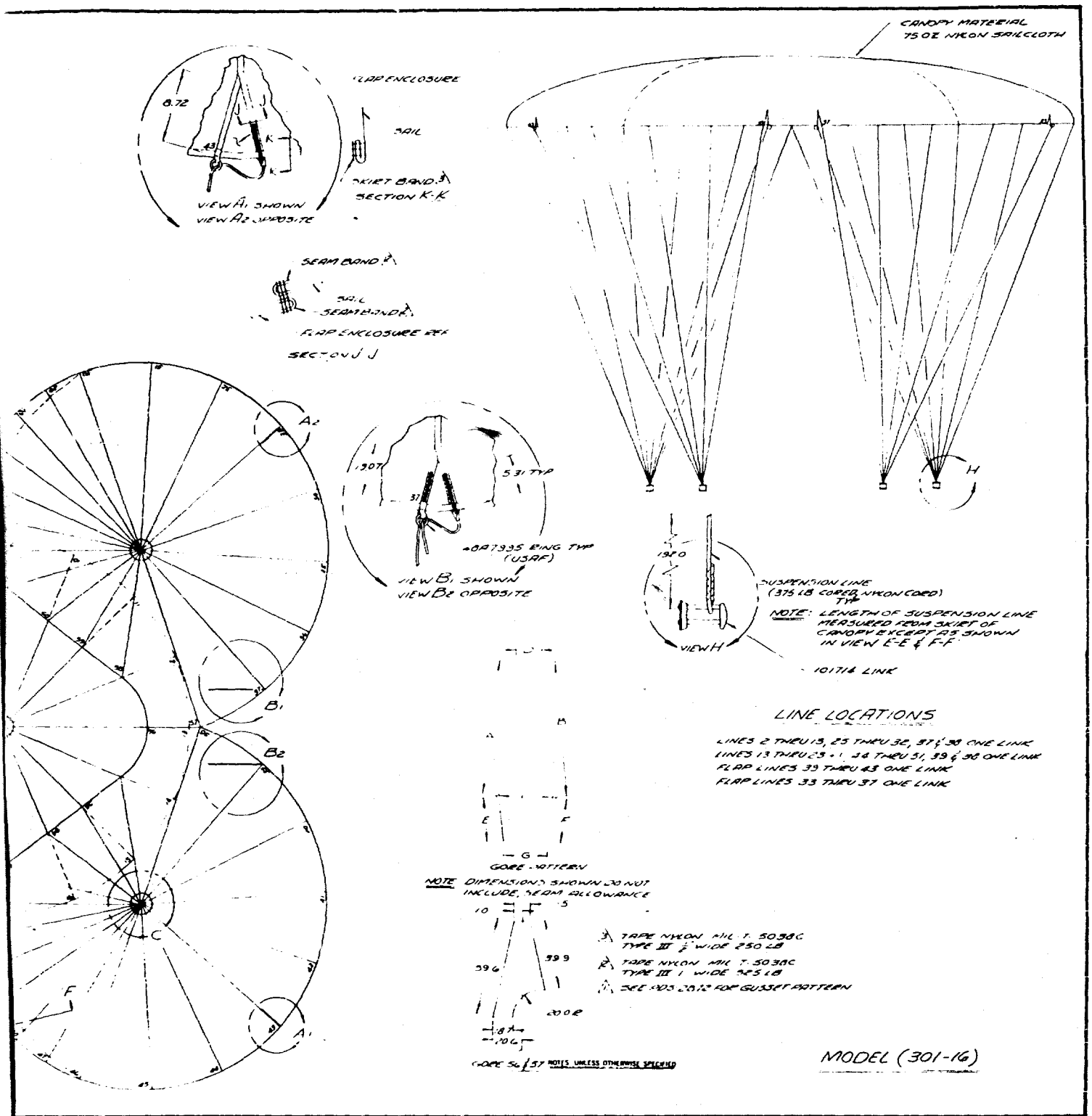

Figure 34.

Steerable Parachute - Model 301-16

2

Reproduced From
Best Available Copy

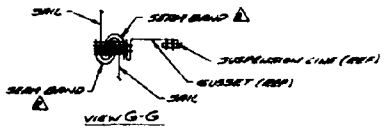

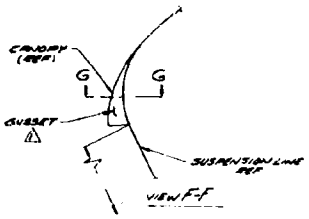

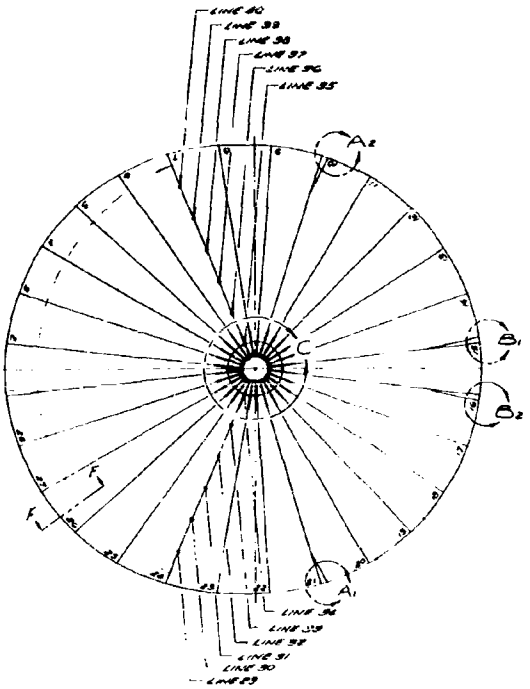

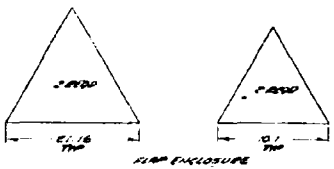

GORE No	A	B	C	D	E
1	77.1	77.1	20.3	19.0	19.0
2	79.4	77.1	19.7	18.5	19.0
3	79.7	78.4	19.1	11.9	18.9
4	78.0	78.7	18.5	8.5	11.9
5	70.4	78.0	17.9	5.9	8.5
6	68.7	70.4	17.9	2.6	5.5
7	67.0	68.7	16.7	0	2.6
8	67.0	67.0	16.1	0	0
9	↓	↓	↓	↓	↓
10					
11					
12					
13					
14					
15					
16					
17					
18					
19					
20					
21					
22	67.0	67.0	16.1	0	0
23	68.7	67.0	16.7	2.6	0
24	70.4	68.7	17.9	5.9	2.6
25	78.0	70.4	17.9	8.5	5.5
26	78.7	78.0	18.5	11.9	8.5
27	78.4	78.7	19.1	18.8	11.9
28	77.1	78.4	19.7	19.0	18.9

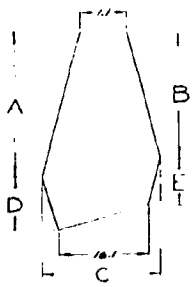

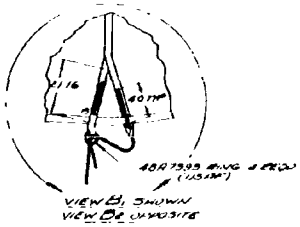

3. TAPE VINYL MIL-T-50396C TYPE III 1/4" WIDE 280 LBS
2. TAPE NYLON MIL-T-5038C TYPE III 1" WIDE 525 LBS
1. SEE POS 2813 FOR GUSSET PATTERN

NOTES UNLESS OTHERWISE SPECIFIED

1

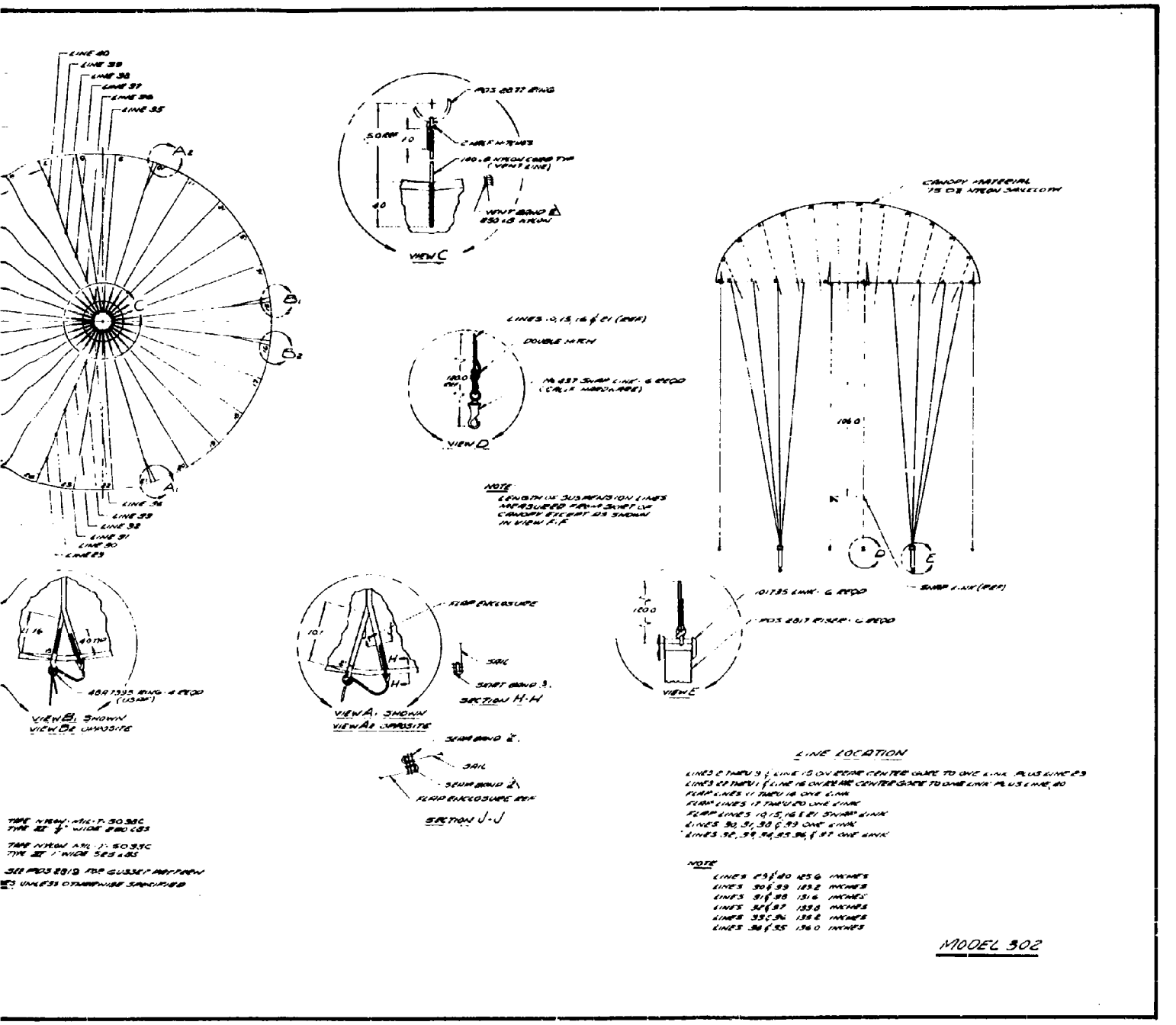

Figure 35.
Steerable Parachute - Model 302

2

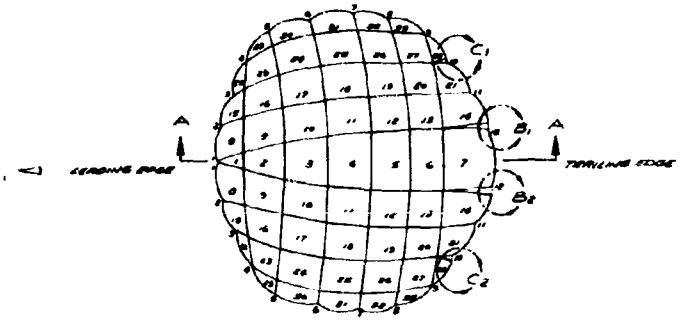

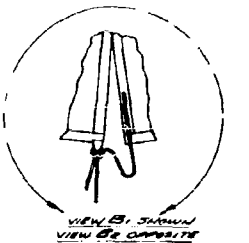

VIEW B_1 SHOWN
VIEW B_2 OPPOSITE

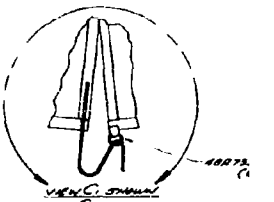

VIEW C_1 SHOWN
VIEW C_2 OPPOSITE

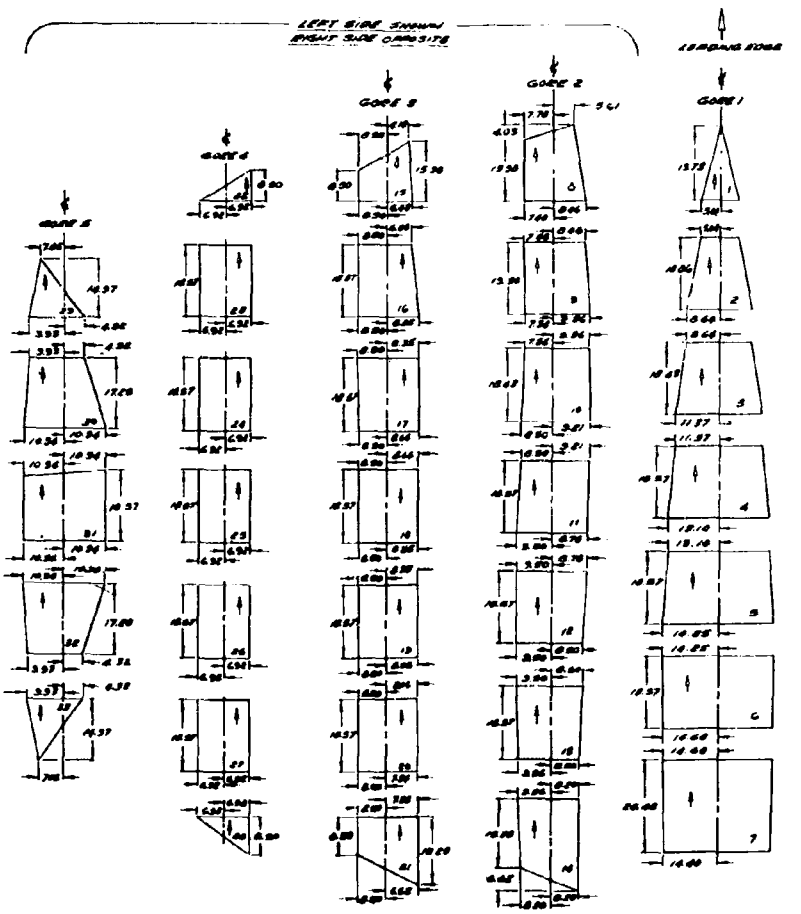

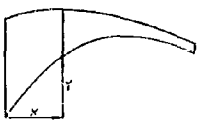

RIB DIMENSIONS

X	0	7.20	14.40	21.60	28.80	36.0	43.20	50.40	57.60	64.80	
Y	33.16	36.42	36.36	35.34	31.33	28.87	26.36	21.43	17.33	12.10	
D_1	0	10.00	19.80	29.17	37.76	44.59	49.30	50.46	46.27	11.56	
X	0	7.20	14.40	21.60	28.80	36.0	43.20	50.40	57.60	64.80	
Y	29.66	30.08	30.03	29.28	27.36	24.91	22.11	18.70	14.97	11.23	
D_1	0	3.76	7.20	10.16	12.88	14.83	15.46	16.70	15.83	5.86	
X	0	7.20	14.40	21.60	28.80	36.0	43.20	50.40	57.60		8/18
Y	24.51	25.38	25.38	24.91	23.76	22.23	20.26	17.83	15.14		
D_1	0	3.73	5.30	6.16	6.86	6.83	7.00	6.88	5.53		
X	0	7.20	14.40	21.60	28.80	36.0	43.20	50.40	57.60	64.80	
Y	19.16	18.01	16.16	13.30	11.83	9.87	7.88	5.83	3.53	1.10	
D_1	0	1.60	2.80	3.17	3.76	3.83	3.30	3.46	2.77	1.56	
X	0	7.20	14.40	21.60	28.80	36.0	43.20	50.40	57.60	64.80	
Y	33.0	30.71	26.10	23.00	21.36	20.31	22.10	18.70	14.97	11.23	
D_1	0	3.76	7.20	10.16	12.88	14.83	15.46	16.70	15.83	5.86	
X	0	7.20	14.40	21.60	28.80	36.0	43.20	50.40	57.60		8/18
Y	27.85	27.32	26.40	25.20	23.25	22.25	20.00	17.83	15.14		
D_1	0	3.73	5.30	6.16	6.86	6.83	7.00	6.88	5.53		

1

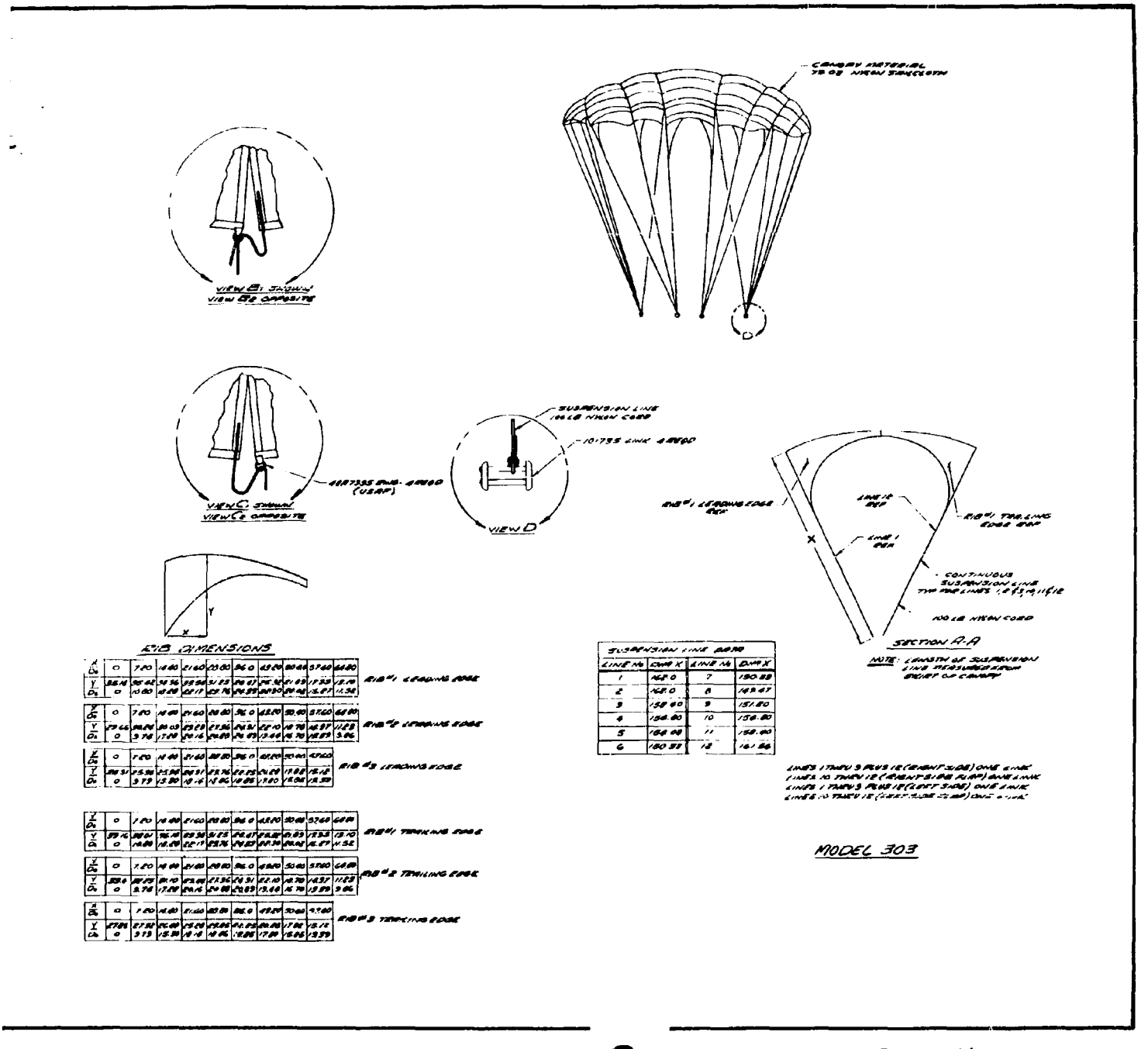

2

Figure 36.
Steerable Parachute - Model 303

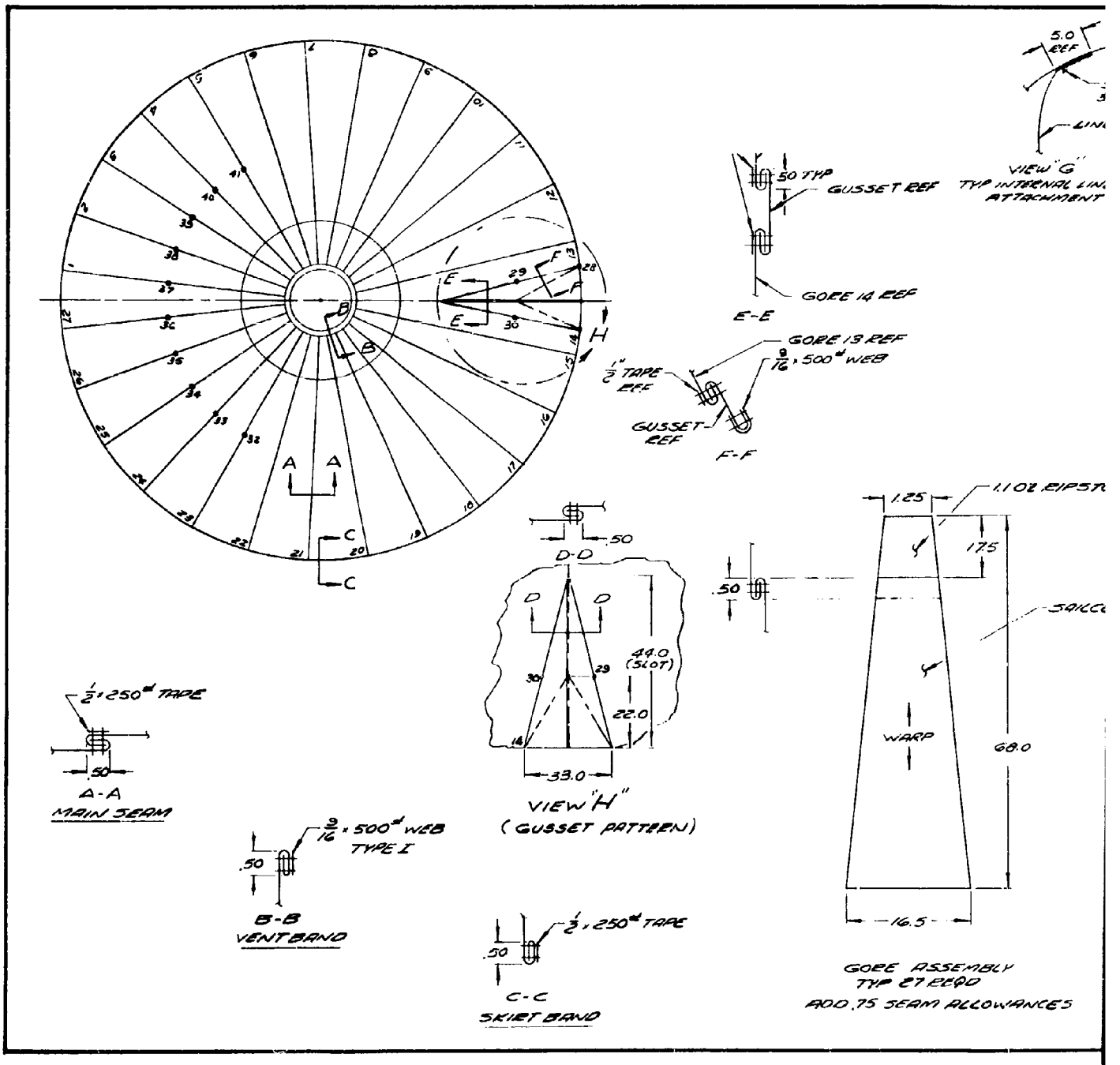
A-A
MAIN SEAM
B-B
VENT BAND
C-C
SKIRT BAND
D-D
VIEW "H"
(GUSSET PATTERN)
E-E
GUSSET REF
GORE 14 REF
F-F
GORE 13 REF
GUSSET REF
VIEW "G"
TYP INTERNAL LINE ATTACHMENT
GORE ASSEMBLY
TYP 27 REQD
ADD .75 SEAM ALLOWANCES
WARP
68.0
16.5
44.0 (SLOT)
22.0
33.0

1

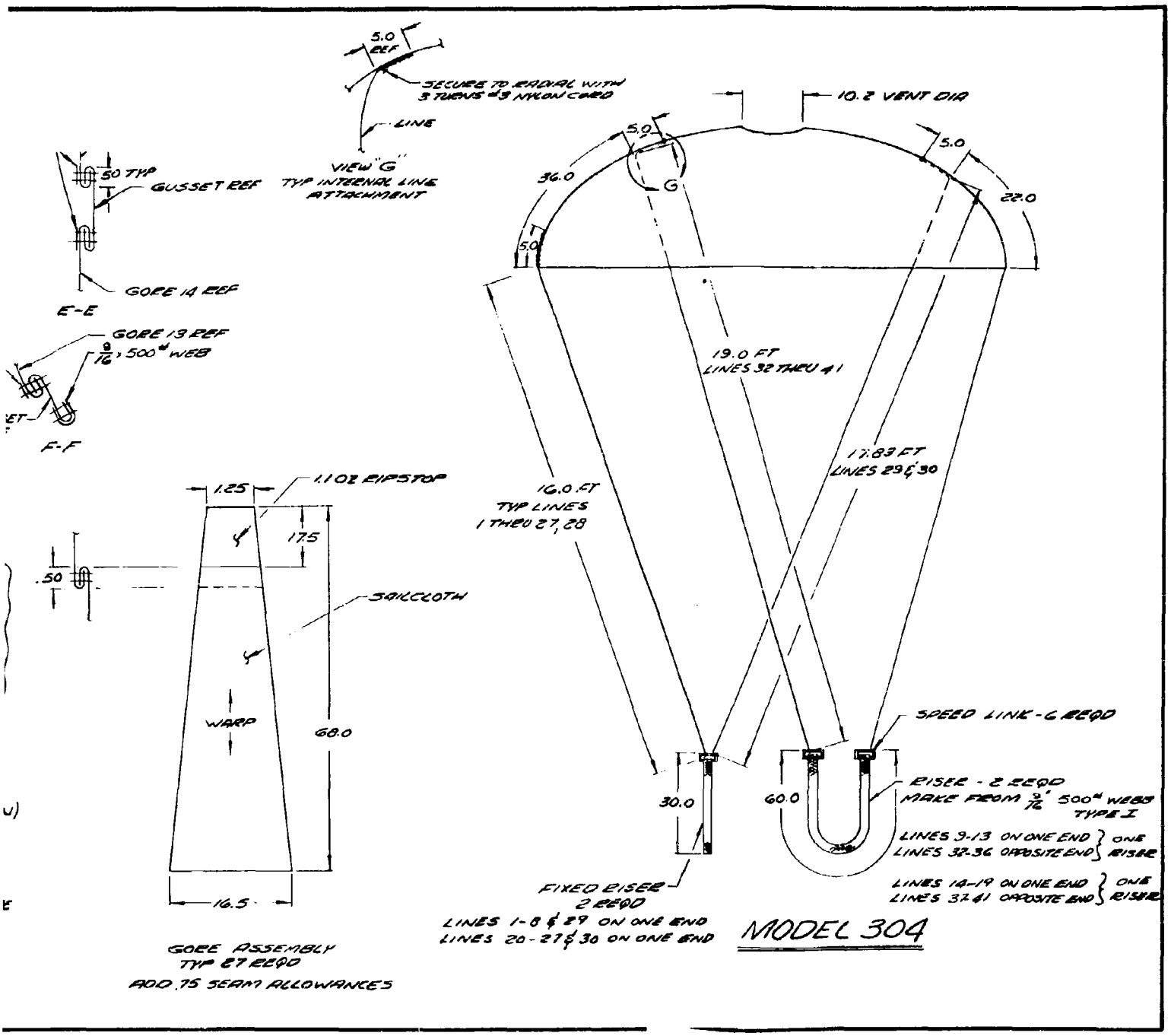

2

Figure 37.
Steerable Parachute - Model 304

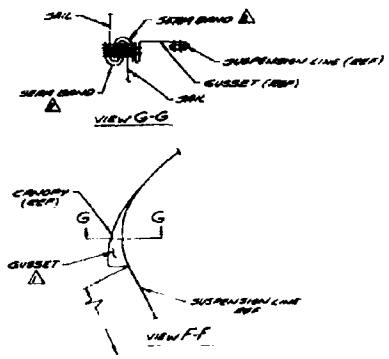

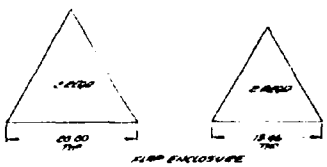

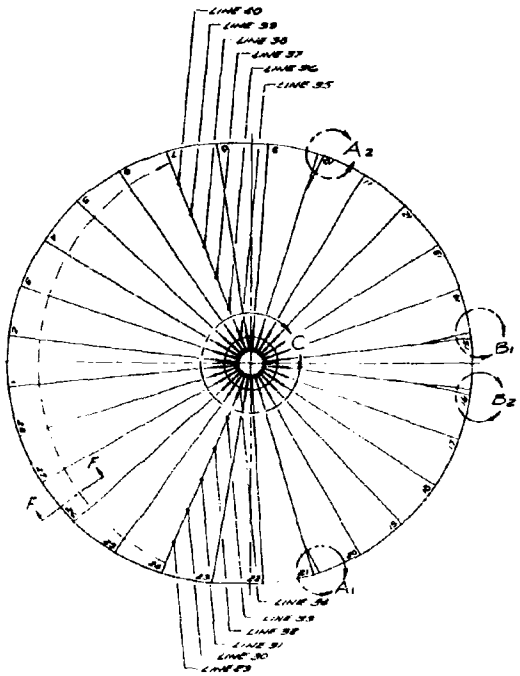

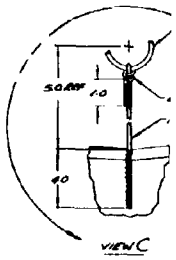

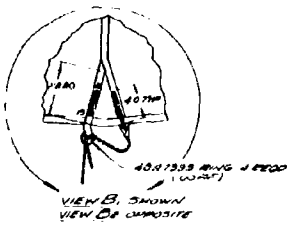

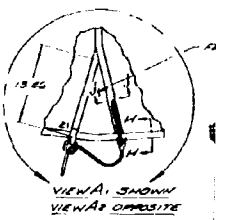

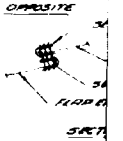

GORE No.	A	B	C	D	E
1	102.00	102.00	27.06	25.33	25.33
2	100.33	102.00	26.86	20.66	23.33
3	98.86	100.33	25.86	15.86	20.66
4	96.0	98.86	24.66	11.33	15.86
5	92.86	96.0	23.86	7.33	11.33
6	91.60	93.86	23.06	3.86	7.33
7	89.33	91.60	22.86	0	3.86
8	89.33	89.33	21.86	0	0
9					
10					
11					
12					
13					
14					
15					
16					
17					
18					
19					
20					
21					
22	89.33	89.33	21.86	0	0
23	91.60	89.33	22.86	3.86	0
24	93.86	91.60	23.06	7.33	3.86
25	96.0	93.86	23.86	11.33	7.33
26	98.86	96.0	24.66	15.86	11.33
27	100.33	98.86	25.86	20.66	15.86
28	102.00	100.33	26.86	25.33	20.66

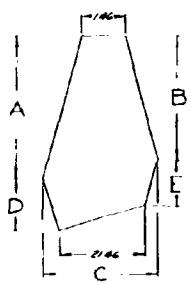

GORE DETAIL

△ TAPE NYLON, MIL-T-50 39C TYPE III 3/4" WIDE 250 LBS

△ TAPE NYLON, MIL-T-50 39C TYPE III 1" WIDE 325 LBS

△ SEE FIG 2.6.7A FOR GUSSET PATTERN

NOTES: UNLESS OTHERWISE SPECIFIED

1

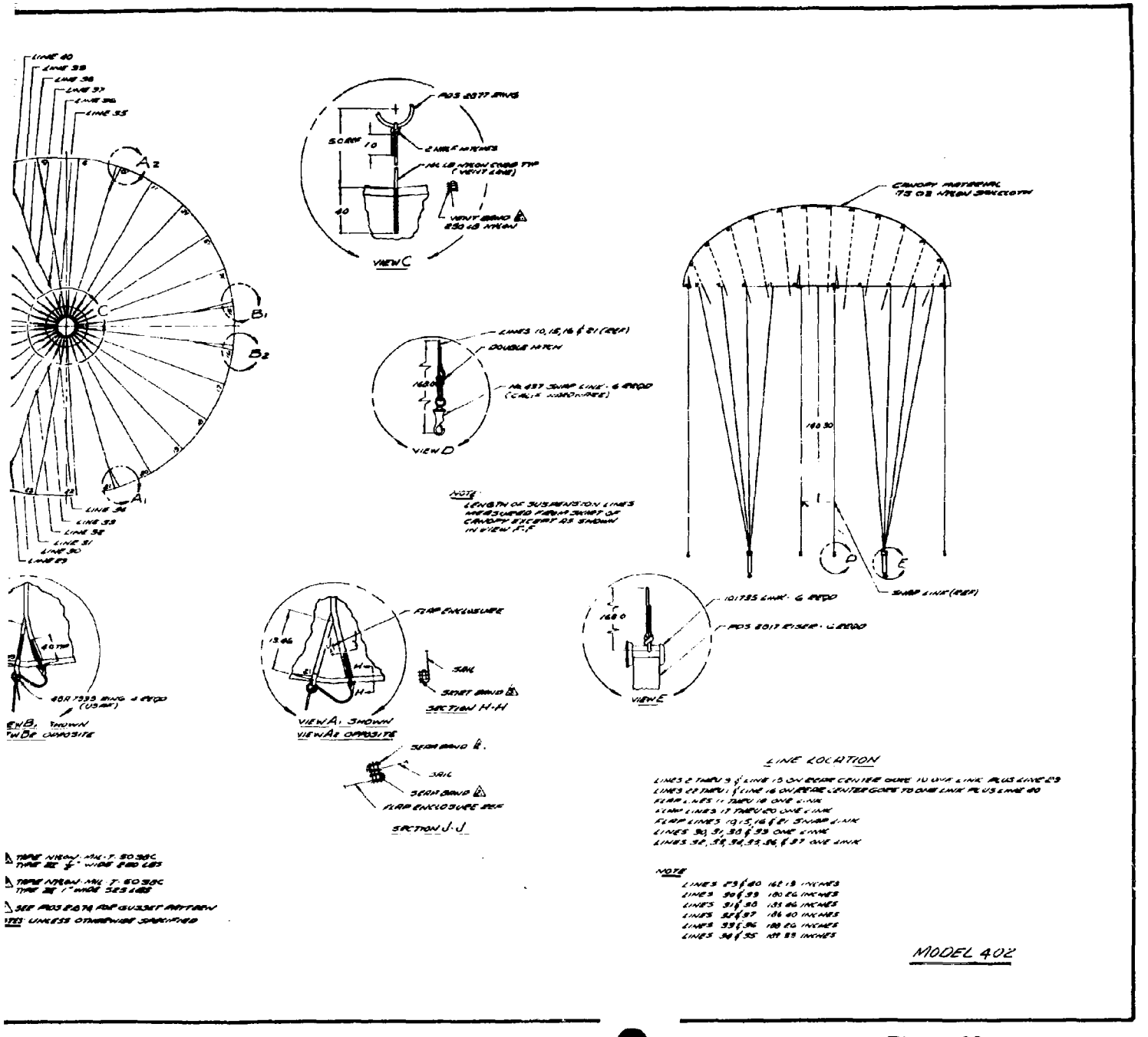

2

Figure 38.

Steerable Parachute - Model 402

APPENDIX II

WIND TUNNEL TEST PROGRAM FOR THE SMALL MODEL TESTS

1.1 TEST PROGRAM OBJECTIVES

The main objectives were to investigate the L/D capability of gliding parachute configurations which had been selected on the basis of the previous data analysis. This program provided the information which resulted in the selection of models to be tested at Ames.

1.2 DATA OBTAINED DURING THE TEST PROGRAM

The following observations were made for each configuration tested, with the model flying free:

(1) L/D as a function of flap setting or rigged angle of attack.

(2) Total resultant force exerted by the model. (This information in conjunction with the L/D of the model can be converted to C_L and C_D.)

(3) Observation and photographs of the canopy condition, that is, leading edge cave in, flutter, etc.

(4) Observation of the stability of the models about the three stability axis, that is, pitch, roll, and yaw.

(5) After the L/D survey was completed, a series of tests were conducted to determine the pitch stability of selected models.

This document contains
blank pages that were
not filmed

1.3 TEST SPECIMENS

Tables 10 and 11 present a list of models tested and the origin of the designs. Figure 32 shows sketches of the models described in Table 10. All models tested were approximately 3-ft D_o and were constructed of .75 oz low porosity nylon sail cloth. Suspension lines were 30-lb, hot-stretched dacron. All Suspension Lines terminated in from 4 to 7 groups which were attached to snaps to facilitate attachment to the wind tunnel model support.

1.4 TEST PLAN

1.4.1 Test Site

Tests were conducted 9 September 1963 to 13 September 1963 and the 2nd and 3rd of October 1963 at the Vertical Wind Tunnel, AFFDL, Wright-Patterson Air Force Base, Dayton, Ohio.

1.4.2 Test Rigging

Figure 39 shows the model attachment apparatus which was installed in the tunnel. The installation of this apparatus was made by AFFDL personnel. All models were pre-rigged before attaching to the model attachment and any change in model rigging required the model to be removed from the wind tunnel.

1.4.3 Instrumentation

The L/D readout system and total force links were furnished by Northrop Ventura as part of the model attachment apparatus. A readout and recording system to read and record the forces measured by the force link was furnished by AFFDL. Photographic coverage, both motion picture and still photographs, was furnished by AFFDL. Placement of cameras and types of shots desired were arranged at the test site. For the second phase of this program, which was the determination of the static

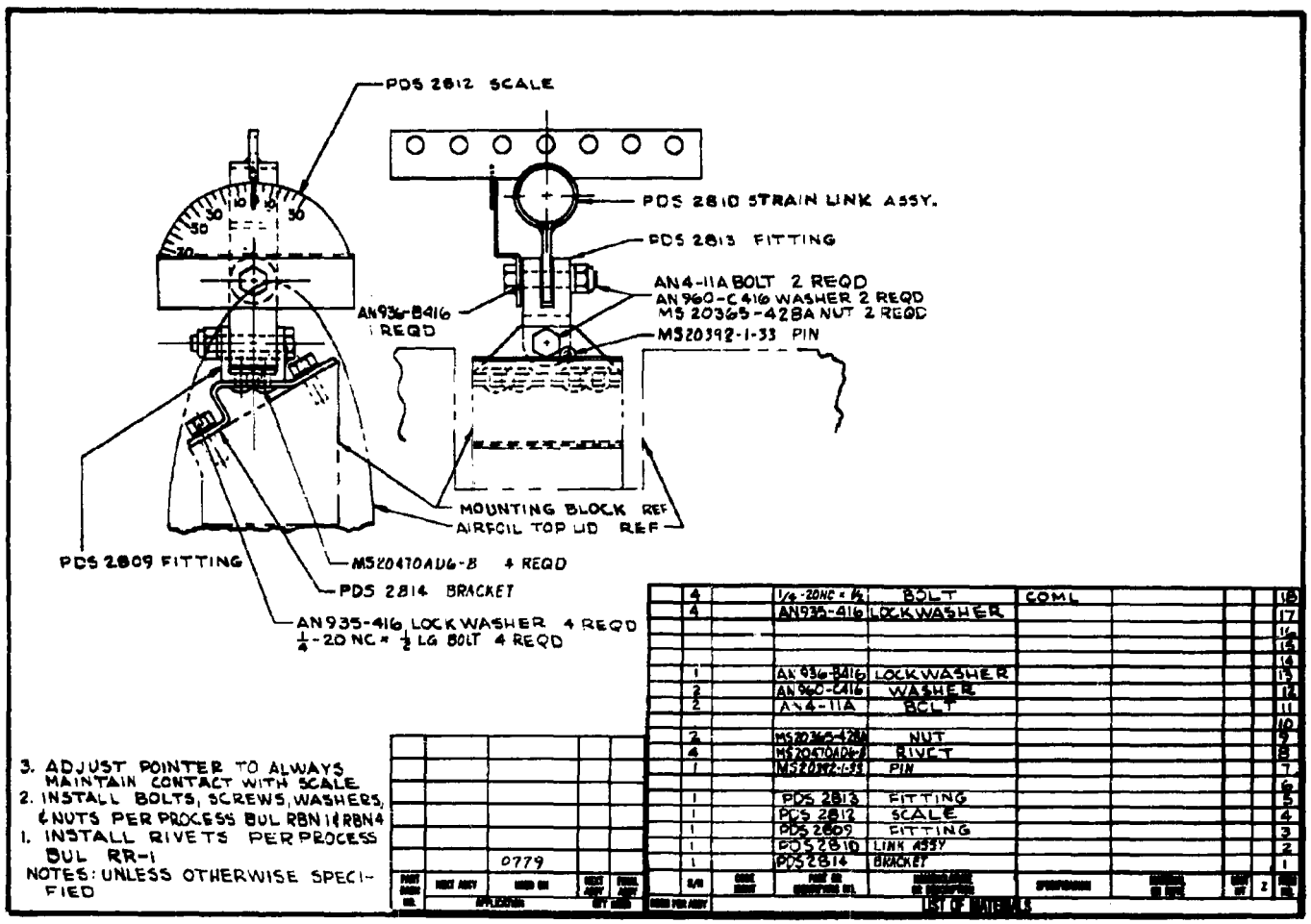

Figure 39. Support Installation - Vertical Wind Tunnel

pitch stability, AFFDL provided a sting balance and the necessary readout and recording instrumentation to obtain pitching moment. The tests were conducted by AFFDL personnel.

1.4.4 Test Procedure

Prior to initiating tests both the L/D readout system and the force link were calibrated. Calibration of the L/D readout system consisted of positioning the protractor so that when a force parallel to the centerline of the tunnel was applied to the parachute attachment bar, the pointer on this bar indicated zero.

Calibration of the force link consisted of loading the force link and recording the output with a strain gage readout and recording system.

During the test run, the glide angle was read visually and also the protractor was photographed to provide an accurate angle measurement. Changes in flap settings were made by providing different length changeable links between the attachment clips and the attachment bar. Resultant force was measured by means of the force link and the attendant recording apparatus.

1.5 DATA SUMMARY

Table 12 and Figures 40 and 41 give a summary of the data obtained from the two series of tests conducted with the models at Wright Field. For the models which do not list values of L/D or force coefficients, data was not available because of instrumentation failure or the model was too unstable to get meaningful data.

The data shown in Figure 40 are summary plots of L/D vs flap extension. As can be seen by comparing the two sets of curves the three lobe type of configuration (such as Model 217) achieved consistently higher values of L/D as compared to the

TABLE 12
SMALL MODEL WIND TUN

MODEL NO.	RIGGING Settings are in inches RC is rear center gore F indicates flaps In indicates riser pulled in Out indicates riser extended	L_D	C_L	C_D	C_M	REMARKS
201	As rigged	1.28	.829	.647		Unstable in roll
202	As rigged	1.4	.512	.319		Moderate instability in yaw
	RC in 1.25 F out 1.75	1.33	.452	.341		Fair stability all axis
	RC in 1.25 F out .75	1.38	.514	.369		Fair yaw stability Good pitch stability
	RC in 1.25 F out 0	1.33	.427	.322		Good stability all axis
203	Front risers out 1.75 F out 2.5	1.21	- -	- -		Poor stability all axis
	FR out 1.75 F out 3.00	1.28	- -	- -		Poor stability all axis
	FR out 3.5 F out 5.9	1.25	- -	- -		Poor stability all axis
	FR out 5.25 F out 5.9	1.28	- -	- -		Unstable in pitch
	FR out 5.25 F out 7.1	1.18	- -	- -		Poor stability all axis
	FR out 0 F out 3.05	1.21	- -	- -		Unstable in roll Fair pitch stability
204	F out 2.50 F out 3.05	1.19 1.28	.401 .454	.252 .286		Poor stability Poor stability
	F out 3.6	1.19	.773	.714		Poor stability
	F out 4.15	1.32	- -	- -		Very unstable, all axis
205	F out 1.75	1.15	- -	- -		Fair stability
	F out 2.15	1.19	- -	- -		Poor stability
	RC in 2.25 F out 2.6	1.15 *(Mod. strained)	- -	- -		Violent pitch instability
206						Violent instability for all rigging positions tried
207	As rigged	1.28	.431	.293		Fair stability all axis All other flap settings very instable
208	As rigged F out 1.75	1.34 *1.35				Yaws about 60 degrees Unstable
209	As rigged	1.31	.498	.441		Very good stability
	F out 1.125	1.37	.541	.349		Very good stability
	F out 1.75	1.42	.521	.305		Good stability
210	As rigged	1.19	.425	.356		Fair stability
	Front riser out 1.75 F out 2.5	1.19	.461	.387		Fair stability
	Front riser out 1.75 F out 3.0	1.15	.337	.293		No data
	Front riser out 1.75 F out 4.15	*1.04	.357	.345		Unstable in yaw
	Front riser out 1.75	* .84	.349	.416		Violent instability, unless restrained
211	Front riser out 1.75 RC in 6.4 F out 4.7	1.21	.513	.423		Fair stability

MODEL NO.	RIGGING Settings are in inches RC is rear center gore F indicates flaps In indicates riser pulled in Out indicates riser extended	L_D	C_L	C
	Front riser out 1.75 RC in 6.4 F out 5.9	1.19	.461	.3
	Front riser out 1.75 RC in 6.4 F out 7.1	1.26	.445	.4
212	Front and rear flaps out 3.6	*1.1		
	Front flap out 4.7 Rear flaps in .55	*1.0		
	Front flaps out 4.7			
	Rear flaps out 4.5			
	Front flaps out 4.7			
213	As rigged F out 1.75	*.885		
	F out 3.6 RC in 1.125			
	F out 3.6	.292		
	F out 3.6 RC in .625	.811		
214	No exact rigging dimensions for this model	1.05		
215	F out 2.5	1.24	.488	.3
	F out 3.7	*1.4	.477	.4
	RC in 6 F out 5.9 Front risers out 1.75	1.3	.511	.4
	RC in 6 F out 7.1 Front risers out 1.75	1.43	.473	.4
	RC in 6 F out 4.7	1.35	.428	.4
	RC in 6 F out 5.9	1.38	.509	.4
	RC in 6 F out 7.1	*1.43	.488	.4
216	As rigged	1.46	.533	.4
	F out 1.25	1.53	.597	.4
	F out 1.75	1.50	.552	.4
	F out 2.25	1.57	.477	.4
	F out 3.0	1.53		
	F out 3.0 RC in 2.5	1.48		
217	F out 0	1.54	.591	.4
	F out 1.25	1.60	.511	.4
	F out 1.75	1.59	.502	.4
	F out 3.25	1.67		
	F out 3.75	1.83		

1

TABLE 12
SMALL MODEL WIND TUNNEL RESULTS

EL.	RIGGING Settings are in inches RC is rear center gore F indicates flaps In indicates riser pulled in Out indicates riser extended	L_D	C_L	C_D	C_M	REMARKS
	Front riser out 1.75 RC in 6.4 F out 5.9	1.19	.461	.387		Good stability
	Front riser out 1.75 RC in 6.4 F out 7.1	1.26	.440	.355		Yaws to about 45 degrees
	Front and rear flaps out 3.6	*1.1				Slightly unstable
	Front flap out 4.7 Rear flaps in .55	*1.0				Slightly unstable
	Front flaps out 4.7					Violent instability of 180 degrees pitch and yaw
	Rear flaps out 4.5					
	Front flaps out 4.7					Oscillates about ± 30 degrees pitch and yaw. This is about the setting for zero glide
	As rigged F out 1.75	*.885				Coned about 40 degrees Fair stability
	F out 3.6 RC in 1.125					Coned about 20 degrees
	F out 3.6	.765				Good stability
	F out 3.6 RC in .625	.811				Good stability
	No exact rigging dimensions for this model	1.65				Several runs made with this model with different line settings.
	F out 2.5	1.24	.488	.395		Fair stability
	F out 3.6	*1.3	.477	.466		Instable
	RC in 6 F out 5.9 Front risers out 1.75	1.4	.511	.395		Excellent stability
	RC in 6 F out 7.1 Front risers out 1.75	1.43	.521	.429		Stable
	RC in 6 F out 4.7	1.35	.468	.347		Stable
	RC in 6 F out 5.9	1.38	.469	.341		Stable
	RC in 6 F out 7.1	*1.40	.489	.275		Unstable
	As rigged	1.68	.609	.411		Very stable
	F out 1.25	1.60	.592	.374		Very stable
	F out 1.75	1.60	.552	.345		Stable, slight flutter of leading edge of rear lobes
	F out 2.25	1.57	.477	.304		Same as F out 1.75
	F out 3.0	1.53				Bad flutter of rear lobes, slight pitch instability
	F out 3.0 RC in 2.5	1.48				Trailing edge flutter
	F out 0	1.54	.591	.384		
	F out 1.25	1.60	.611	.319		Excellent stability and canopy inflation
	F out 1.75	1.60	.602	.314		
	F out 3.25	1.67				
	F out 3.75	1.63				Pitch instability

MODEL NO.	RIGGING Settings are in inches RC is rear center gore F indicates flaps In indicates riser pulled in Out indicates riser extended	L_D	C_L	C_D	C_M	REMARKS
	F out 3.25	1.73				Fairing over upper rear portion of canopy, and inside web partly cut away
	F out 3.25	1.73				Unmodified configuration but velocity reduced to 30 to 35 fps
218	30-inch line lengths except as noted for this model. F out 0 Front group of internal lines 40 Rear group of internal lines 40.75	*1.26				Unstable in yaw Good inflation
	F out 1.25 Front group of internal lines 40.00 Rear group of internal lines 42.5	*1.19				Very unstable in yaw
	F out 1.25 Lines (14 & 16) 37.5 Lines (41 & 43) 39.0 Line (44) 38.5 All other lines same as preceding run.	*1.38	.590	.428		Slight yaw instability Good inflation
	F out 1.75 All other lines same as F out 1.25	*1.4	.520	.414		Same as F out 1.25
	F out 2.75 All other lines same as F out 1.25	*1.19				Very unstable
219	F out 0	*1.0				Unstable all axis. Longitudinal rib flapping around loose. Also tried several other flap settings which were all unstable.
	F out 1.25	*1.19				Roll and yaw instability. Most of longitudinal rib was cut away.
	F out 1.25 RC in 6.5	*1.19	.438	.368		Good inflation, needs to be restrained.
	F out 1.75 RC in 6.5	*1.23	.419	.339		Same as F out 1.75
	F out 2.75 RC in 6.5	*1.33				Violently unstable unless restrained
C-1	F out 3.6	*1.58				Unstable
C-2	F out 1.75	.93	.434	.470		Very good stability and canopy inflation
	F out 1.5	1.11	.457	.395		Stable
	F out 3.6	1.19	.432	.363		Stable
	F out 4.7	*1.33	.412	.311	S	Stable in pitch has tendency to yaw
	F out 3.6	*1.58				Leading edge of front chute collapsed due to insufficient pressure in tubes

*Indicates Model Restrained

2

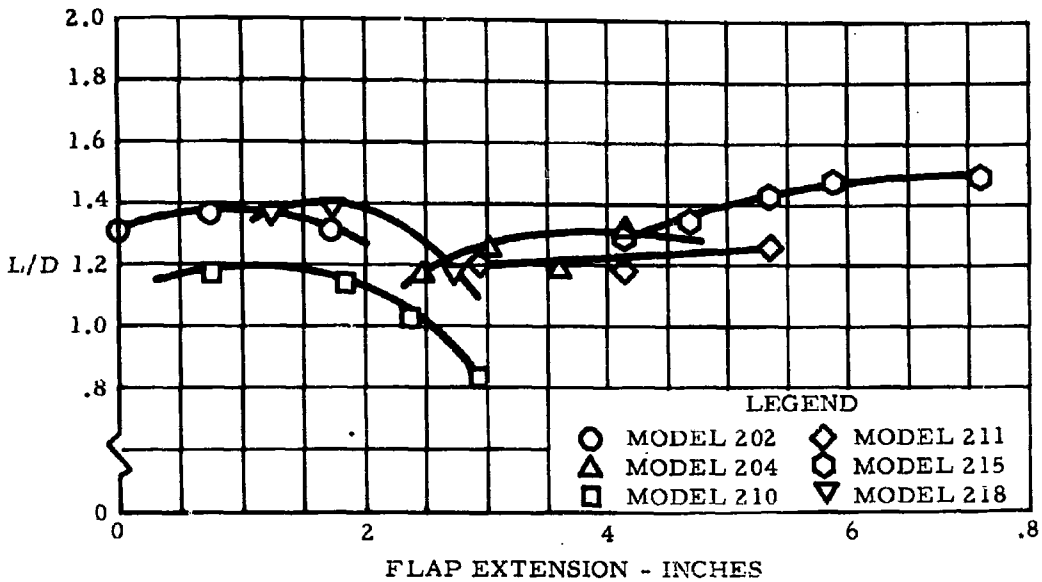

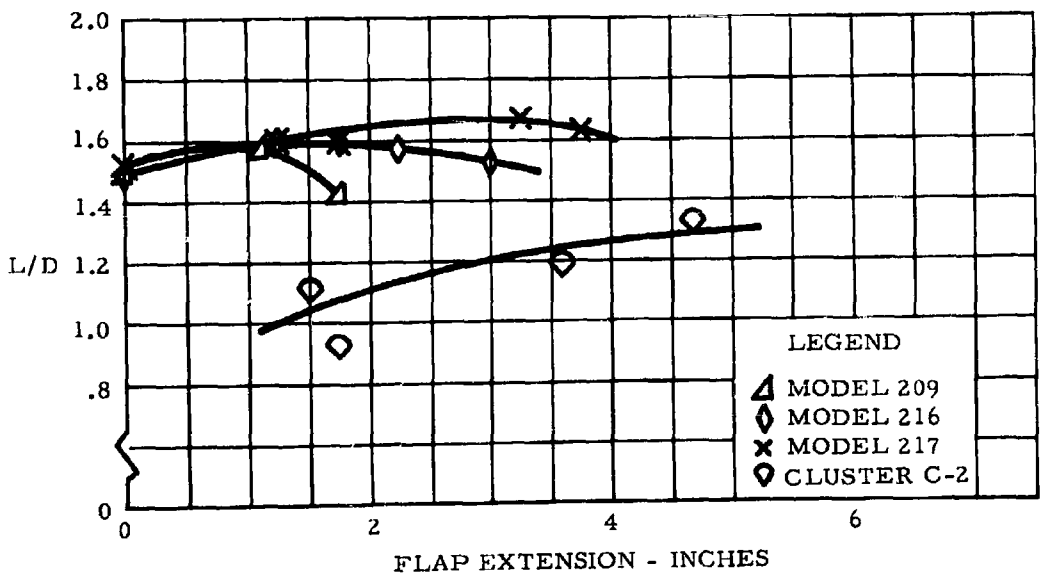

Figure 40. L/D Vs Flap Extension

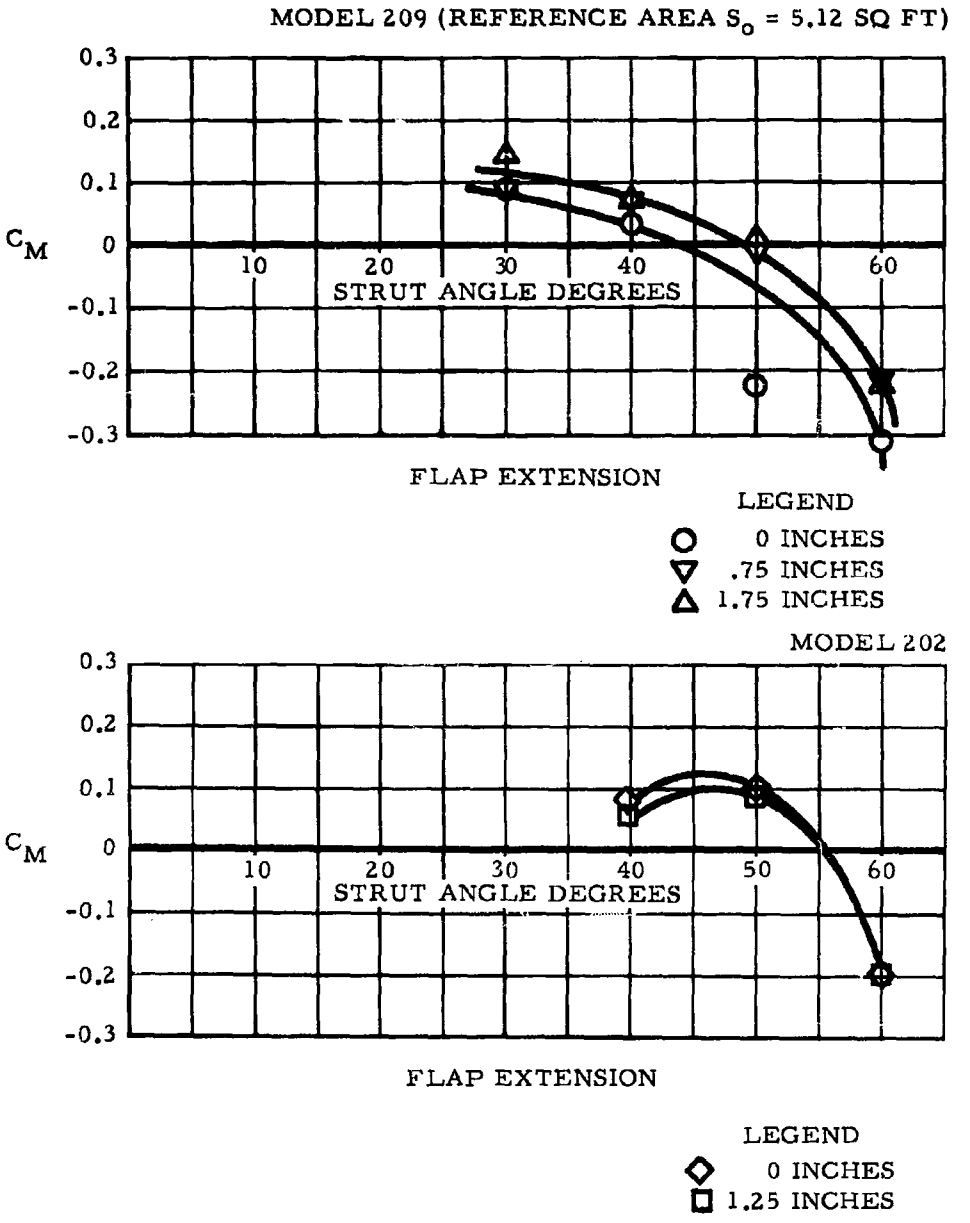

Figure 41. C_M Vs Strut Angle

performance of the single canopies (such as Model 204). This was true even in the case of Model 215 which had inflated tubes to stiffen the leading edge of the canopy.

Figure 41 gives the results of tests to determine stability in pitch of Models 209 and 202. It should be noted that C_M is plotted vs strut angle. In order to measure pitching moment, the model is attached at the crown of the canopy and the confluence point of the suspension lines to a strut. The moment is measured at the base of the strut as the strut is deflected in pitch, forcing the model to fly at an attitude other than one which gives zero moment. Using this measured moment, C_M is computed as a function of strut angle. C_M is not obtained as a function of absolute glide angle because the exact location of the center of pressure of the parachute is not known. Therefore, it is necessary to refer to Figure 40 to determine the glide angle corresponding to the flap settings shown on Figure 41. The major result shown by Figure 41 is that Model 209 (which is the basic three-lobe design) is stable over the flap travel range.

1.5.1 First Series of Small Model Tests

As shown in Table 12, the highest L/D obtained with a non-stiffened model was 1.57. Model 209 which gave this result is one of a series of three models designed to duplicate the design features of a three chute cluster in a single chute. This model also was the most stable and had the best canopy inflation. Of the other non-stiffened models, Model 202 and Model 203 had L/D max values of 1.4 and 1.375 respectively.

Model 204, which is a scale model of the design which had an L/D max of 1.54 in the Aerosail test program at Ames, had an L/D max of 1.28 and was moderately unstable. Model 211, which is a variation of Model 204 with a modified leading edge, achieved an L/D max of 1.26 and when the rear center gore was pulled in was quite stable.

Two models which had canopy stiffening were tested. These were Models 214 and 215. Model 214 was a circular flat chute with two booms arranged in a V as stiffeners. It attained an L/D max of 1.65 and appeared capable of doing better if the rigging could be optimized. Model 215 has inflated tubes in the forward portion of the canopy. This model held its shape quite well, was very stable, and attained an L/D max of 1.43.

Three cluster configurations also were tested and the results of these tests are given in Table 12.

1.5.2 Second Series of Small Model Tests

Based on the results obtained from the small models tested at Wright Field during the first test program, four additional models were designed and tested. Of the four models tested during this phase of the test program, Model 217 gave the best results. It achieved an L/D value of 1.67 and had excellent stability about all three stability axis. Model 216, which was a modified version of Model 209, also gave excellent results. Model 218 was an attempt to get a favorable gliding configuration by distorting the canopy to the desired shape by pulling lines attached to the interior of the canopy. With the line arrangement used an L/D of about 1.4 was obtained.

From observations of Model 218 in the wind tunnel, it was felt that the line arrangement used on this model was far from optimum. It was thought that this design would be simpler to construct and deploy for a full scale canopy and that this type of design warranted further investigation.

Model 219 was also a design with which an attempt was made to simplify the canopy configuration. Internal webs were used to get a forward pocket and to support the rear portion of the canopy. This model had poor performance characteristics, both L/D capability and stability.

1.6 MAJOR TEST RESULTS

The following comments summarize the major results of the small model tests.

(1) The highest value of L/D (1.67 at 47 fps and 1.73 at about 30 fps) was obtained with Model 217. This model also displayed the best stability of any of the designs tested.

(2) Lack of stability, especially about the yaw axis was a characteristic of all the designs tested with the exception of Models 209, 215, 216, and 217 and to a lesser degree, Models 201 and 202.

(3) The rolled under leading edge, such as used on Model 217, resulted in an inflated leading edge which was stable at values of L/D of 1.73. The leading edge on Model 217 was stable to the extent that the canopy can be pulled over and forced to fly at lower angles of attack without collapsing.

(4) Trailing edge flutter which was noticed on models which had flaps with open sides was not evident on Models 216 and 217. These models had seals from the edge of the flaps to the canopy.

(5) The three lobe designs such as Models 209, 216, and 217 showed very good stability about all axis. These models approximate wings with sweepback and an aspect ratio of about 1.9.

(6) Model 217 was flown with tufts on the upper surface of the canopy. The tufts showed attached flow over the forward portion of the canopy. This is the type of flow pattern shown by wings.

(7) An exact scale model of a parachute which attained an L/D of 1.54 in the Ames Aerosail tests (Model 204) achieved an L/D of 1.28 in the Wright Field Tests.

(8) The tunnel velocity inadvertently used for these tests was 47 fps rather than the desired 30 fps. Previous test results have shown a decrease in L/D with increasing velocity. Therefore, it can be assumed that the L/D values obtained during this test program are lower than can be obtained at 30 fps which has been the maximum design velocity for this program. One data point with a velocity in the order of 30 to 35 fps was obtained with Model 217 and gave an L/D of 1.73. Also, a data point was taken at V = 94 fps and gave an L/D of about 1.55.

APPENDIX III

TRUCK TOW TESTS

1.1 GENERAL DISCUSSION

During the tow truck test program, conducted January 24, 27th, and 28th, 1964, Models 301A, 302, 303, 304, 402, and 101 were tested. The data obtained during the three days of testing consisted of indicated glide angle and control riser forces. The glide angle was obtained by visually reading the indicated angle from a protractor and the control riser forces were measured with strain gage force links and recorded by a light beam oscillograph. A complete description of the tow test rig, instrumentation and test procedures is given in Paragraph 1.2.

The data obtained during the test program is presented in Figures 42 to 63. The L/D data shown on these plots exhibits a good deal of scatter. There are two reasons for this scatter: (1) due to surface irregularities of the runway used, the L/D indicator oscillated ± 2 to 3 degrees which made it necessary to visually estimate the extent of the oscillation, therefore, the L/D value is dependent on the accuracy of this visual estimation (2) the airspeed indicator could not be read visually during the test runs; this made it necessary to use the truck speedometer to determine ground speed which was corrected by estimating wind velocity. This, in turn, led to a variation in dynamic pressure, which affected the consistency of the L/D performance of the parachute being tested.

This document contains
blank pages that were
not filmed

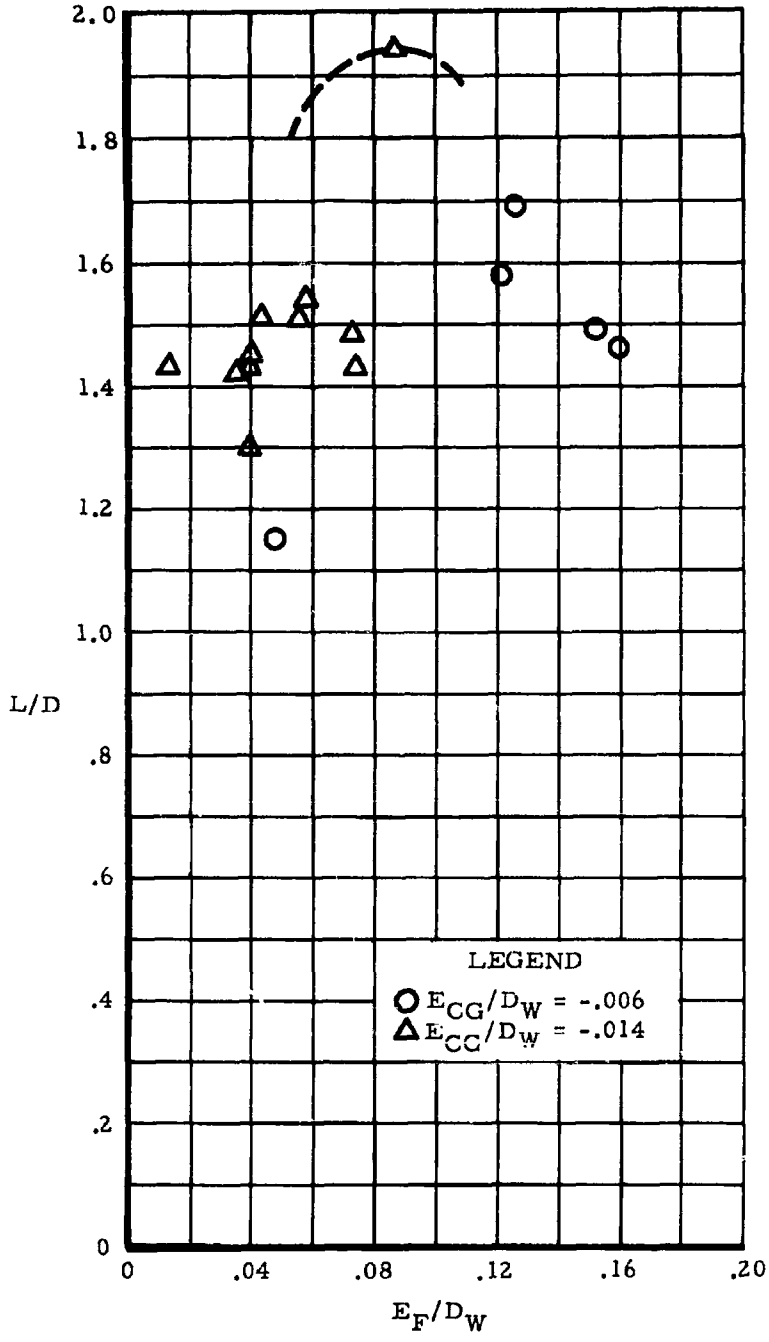

Figure 42. L/D Vs Flap Extension, Model 301A

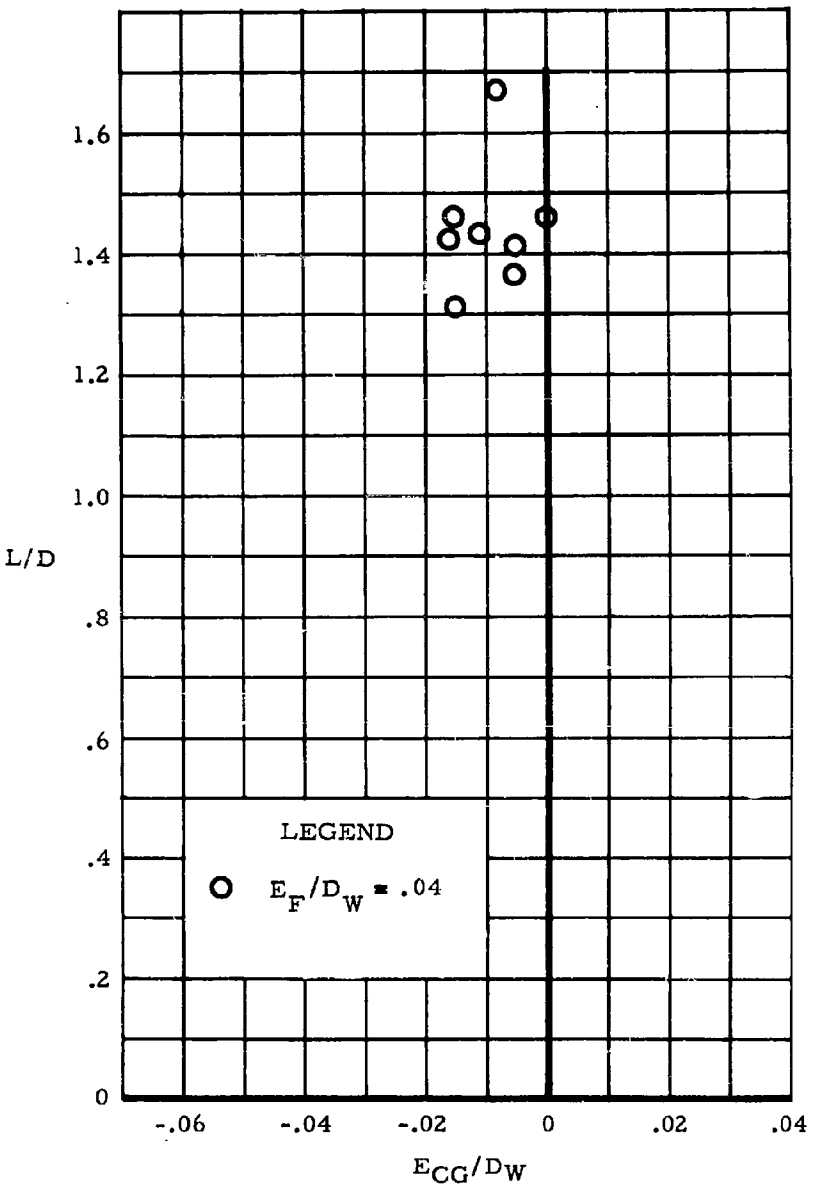

Figure 43. L/D vs Center Group Extension, Model 301A

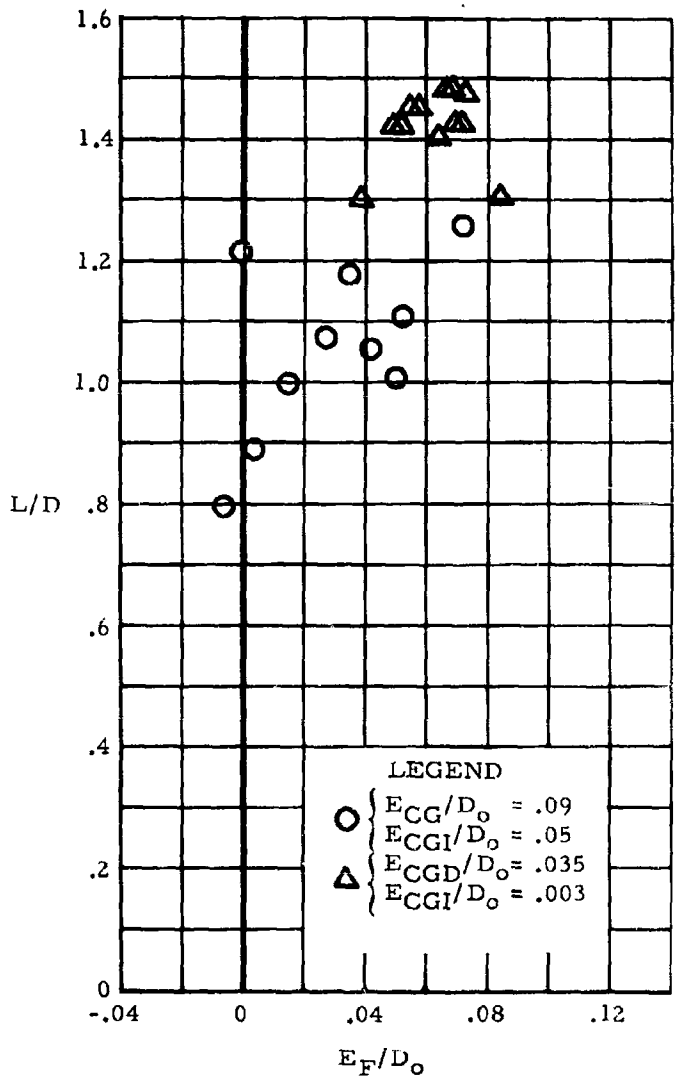

Figure 44. L/D Vs Flap Extension, Model 302

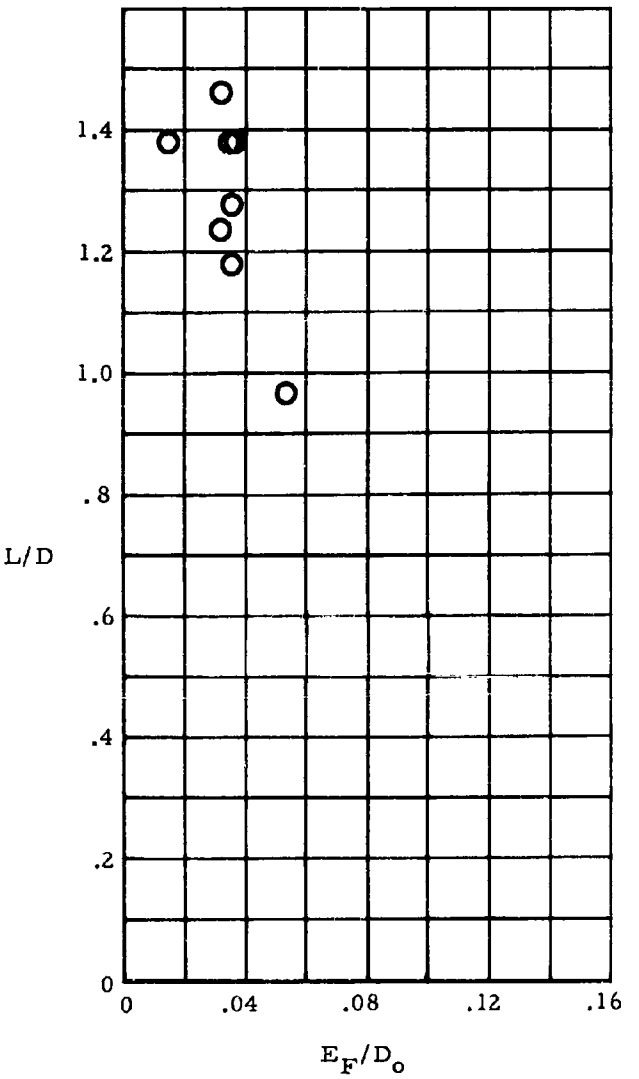

Figure 45. L/D Vs Flap Extension, Model 303

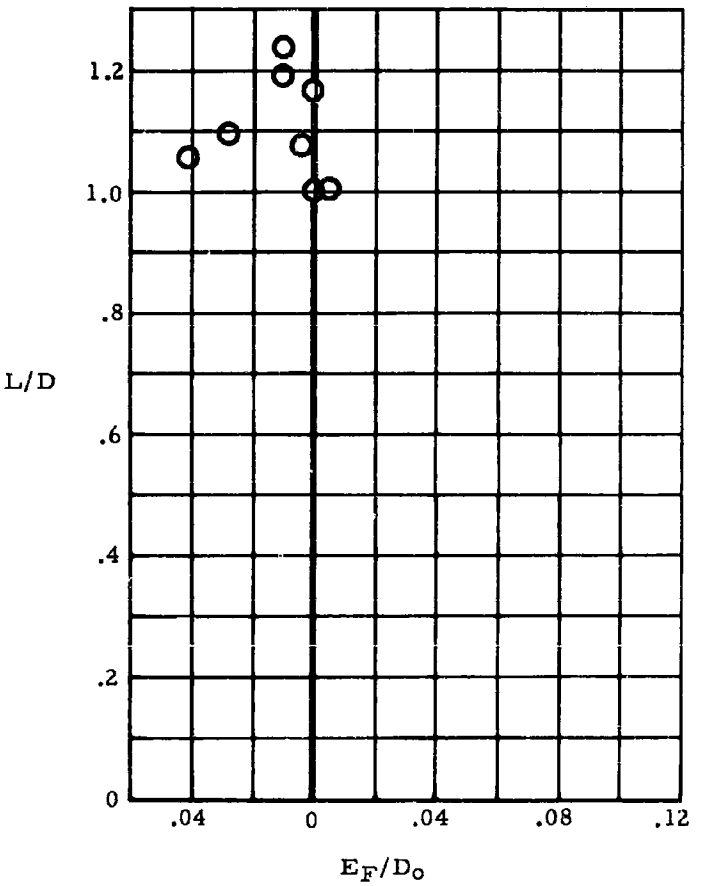

Figure 46. $L/_D$ Vs Flap Extension, Model 304

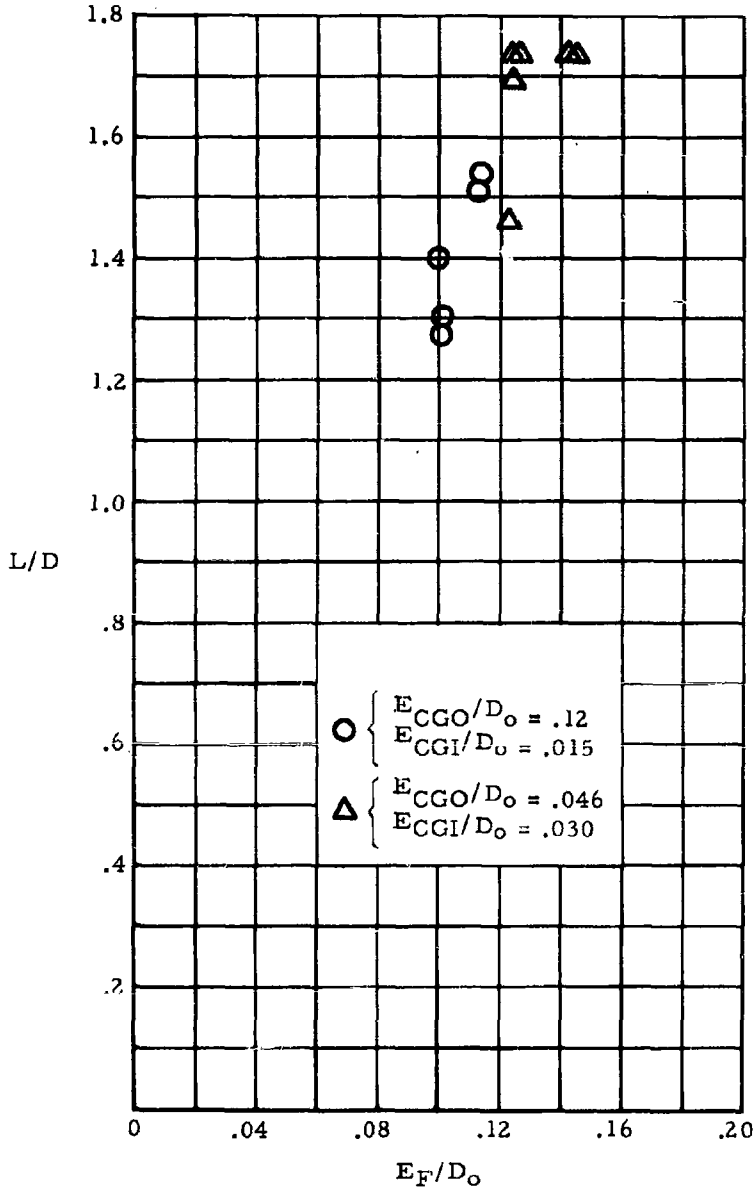

Figure 47. L/D Vs. Flap Extension, Model 402

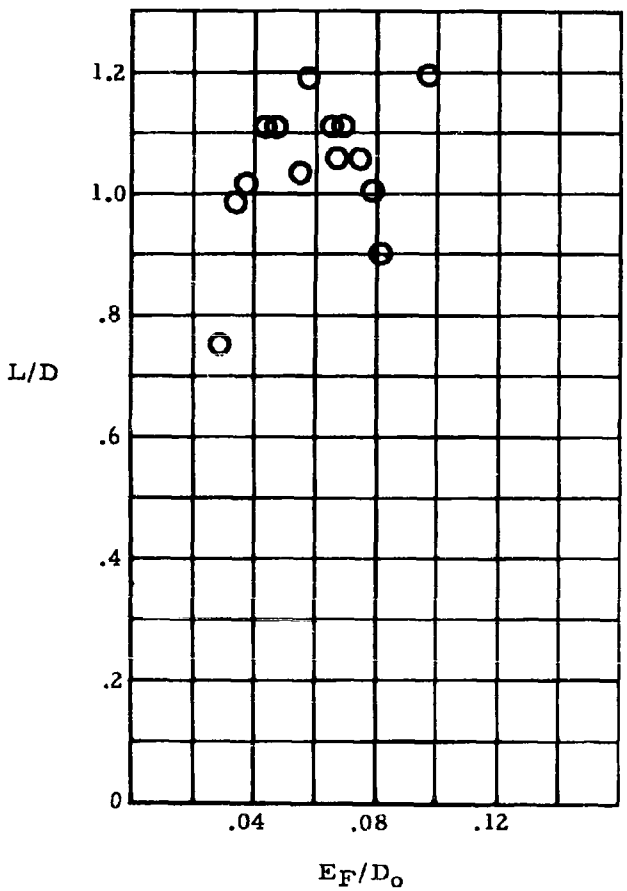

Figure 48. L/D Vs. Flap Extension, Model 101

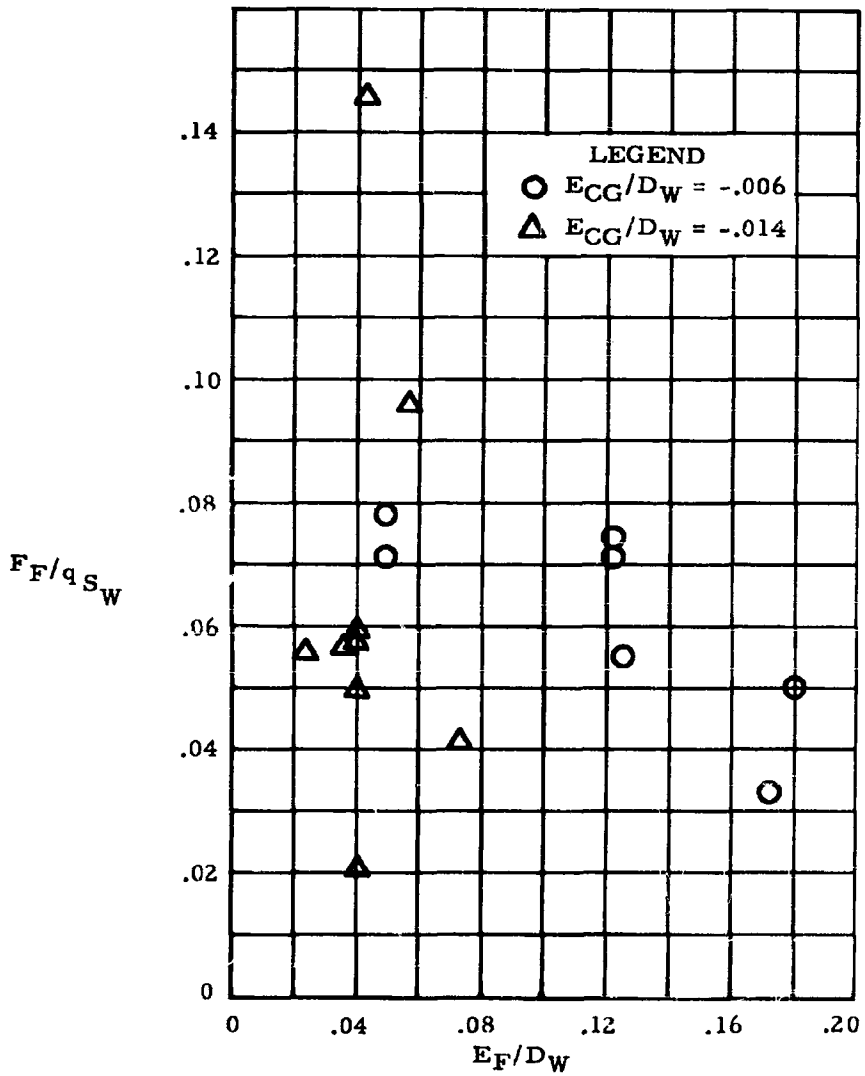

Note: This data is for one flap only

Figure 49. Force Coefficient Vs. Flap Extension, Model 301A

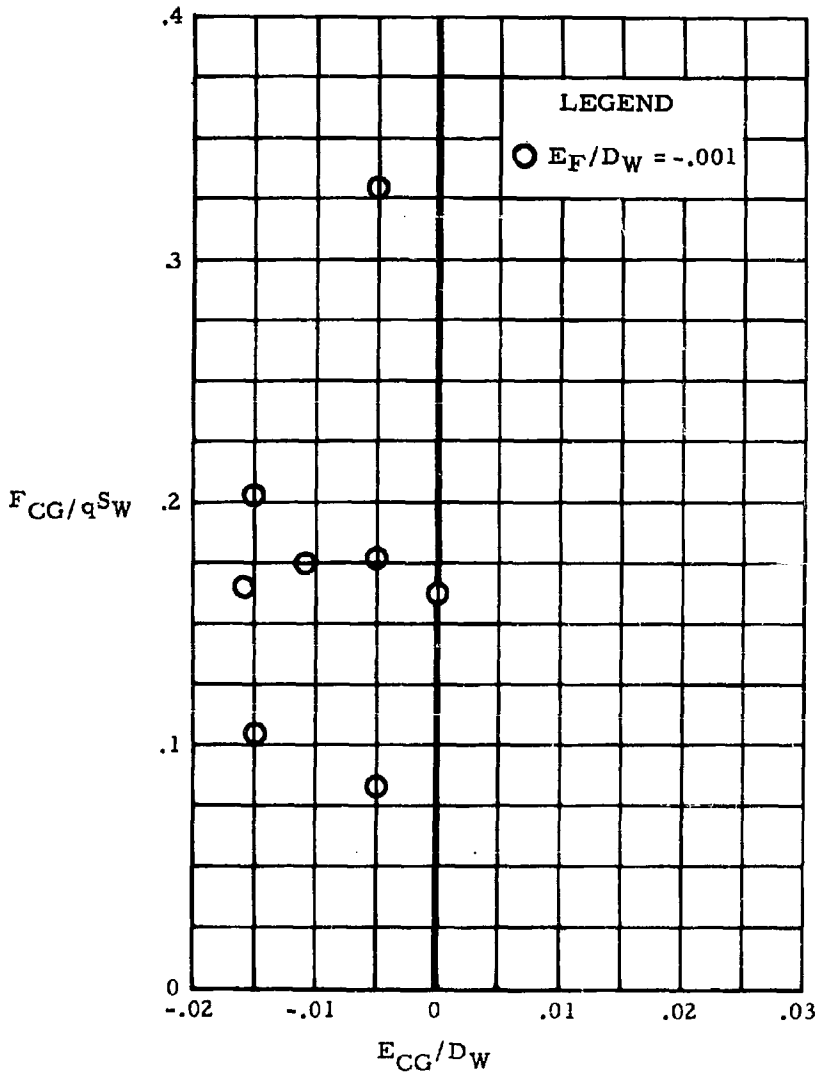

Figure 50. Force Coefficient Vs Riser Extension, Model 301A

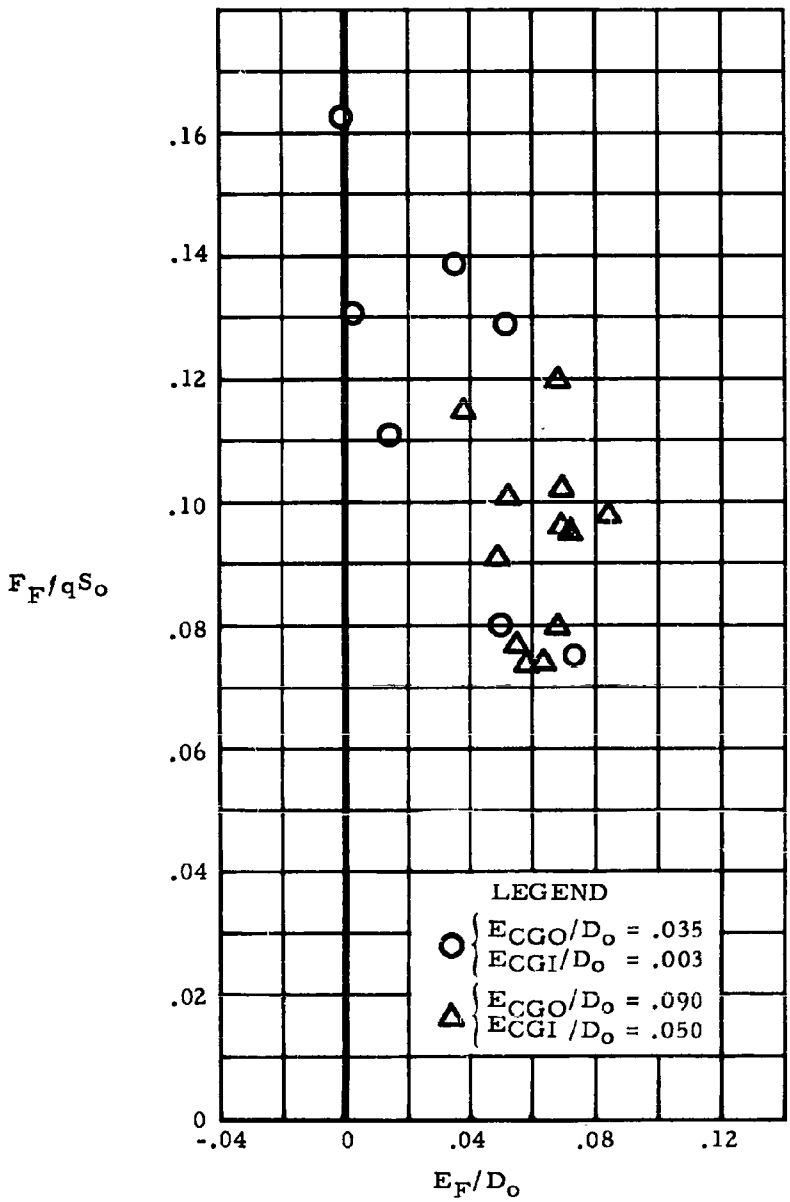

Note: This data is for one flap only

Figure 51. Force Coefficient Vs Flap Extension, Model 302

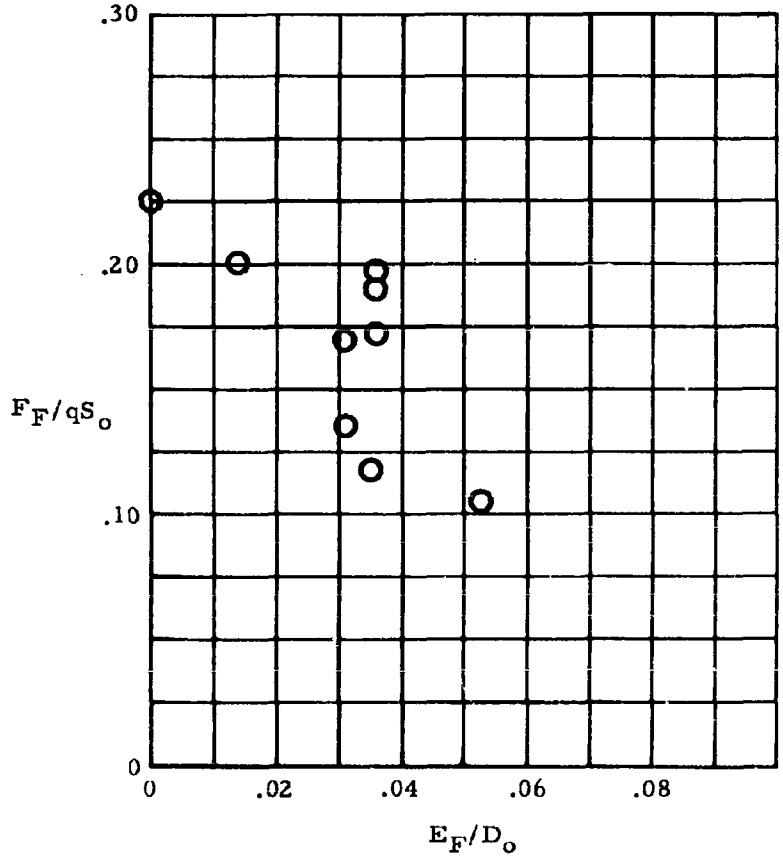

Note: This data is for one flap only

Figure 52. Force Coefficient Vs Flap Extension, Model 303

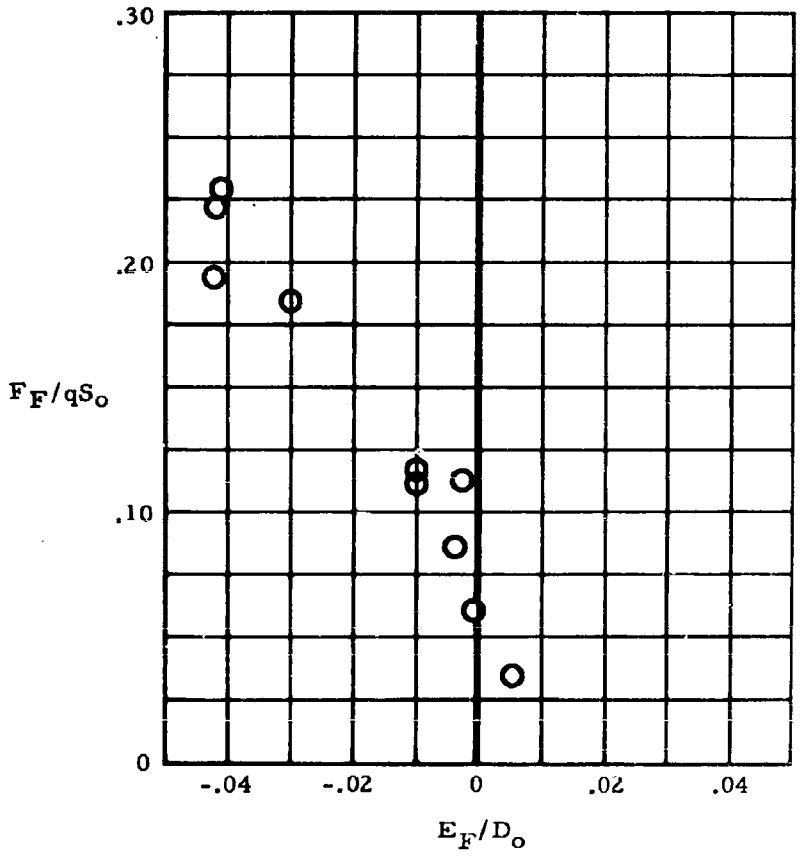

Note: This data is for one flap only

Figure 53. Force Coefficient Vs Flap Extension, Model 304

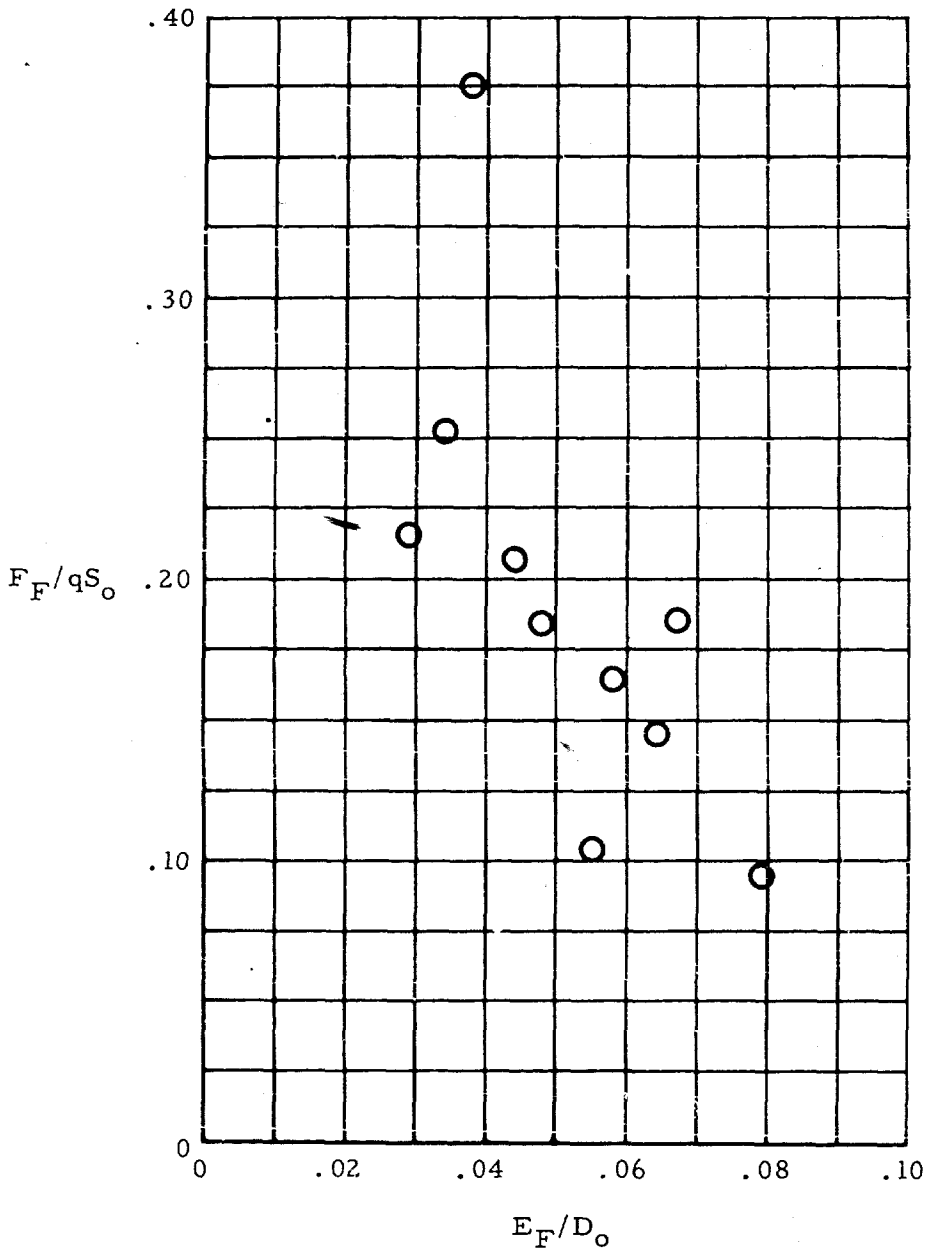

Note: This data is for one flap only

Figure 55. Force Coefficient Vs Flap Extension, Model 101

This Document Contains Missing
Page/s That Are Unavailable In
The Original Document

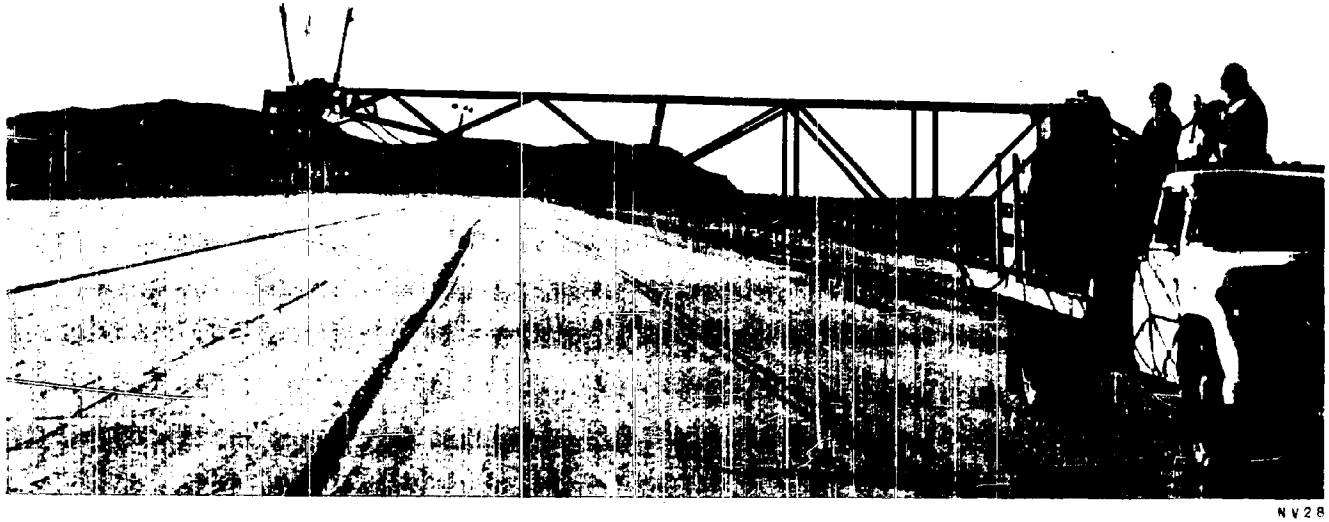

Figure 56. Model 301A

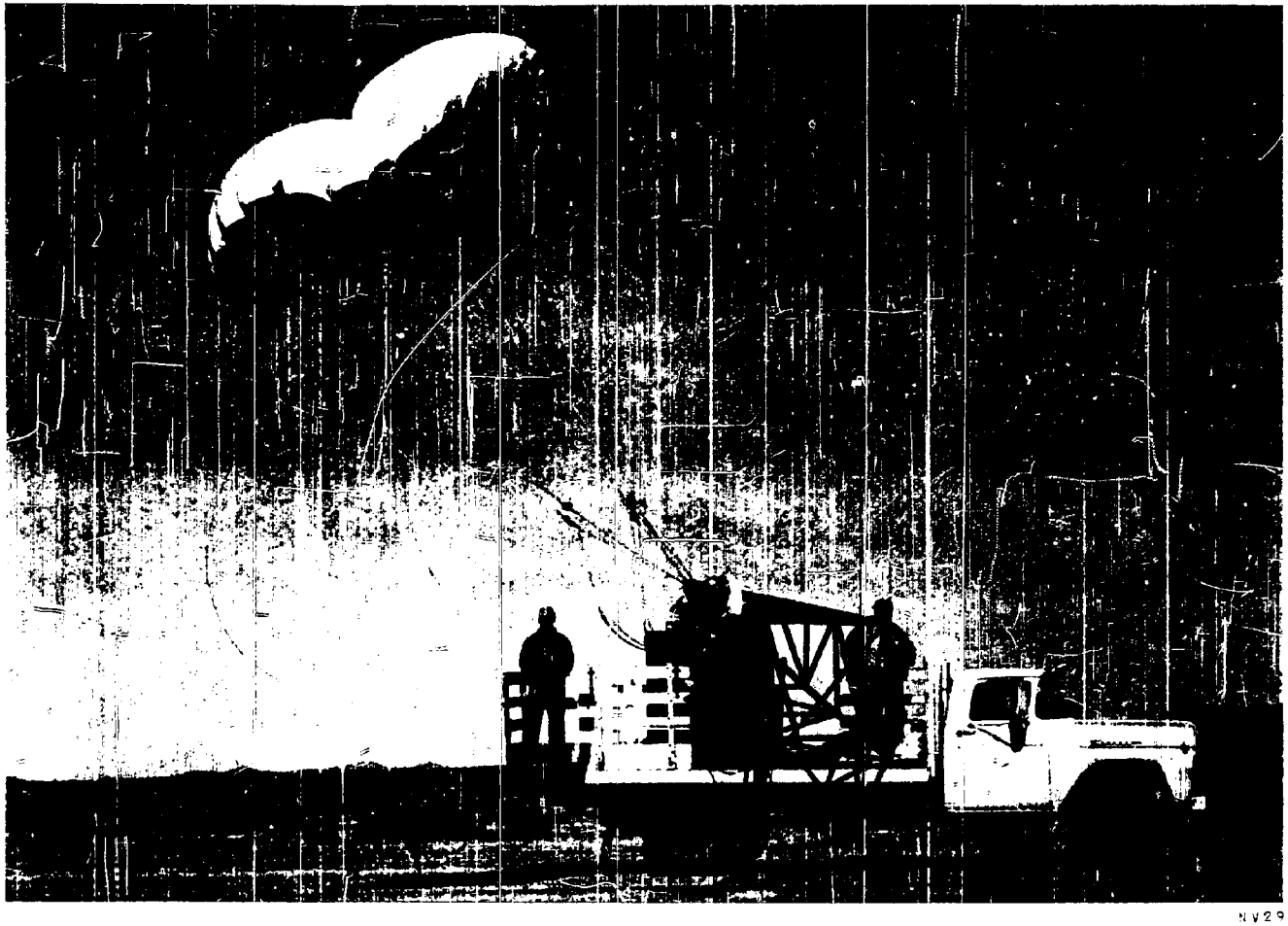

NV29

Figure 57. Model 302

Figure 58. Model 303

Figure 59. Model 402

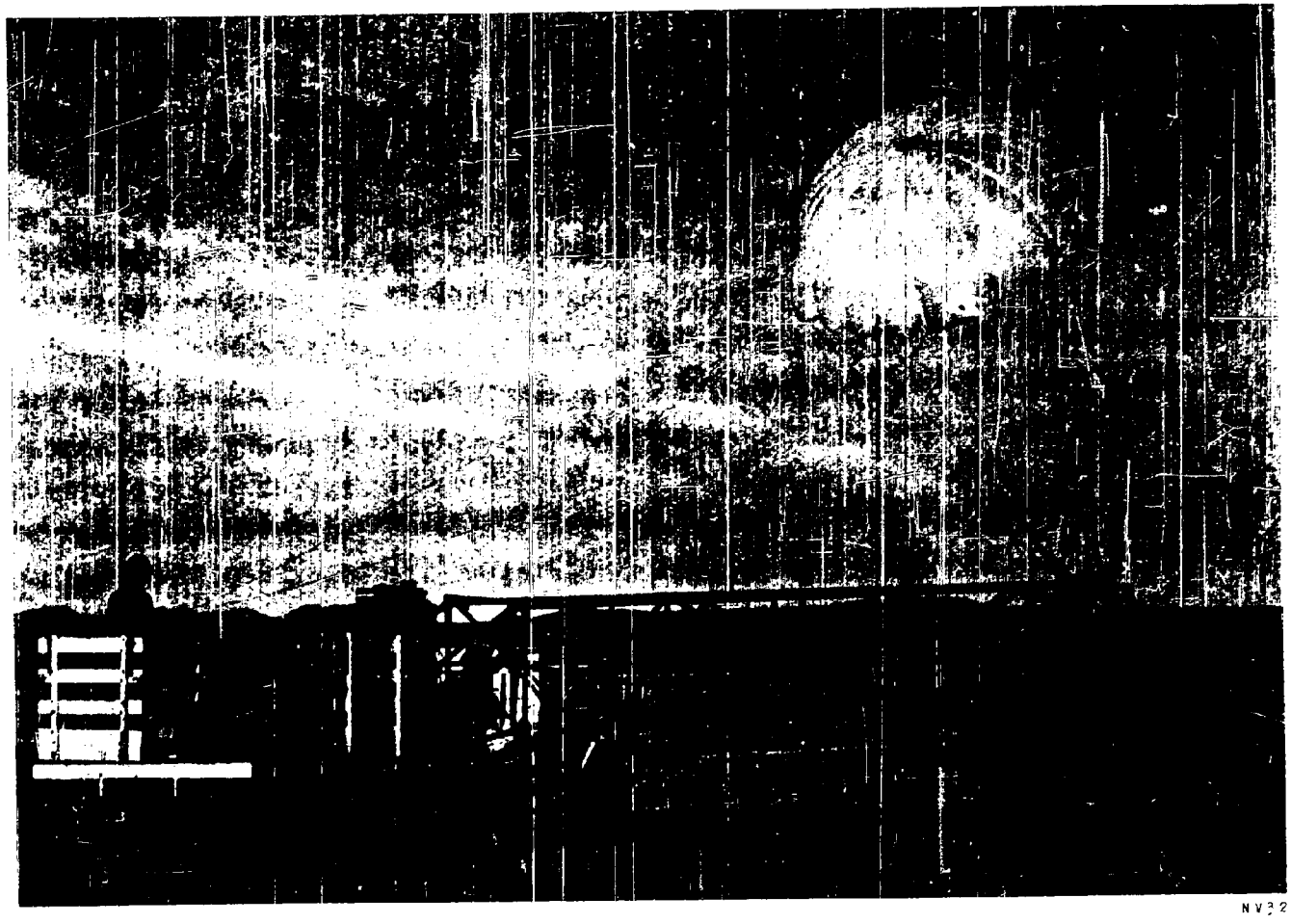

Figure 60. Model 101

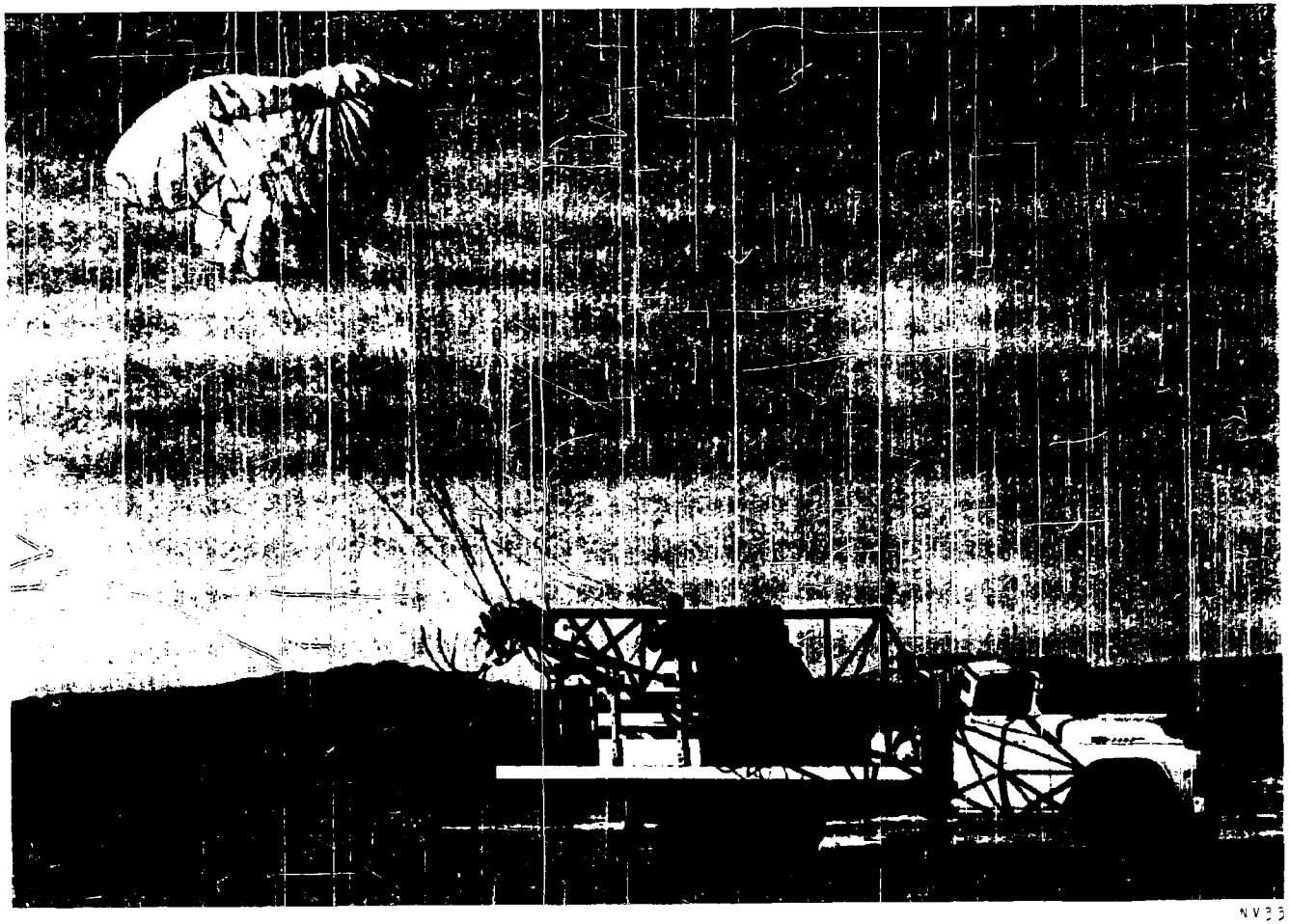

Figure 61. Boom Assembly Mounted on Truck

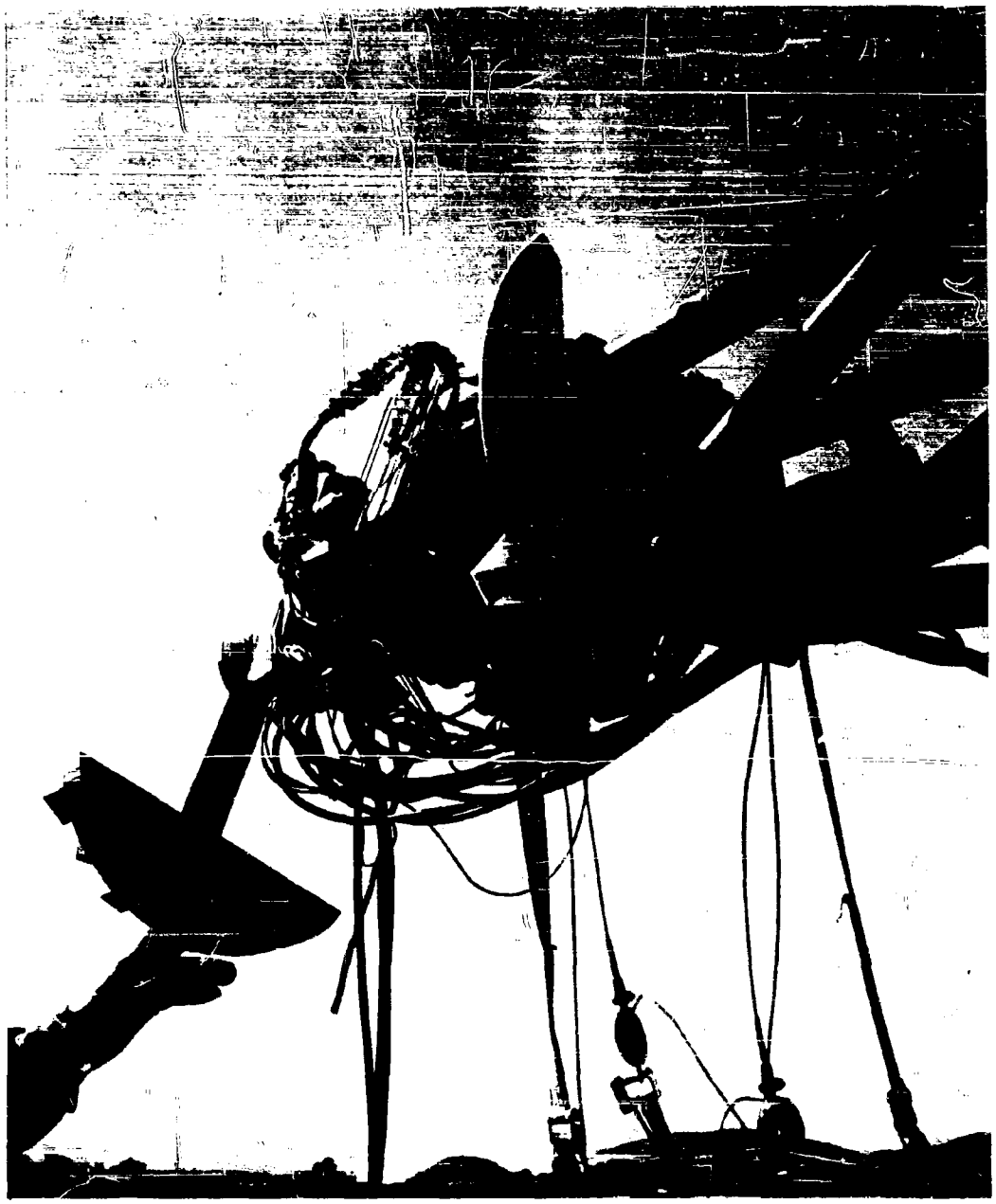

Figure 62. Control Mechanism Mounted on Boom

NV35

Figure 63. Instrumentation on the Truck

1.2 TOW TRUCK TEST PROCEDURE AND SET-UP

1.2.1 Test Set-Up

The test set-up used for the two truck tests consisted of a 20-ft boom with a control mechanism mounted at the end of the boom, cantilevered out to the side from the bed of a truck. Figure 61 is a photo showing the truck and boom with a parachute flying from it. The control mechanism had four remotely controllable winches to control flap deflections and vary parachute rigging.

These four controls were equipped with potentiometers for the purpose of recording control cable positions. The complete control mechanism was mounted in bearings on a shaft on the end of the boom. The positioning of the control mechanism due to forces applied to it by the parachute was used to determine the glide angle of the parachute. A protractor was attached to the end of the boom and a pointer was attached to the control mechanism, after proper positioning of the pointer with respect to the protractor and counter-balancing of the control mechanism, glide angle could be read directly. Strain gage force links were used between the cable ends and the control risers to obtain control line forces. An anemometer was used to obtain air speed. Airspeed, control line loads and control line positions were recorded with a light beam oscillograph. Power for the recorder and control motors was provided by storage batteries through a regulated power supply. Figures 62 and 63 show photos of the control mechanism on the boom and the instrumentation on the truck.

1.2.2 Test Procedure

Test procedure was to attach the parachute to the control mechanism and spread the parachute out on the ground behind the truck. The truck was then brought up to speed and

the desired range of control settings run. Since there was no provision made to read airspeed during the test run, the truck speedometer was used to determine ground speed and an estimated correction made for wind. Also, it was not possible to read control line position while in motion and this made it necessary to estimate control settings. As much as possible, all runs were made directly into or with the wind. Because of the yaw instability of some of the models, tag lines were attached to all the models tested and manually manipulated as necessary to control the model. These lines from the canopy to the truck bed, are the ones seen in the photos of the models in flight.

1.3 PERFORMANCE OF TOW TRUCK TEST RIG

The performance of the test rig was in general satisfactory. The data provided by the test rig used provided data which was in general, substantiated by later tests at the Ames Wind Tunnel. There were, however, due to lack of time in which to set-up, deficiencies in the test rig which introduced the large amount of scatter in the L/D values obtained. These deficiencies were: (1) lack of ability to accurately read airspeed during the test run; (2) the need to visually read the indicated glide angle and manually record it; (3) oscillations of the control mechanism, which made it difficult to determine L/D accurately; (4) no provision to read flap position while the truck was in motion. These deficiencies could be corrected by: (1) the addition of a direct reading airspeed indicator which can be read in the cab of the truck; (2) the addition of a system to record indicated glide angle; (3) damping the control mechanism to reduce the affect of ground surface irregularities; (4) adding a direct readout system for flap control line position. One additional factor which had an affect on the data obtained from the tow tests was the counter balancing of the control mechanism. The short moment arm, through which forces

from the parachute act to align the control mechanism with the resultant line of force of the parachute, makes the indicated L/D given by the system sensitive to any unbalance due to off center weight distribution. This factor showed up as a change in indicated performance for Model 301A, as indicated when the results of the data obtained from a check run made later in the test program.

1.4 RESULTS OF TRUCK TOW TESTS

Figures 42 to 48 present the gliding performance of the configurations tested. These figures give L/D as a function of flap extension and in some cases the rigging of groups of lines attached to the interior of the canopy. Figures 49 to 55 give control line forces, in coefficient form, as a function of control line extension.

1.4.1 Model 301A

Data for Model 301A is presented in Figures 42, 43, 49, and 50. Figure 42 is a plot of L/D vs flap extension. There are two sets of data points and one curve presented on this plot. The data points are for the data obtained during the first day of testing and are for two different riggings of the group of lines which attach to the rear portion of the front lobe of the parachute. The upper curve is based on the results obtained during a check run made late in the final day of testing. Unfortunately, lack of time made it impossible to rerun the complete range of flap extensions. The curve presented, which is based on the one data point taken by manually measuring the flap extension at the end of the run, is indicative of the performance of Model 301A rather than the lower data.

After the first day of testing, corrections in the counter-balancing of the indicator assembly were made which resulted in more accurate indicated L/D values and, therefore,

the curve should be considered as being representative of the parachute performance. Figure 43 gives the affect of changing the rigging of the parachute by pulling down the interior canopy lines while holding a constant flap setting. As can be seen from Figure 43, the most effective rigging is at a E_{GG}/D_W of about -.01. Figures 49 and 50 give the control line forces as a function of line extension. This parachute showed the best combination of performance and stability of the models tested. Figure 56 is a photo of Model 301A flying from the test rig.

1.4.2 Model 302

Figures 44 and 51 give the L/D performance and force data obtained from Model 302. Model 302 was set up with groups of internal lines which could be adjusted. During the test run, the internal lines were set at what appeared to be an optimum setting and a range of flap settings run. A second test run was made with the group of interior lines attached to the crown of the canopy very close to zero extension (see Figure 44). The stability of Model 302 was fair. Tag lines attached to the skirt of the canopy were necessary to maintain stable flight. Figure 57 is a photo of Model 302 flying from the test rig.

1.4.3 Model 303

Figures 45 and 52 give the L/D performance and force data obtained from Model 303. Model 303 is the University of Minnesota design modified by the addition of flaps. This model was the most stable design tested during the tow truck test series.

1.4.4 Model 304

Figures 46 and 53 give the results for Model 304. Model 304 is rigged with the flaps connected to interior canopy lines which reduces the forces required to actuate the flaps when the parachute is operating near its maximum L/D capability. This

parachute was rigged to obtain maximum L/D at flap riser settings near zero. As a result of this rigging, flap riser loads are low as can be seen in Figure 53.

1.4.5 Model 402

Figures 47 and 54 give the results for Model 402. Model 402 is identical to Model 302, with the exception that D_o for Model 402 is 16 feet. Model 402 showed an increase in L/D performance as shown by a L/D max of 1.72 for Model 402 as compared to an L/D max of 1.485 for Model 302. As with Model 302, two different arrangements of interior lines was used. This model was extremely stable and did not require guidance from the tag lines to control oscillations in yaw. Figure 59 is a photo of Model 402 flying from the test rig.

1.4.6 Model 101

Figures 48 and 55 give the data for Model 101. This model was the same model tested in the Aerosail test program. The best results which could be obtained from this model on the tow test rig was L/D = 1.19, which is much lower than the performance reported for this model in the Ames Wind Tunnel. Figure 60 is a photo of Model 101 flying from the test rig.

1.5 OBSERVATIONS

Based on the results of the truck tow tests, the following observations were made:

(1) Model 301A gave the best L/D performance and excellent yaw stability. Therefore, this model has the best chance of achieving an L/D of 2.0.

(2) A definite improvement in maximum L/D performance was noted between Model 302 and Model 402 which seems to indicate an increase of L/D capability with increasing size for a given design.

(3) Either Model 101 has deteriorated, with a resultant loss in L/D capability, since the Aerosail Wind Tunnel tests, or the wind tunnel data is in error.

(4) None of the models tested appear to have the potential of matching the performance of the three lobe type of design.

(5) Relatively small flap riser extensions are necessary to achieve maximum L/D performance. This results in low control line extension capability being required to operate the parachute.

APPENDIX IV

AMES WIND TUNNEL TESTS

1.1 GENERAL DISCUSSION

The data presented in this section is data from the Wind Tunnel Tests conducted at the Ames Research Facility - February 6th to February 10th, 1964 and February 17th to February 18th, 1964. Because of difficulties encountered with the wind tunnel instrumentation during the first series of tests conducted February 6th to February 10th, the validity of the data obtained during these tests was questioned. Therefore, a second series of tests was conducted February 17th and 18th. The question of the validity of the data obtained during the first series of tests was brought up because of the low values of L/D obtained with Model 101. Model 101 in the Aerosail Wind Tunnel test program reached an L/D of 1.76 while the highest value that could be obtained in the current test program was an L/D of about 1.3. Checks of the wind tunnel instrumentation by Ames personnel showed that the strain gage balances and associated electronics, used as the primary system for measuring L/D, were giving unreliable data. As a result of this, it was necessary to depend on the back-up system to get data. The back-up system was a mechanical scale system. During the first part of the February 6th to February 10th tests, data was not taken with the scale system, and, therefore, the results of these tests were lost. Because of the incomplete

Preceding Page Blank

data coverage obtained during the first series of tests, a second series of tests was necessary. The purpose of the second series of tests was to rerun the tests from which erroneous data were obtained. Also, during the second test series, many of the models tested during the Aerosail Wind Tunnel Test Program were retested. Figures 64 to 86 present data obtained during the complete test program.

During the first series of tests, the models were flown horizontally from a vertical strut. Because this method of testing required the model to support its weight in a direction perpendicular to the direction of the lift vector, it was felt that the performance of the models may have been degraded.

Therefore, during the second series of tests, the models were flown vertically from a strut mounted on the floor of the tunnel. Although the parachute has to support its weight when flying vertically from the floor of the tunnel, this flight condition approximates free flight conditions better than flying horizontally.

The remote control mechanism and strain links were the same as used for the tow truck tests and are described in Appendix III. The same type of instrumentation as used for the truck tests was also used to record control riser positions and forces. For the tests with the models flying horizontally, the control mechanism was mounted on a vertical strut. For the tests with the models flying vertically, the control mechanism was mounted on a short strut attached to the mechanical balance system. Figure 84 is a photo showing the set-up for vertical flight and Figure 85 shows the horizontal flight set-up.

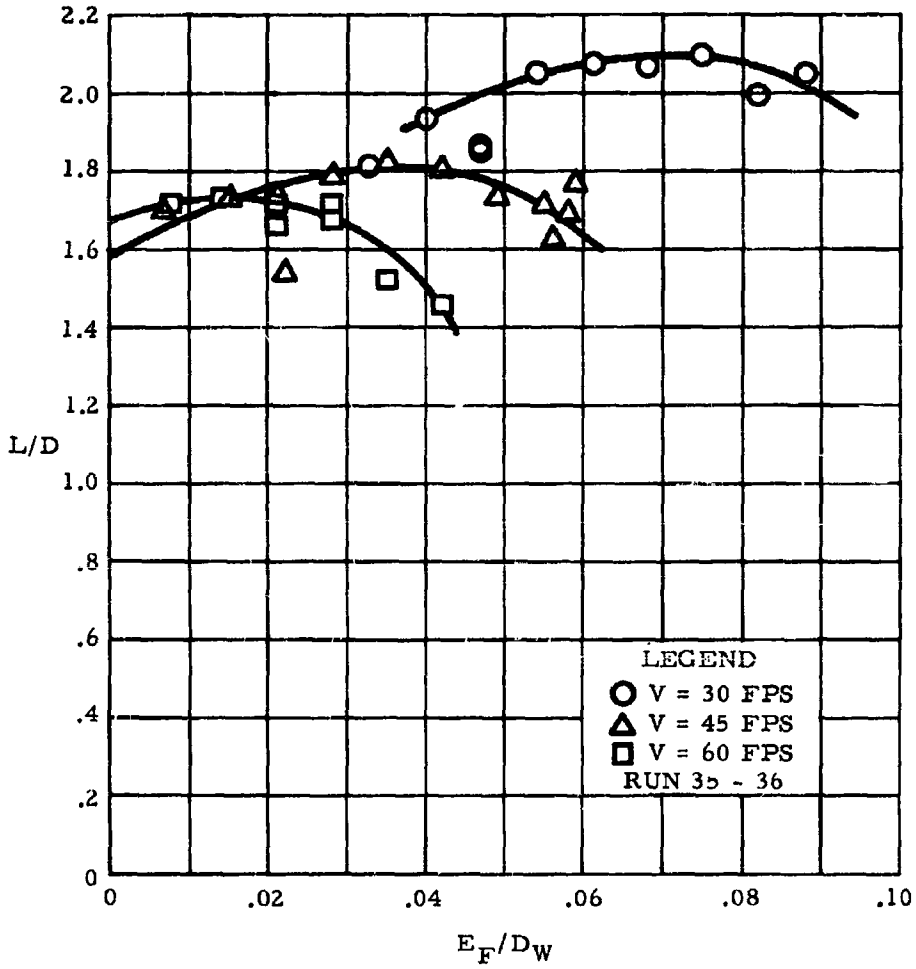

Figure 64. L/D vs Flap Extension - Ames Wind Tunnel Tests

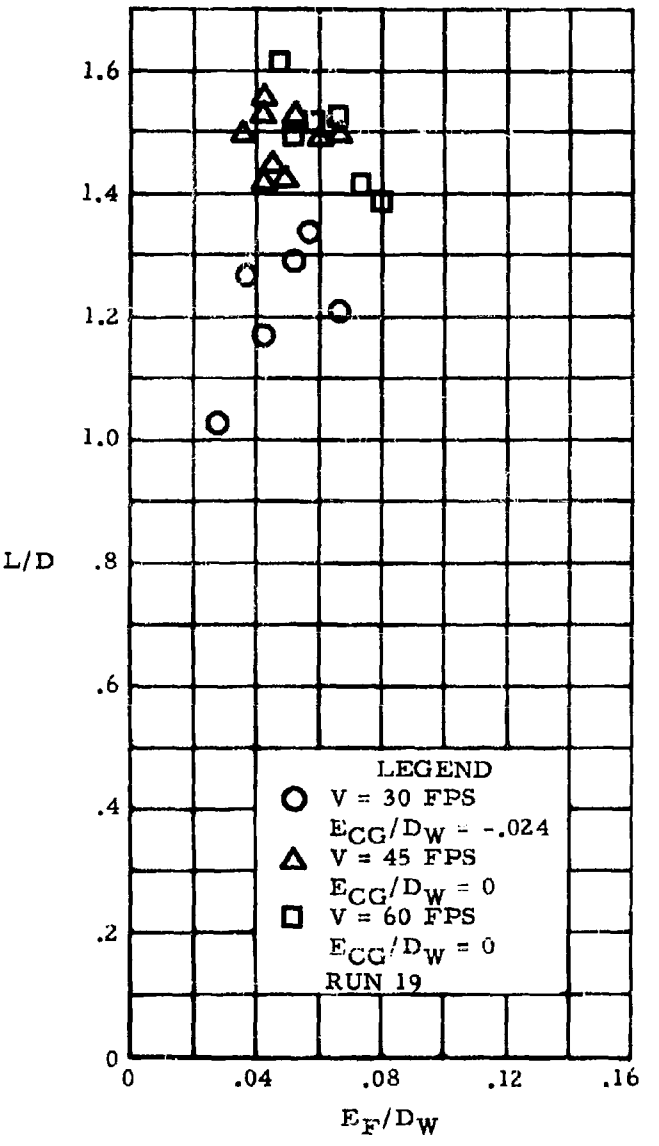

Figure 65. L/D Vs Flap Extension, Model 301

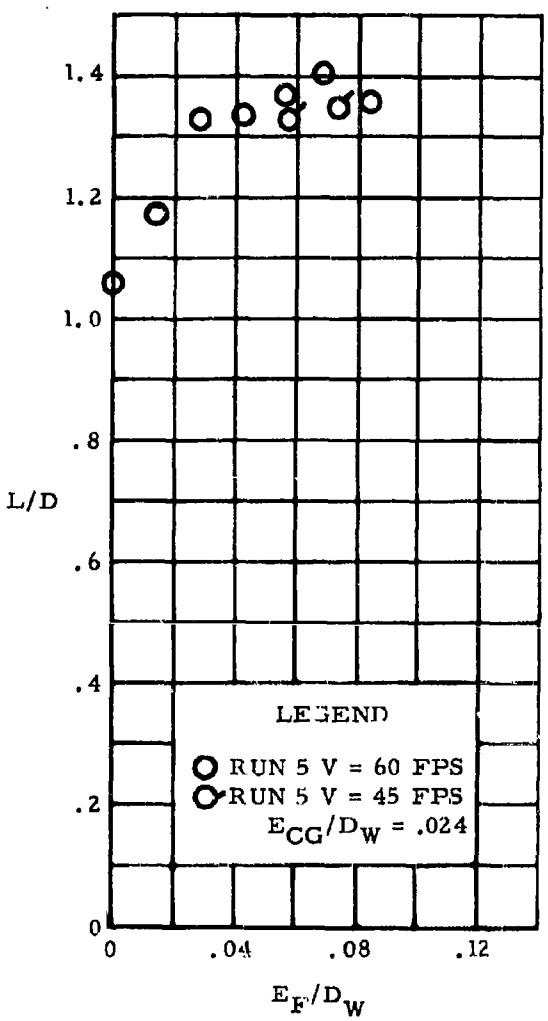

Figure 66. L/D Vs Flap Extension, Model 301A

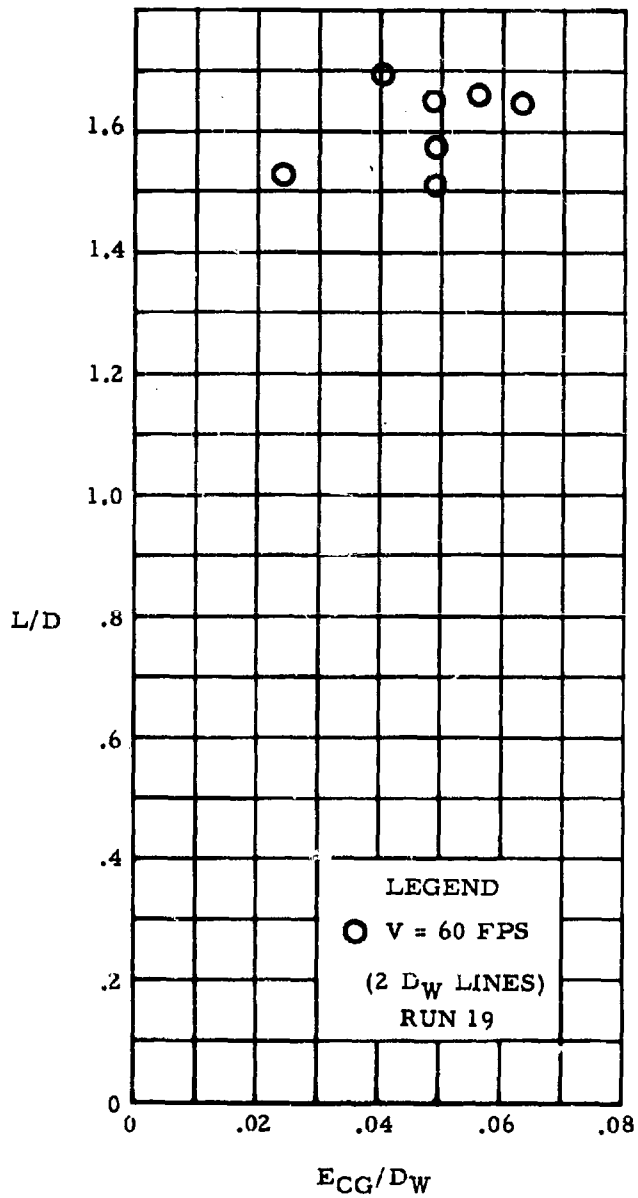

Figure 67. L/D Vs Extension of Interior Lines

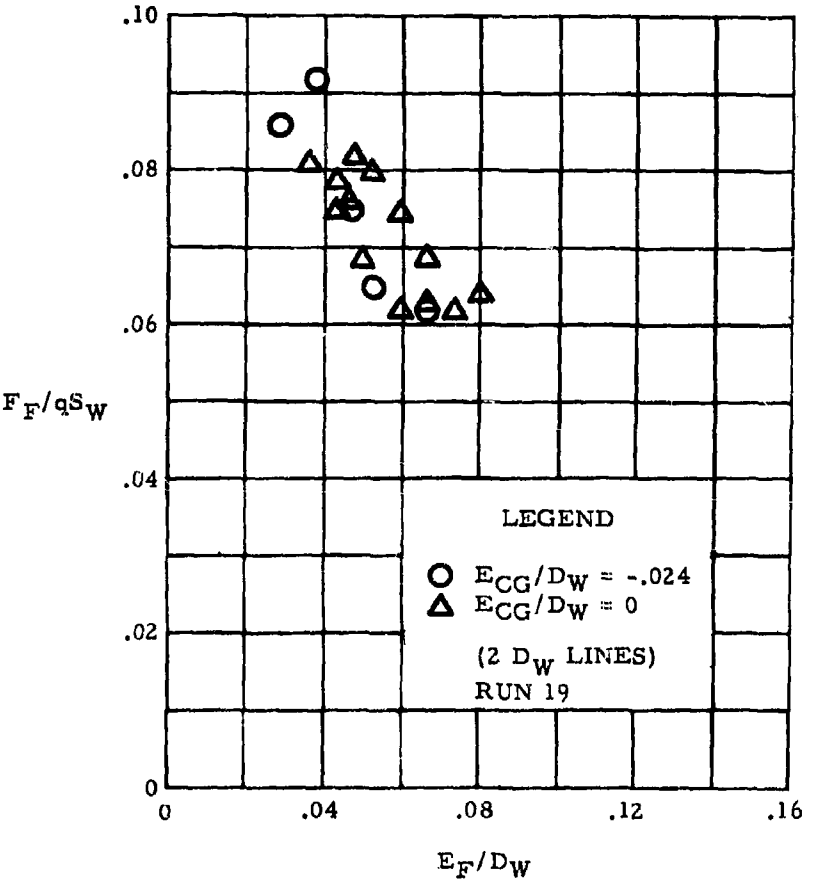

Note: This data is for one flap only

Figure 68. Flap Riser Force Vs. Flap Extension, Model 301

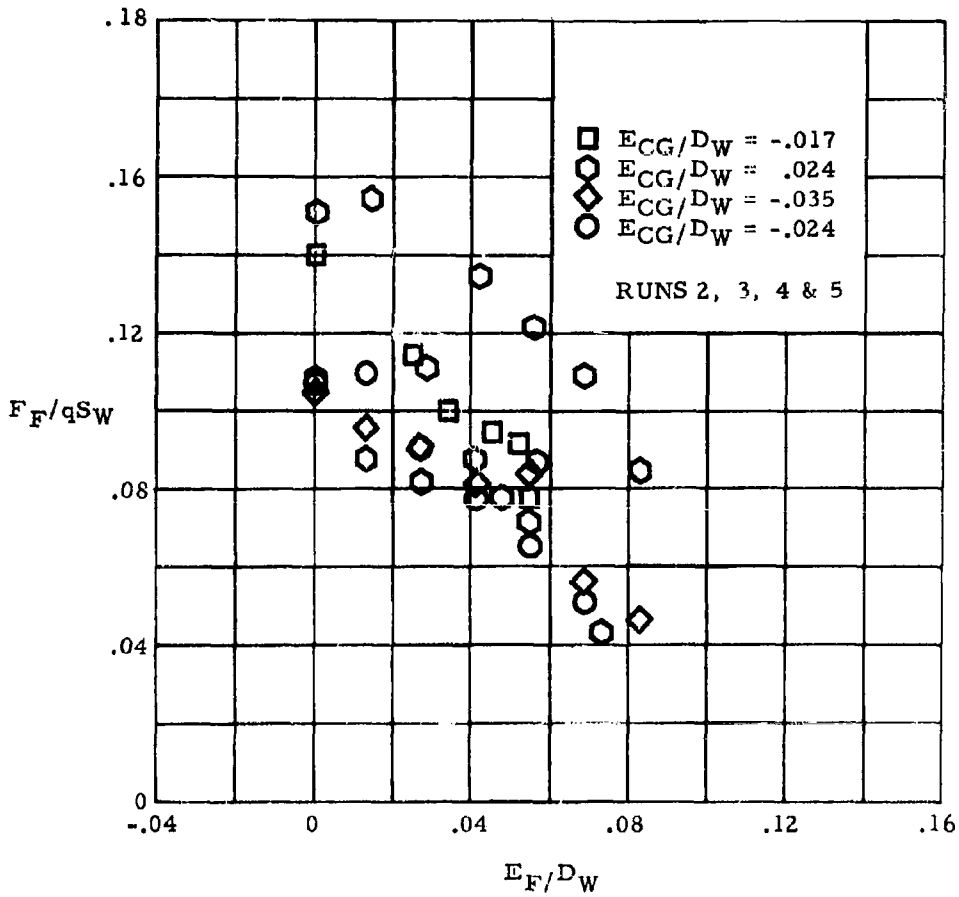

Note: This data is for one flap only

Figure 69. Flap Riser Force Vs. Flap Extension, Model 301A

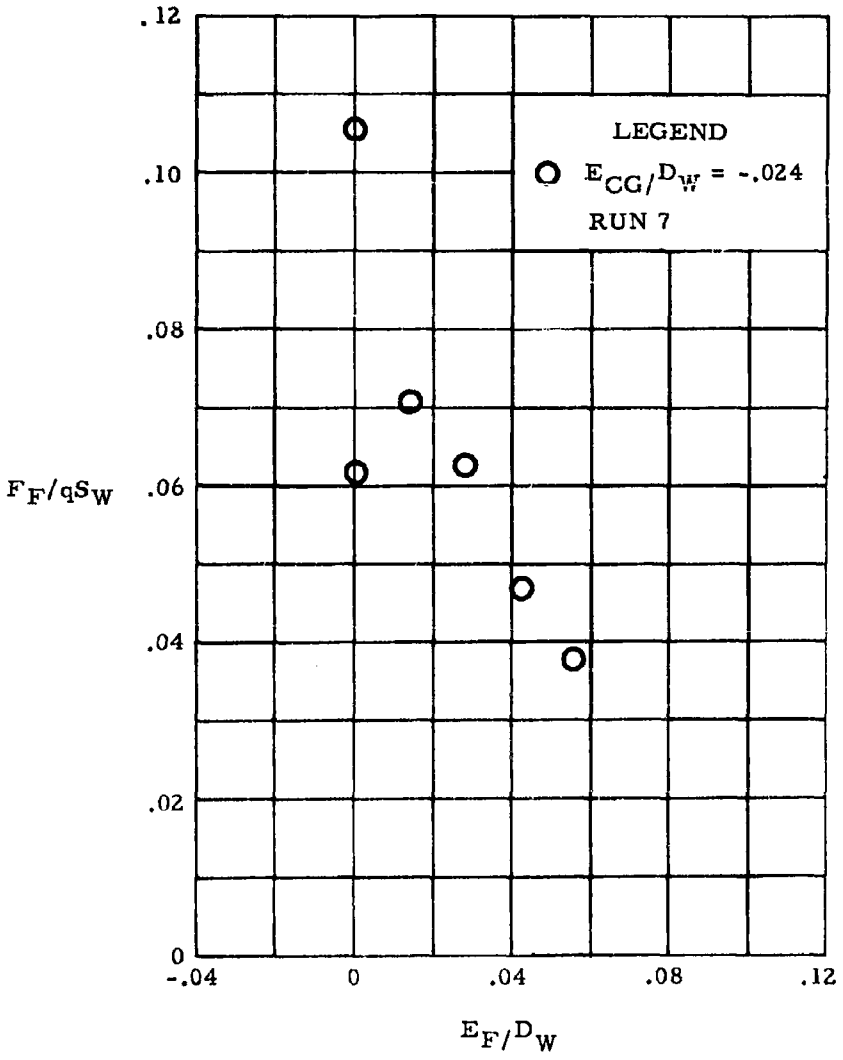

Note: This data is for one flap only

Figure 70. Flap Riser Force Vs. Flap Extension, Model 301

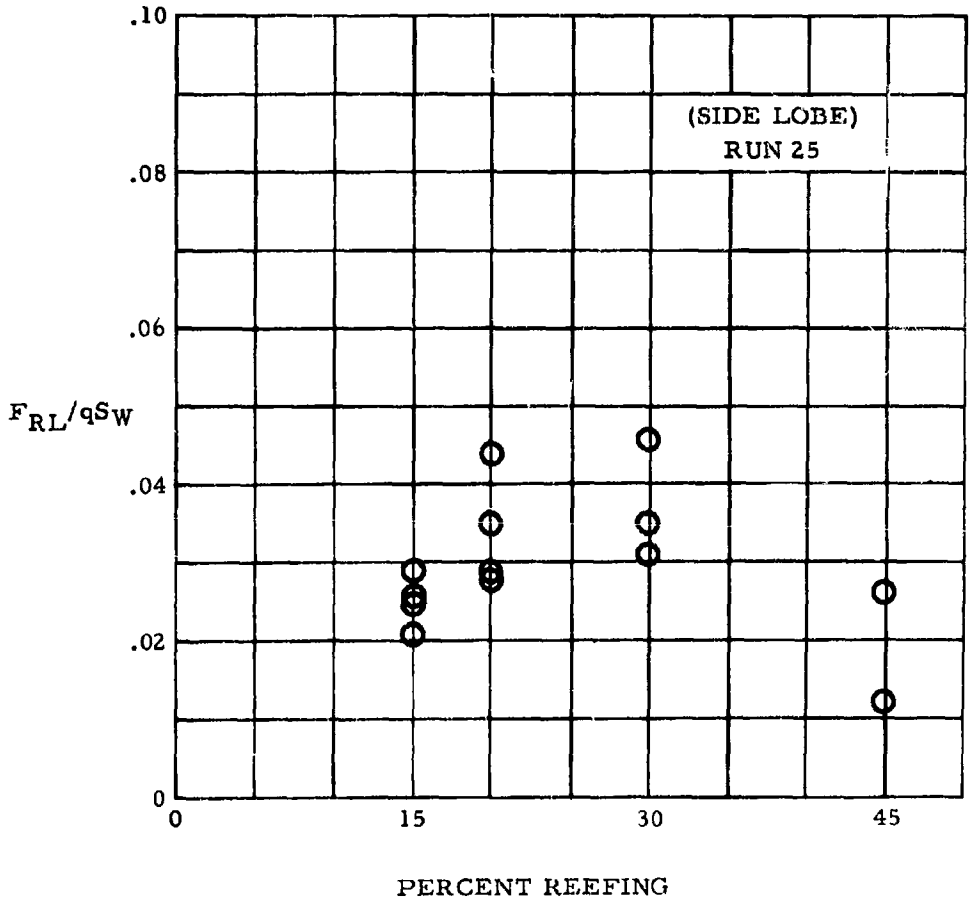

Figure 71. Reefing Line Force Vs. Percent Reefing

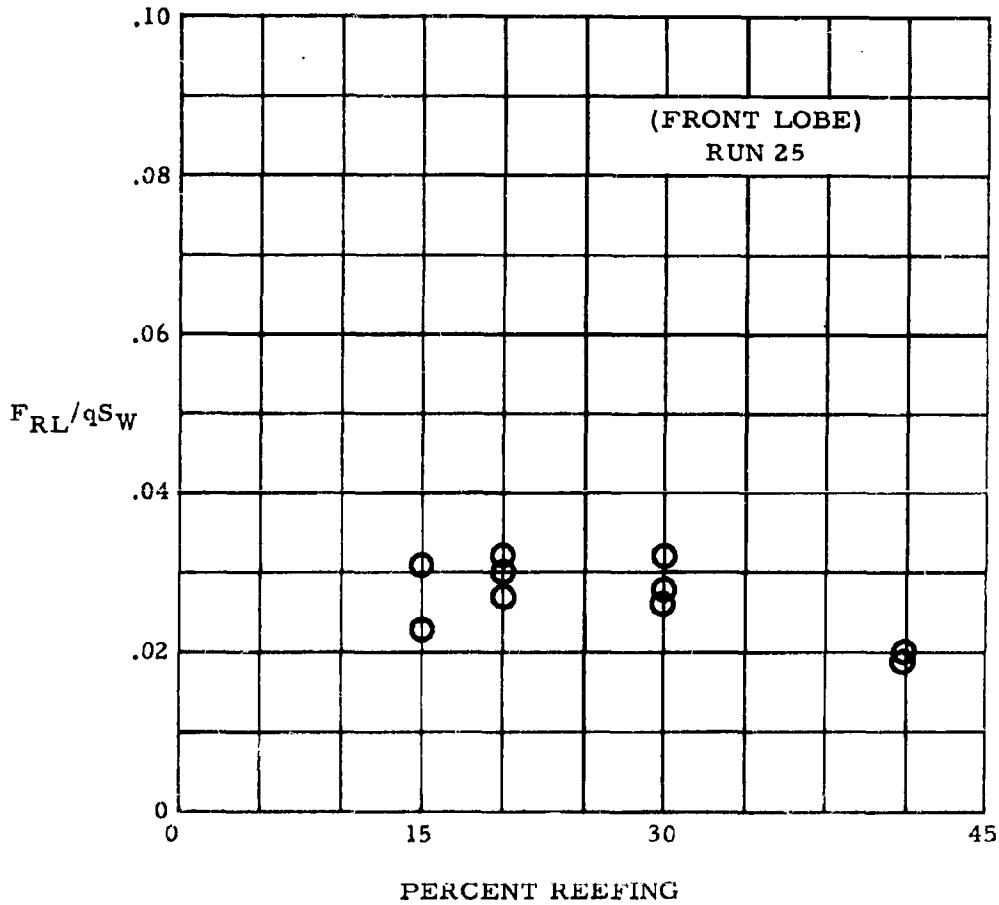

Figure 72. Reefing Line Force Vs. Percent Reefing

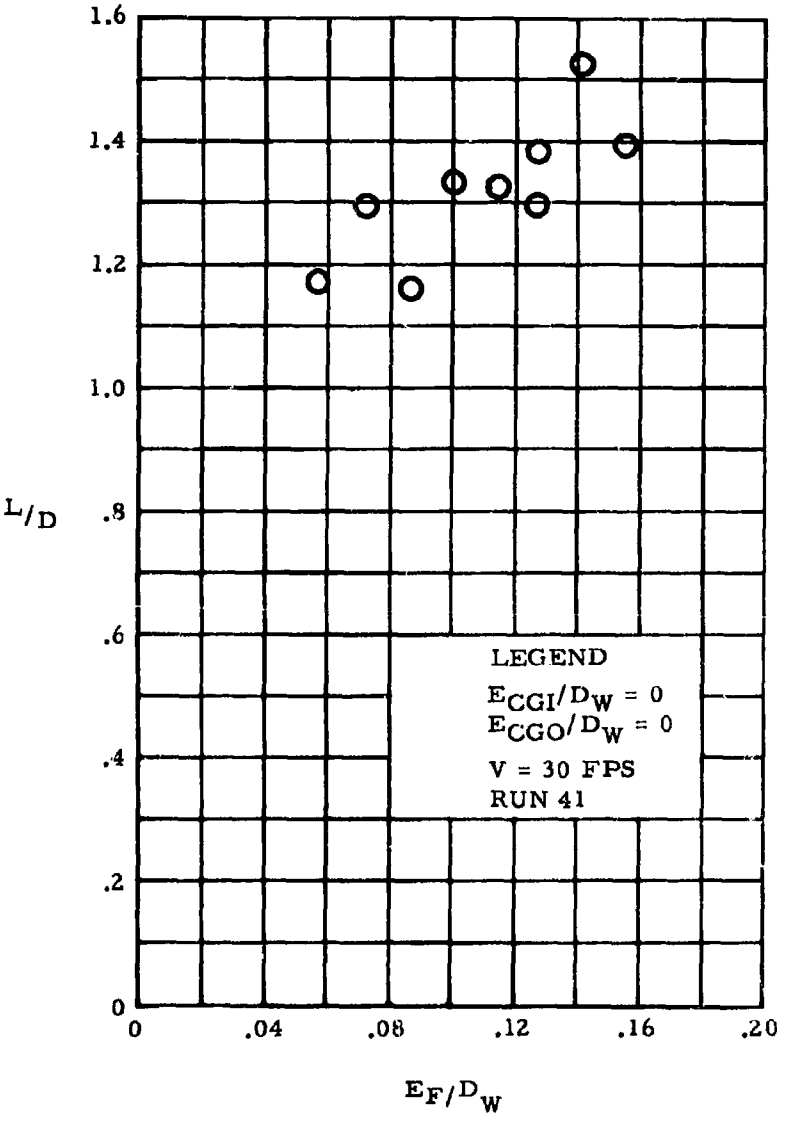

Figure 73. L/D Vs. Flap Extension, Model 302

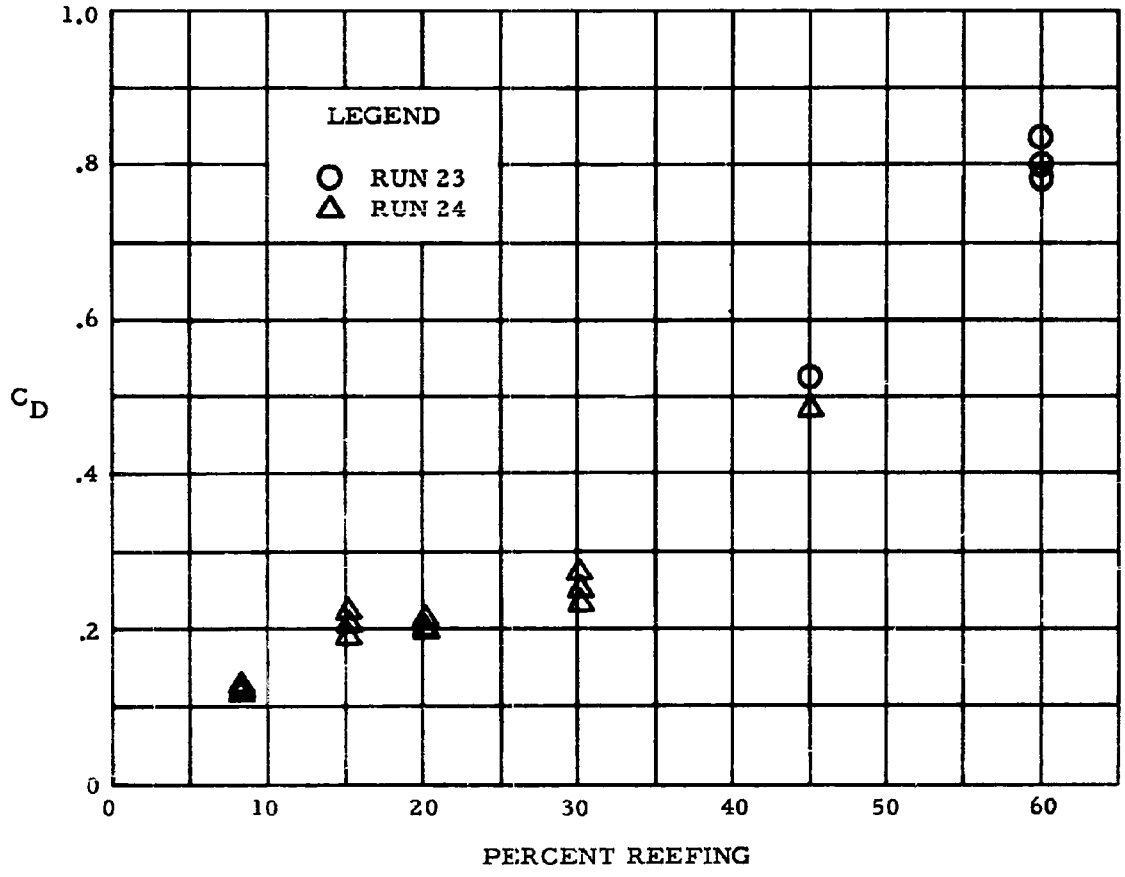

Figure 74. C_D Vs. Fercent Reefing, Model 302

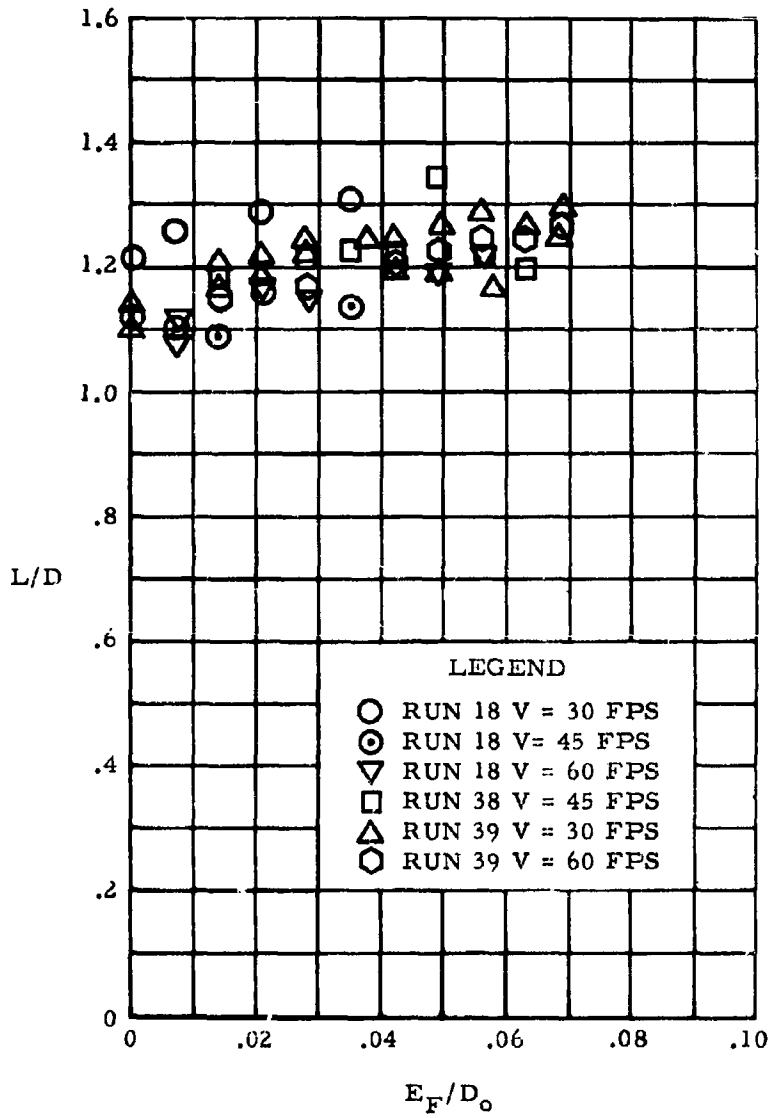

Figure 75. L/D Vs. Flap Extension, Model 303

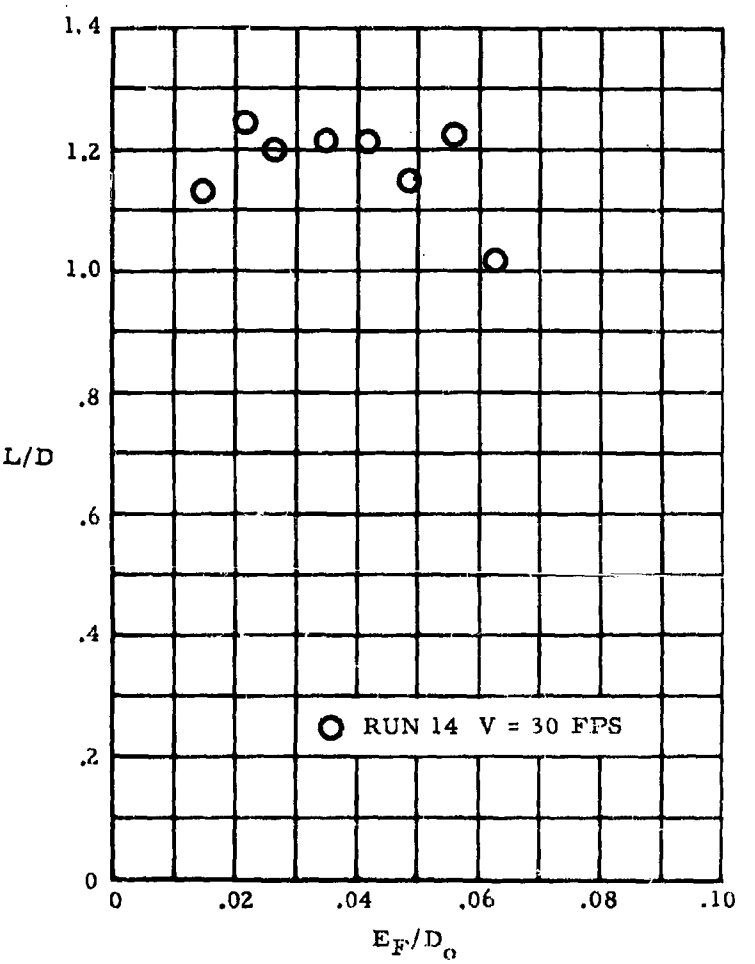

Figure 76. L/D Vs. Flap Extension, Model 304

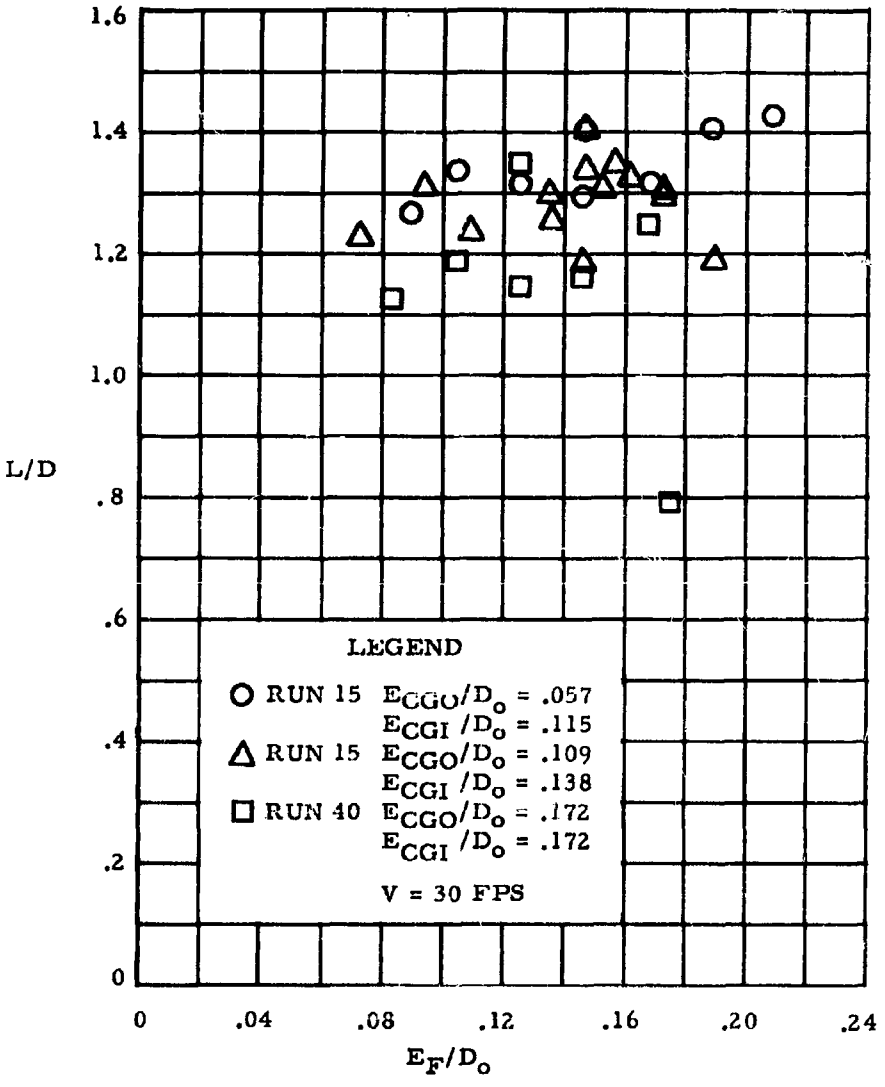

Figure 77. L/D Vs Flap Extension, Model 402

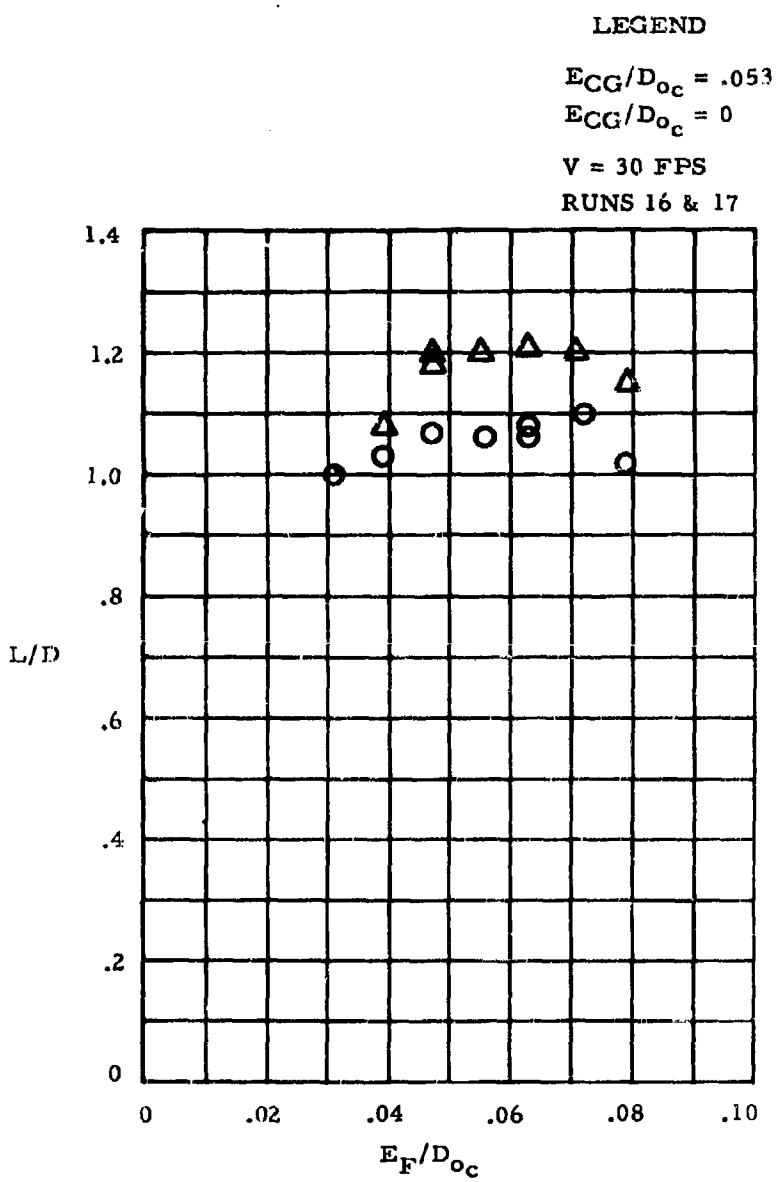

Figure 78. L/D Vs Flap Extension, Cluster 302's

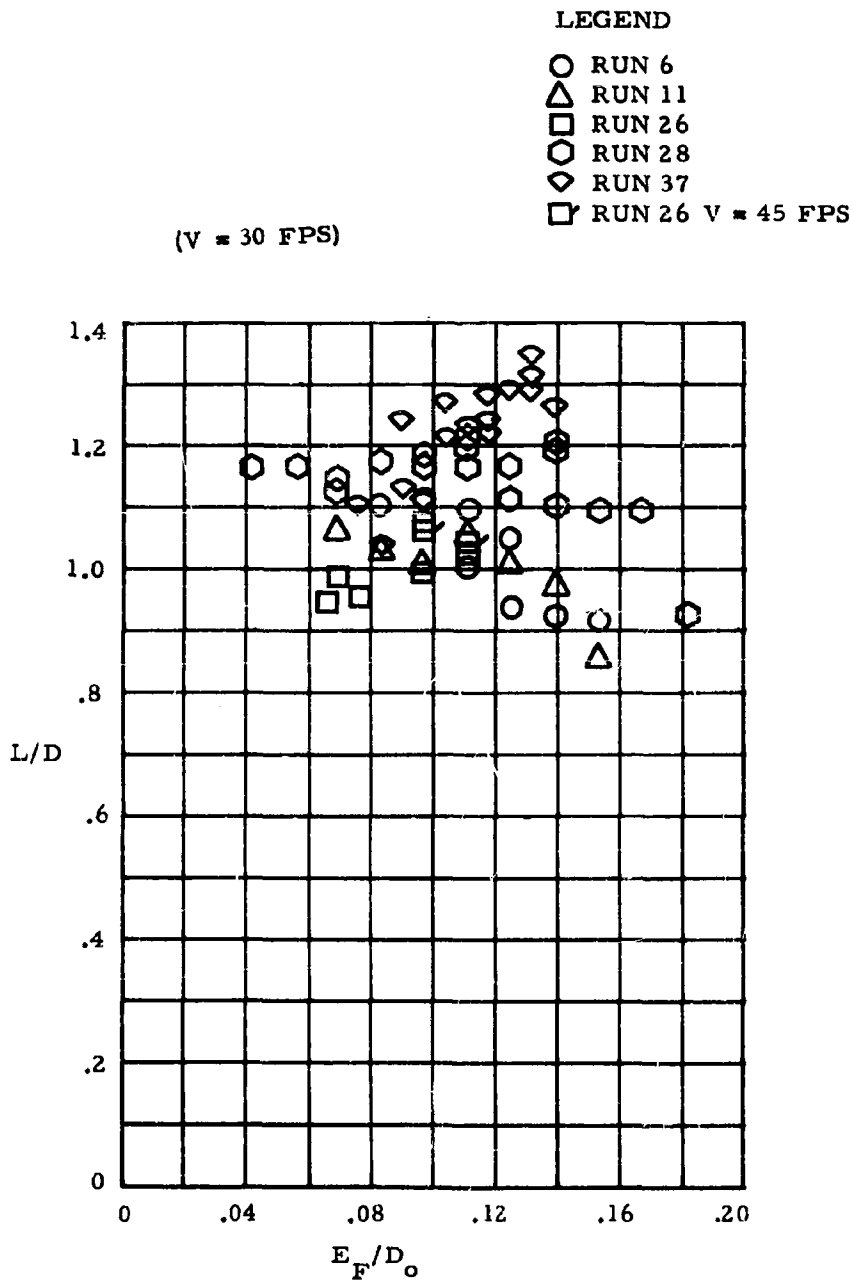

Figure 79. L/D Vs Flap Extension, Model 101

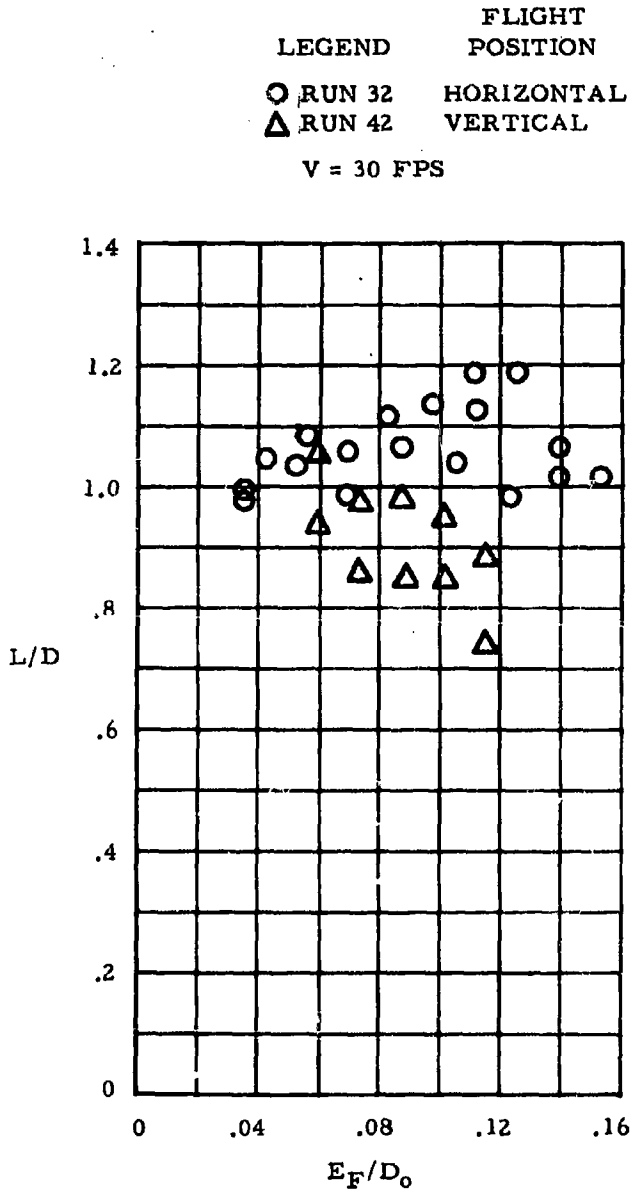

Figure 80. L/D Vs Flap Extension, Model 105

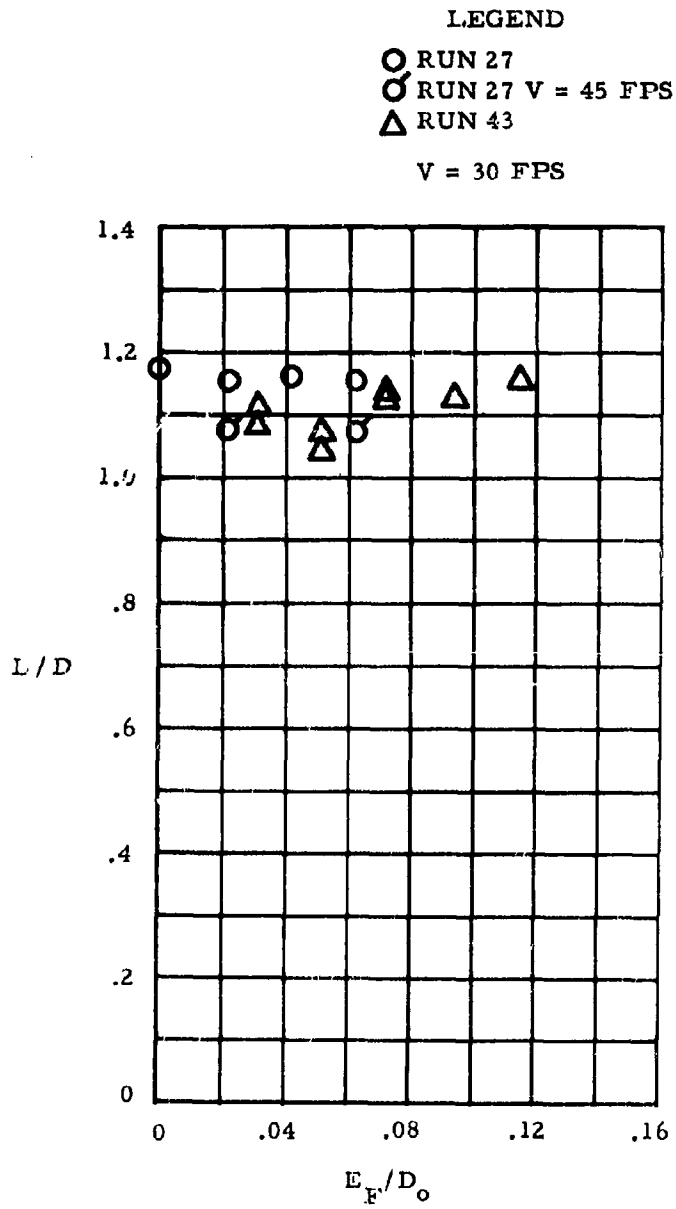

Figure 81. L/D Vs Flap Extension, Model 107

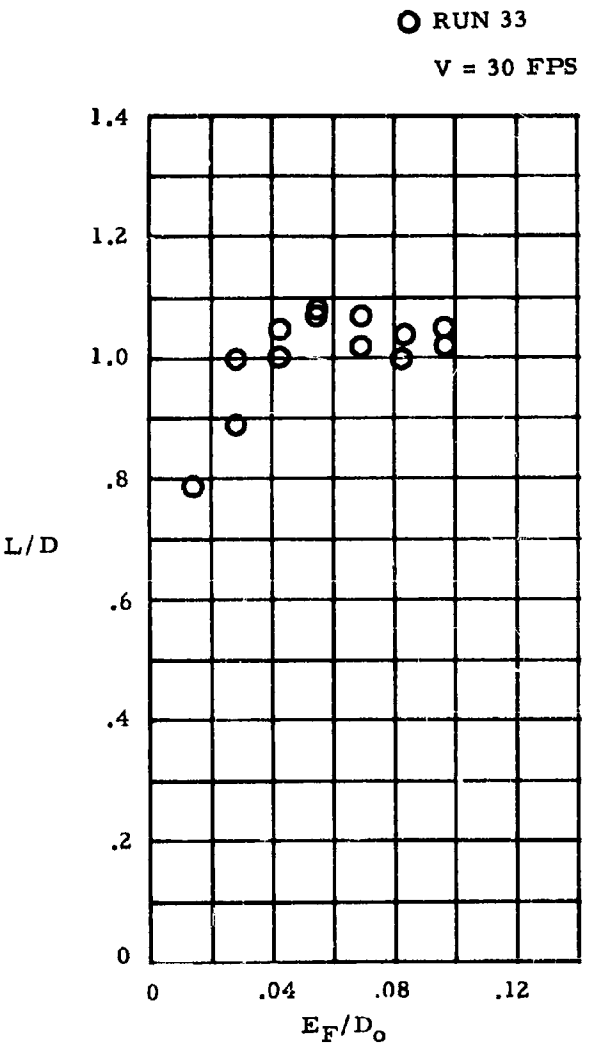

Figure 82. L / D Vs Flap Extension, Model 113

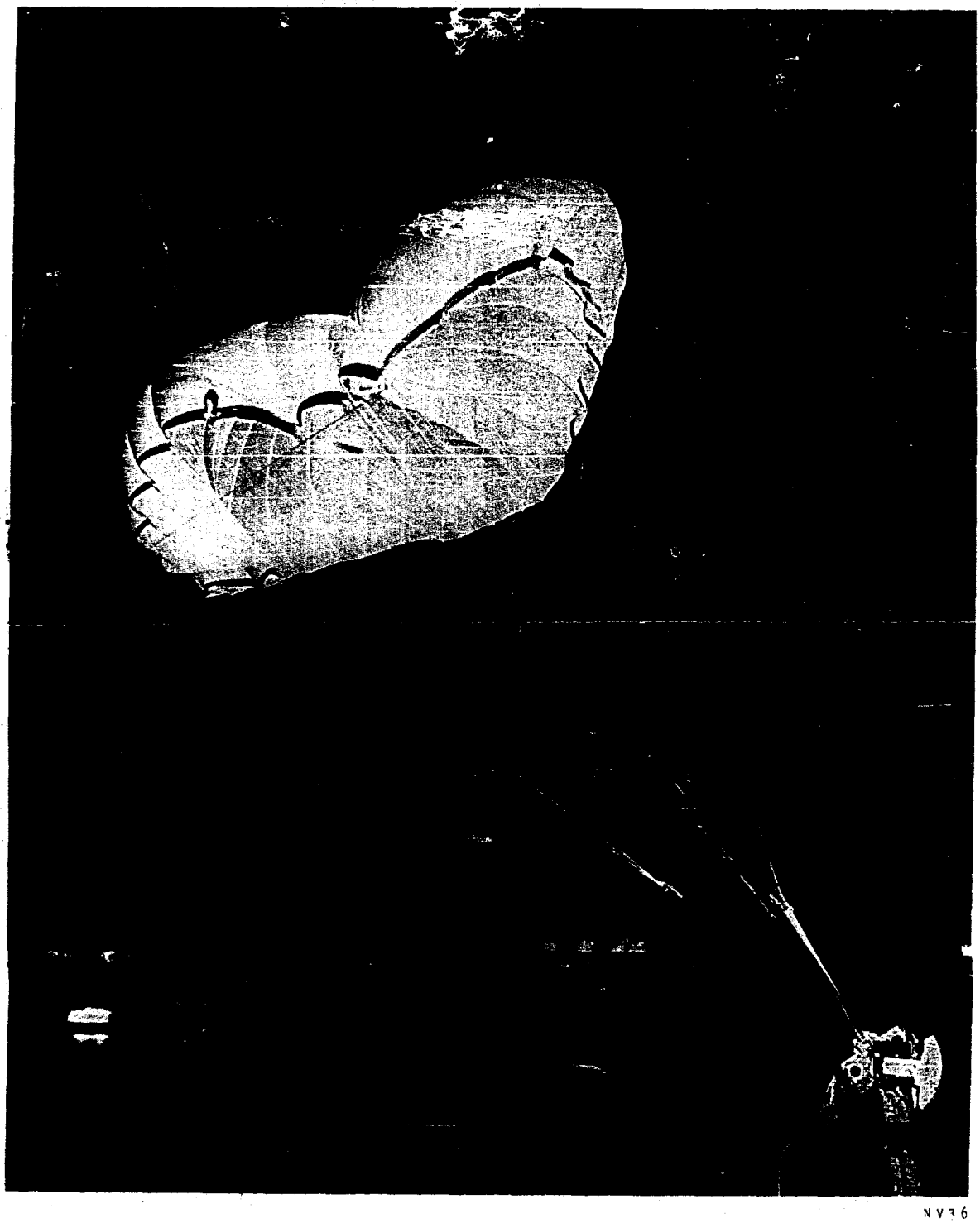

NV36

Figure 83. Model 302 Flying Vertically in the Wind Tunnel

Reproduced From
Best Available Copy

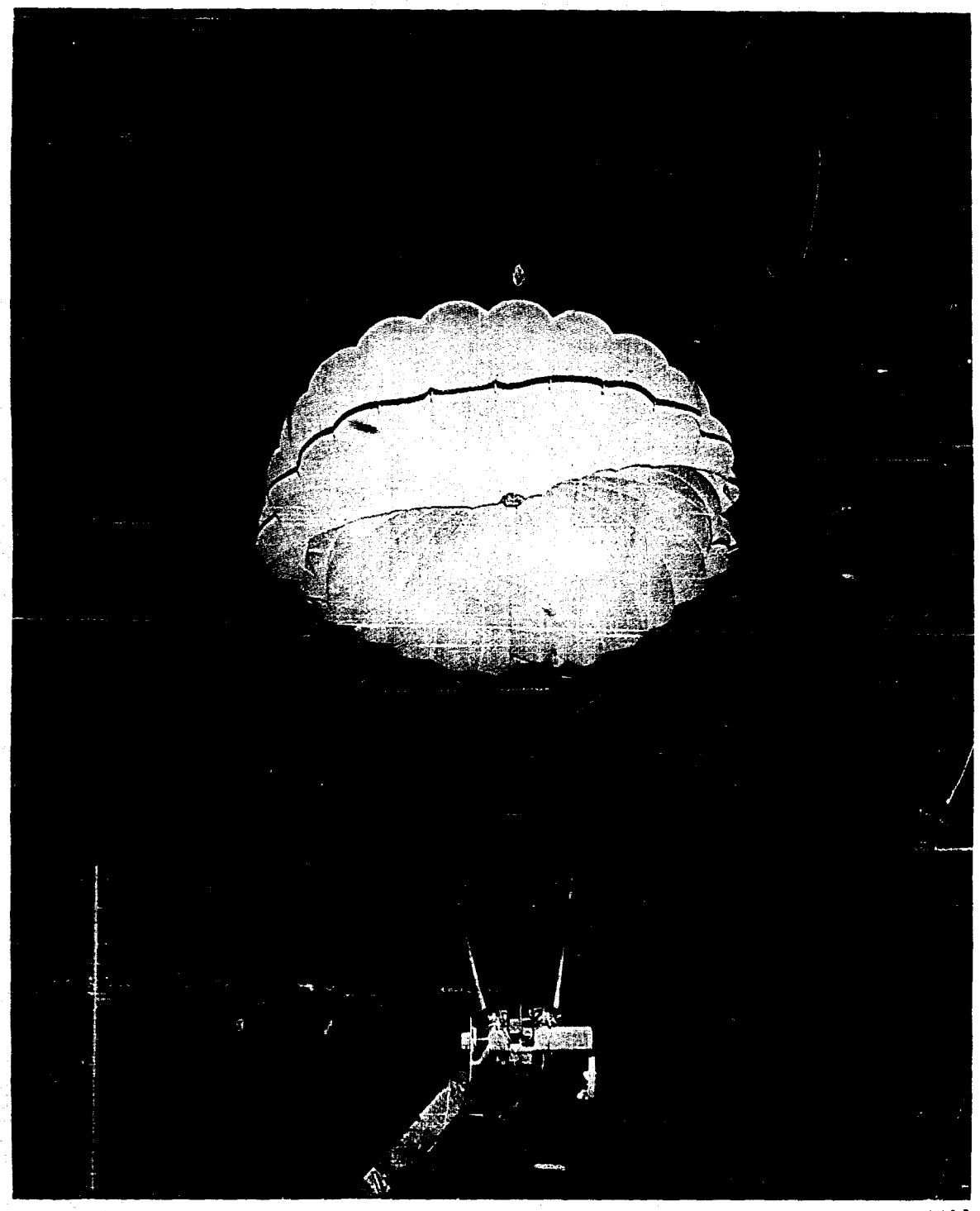

NV37

Figure 84. Model 302 Flying Vertically in the Wind Tunnel

Reproduced From
Best Available Copy

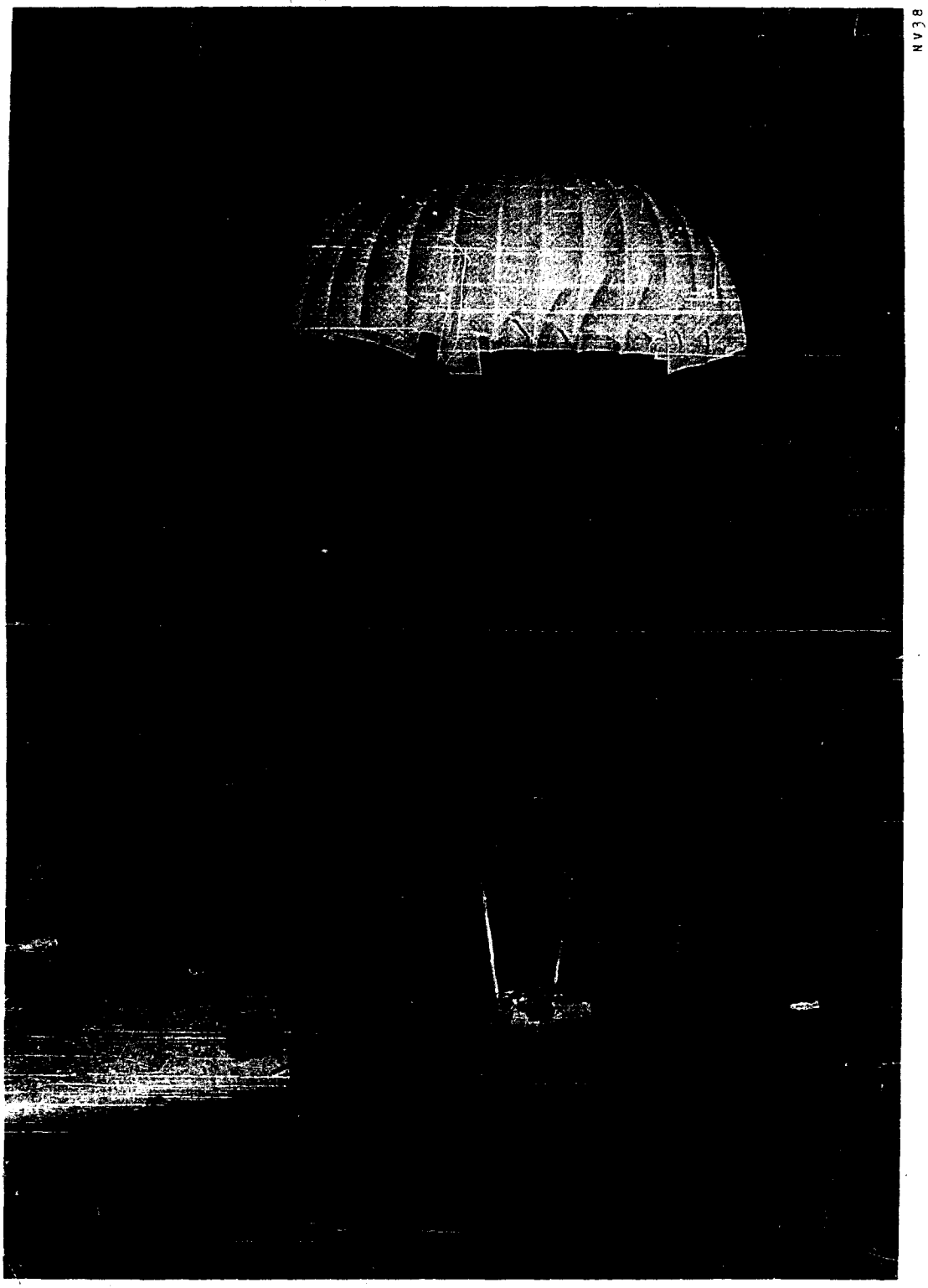

Figure 85. Model 101 Flying Horizontally in Wind Tunnel

Reproduced From
Best Available Copy

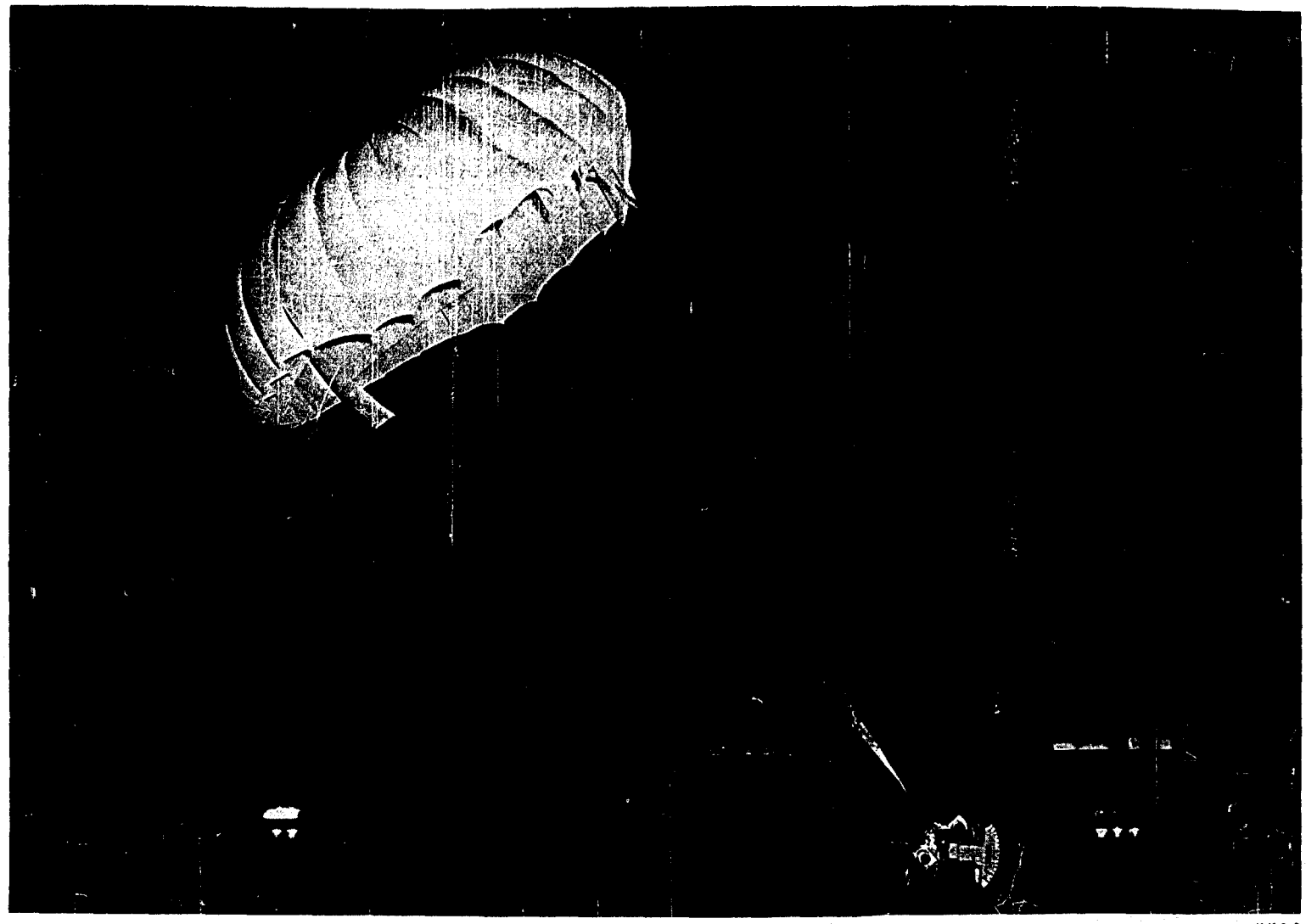

Figure 86. Model 101 Flying Vertically in the Wind Tunnel

Reproduced From
Best Available Copy

1.2 DATA PRESENTATION

The following paragraphs present the data obtained during the Ames Wind Tunnel Tests. The presentation is broken down by model number. For the models from the Aerosail test program, which were retested, corrected values of L/D max as well as the data obtained during this test program are given. The corrected values were obtained by using mechanical scale data that was taken during the Aerosail test program. It should be noted that for runs 1 to 34 the models were flown horizontally and for runs 35 to 43 the models were flown vertically.

1.2.1 Models 301 and 301A

The following is a discussion of the Model 301 and Model 301A data presented in this appendix. Data for both models are presented under one heading because of the similarity of the two configurations. Model 301A is identical to Model 301 except for a fairing over the rear center portion of the Model 301A canopy. Figure 64 is a plot of L/D versus flap extension for Model 301. Data for velocities of 30, 45, and 60 fps are shown. Figure 65 gives the affect of velocity on the L/D performance of Model 301 rigged with 2 D_W suspension lines. The data presented in this figure was obtained with the model flying horizontally. Unfortunately, because of trouble experienced with the wind tunnel instrumentation during the first series of Ames tests and the lack of time necessary to completely rerun the test program during the second series of Ames tests, there is no data for Model 301 with 1 D_W lines and flying horizontally. Therefore it is not possible to get the affect of the increased suspension line length on L/D. It is not possible to compare results between tests conducted with Model 301 flying horizontally to tests conducted with the model flying vertically because of an observed deterioration in

performance when flying horizontally. As shown by Figure 65, Model 301 with 2 D_W suspension lines had an increase in performance with increasing velocity. This trend is directly opposite to the results obtained with Model 301 with 1 D_W lines flying vertically. The reason for the indicated increase in performance with velocity is probably due to the weight of the canopy making it necessary to fly yawed in order to keep the parachute out in a horizontal position. Because the vertical component of force necessary to support the parachute weight becomes a smaller percentage of the total force vector acting on the parachute as velocity increases, it is not necessary to fly at as great an angle of yaw. This results in higher indicated L/D values as the velocity increases. Figure 66 gives L/D versus flap extension for Model 301A. This data, at 60 fps, was the only data for Model 301A salvaged from the first test series. Because Model 301A was made by modifying Model 301, and this modification was removed after it was tested and could not be replaced, Model 301A was not retested.

Figure 68 is a plot of flap extension force coefficient as a function of flap extension for Model 301 with 2 D_W lines. Figures 69 and 70 are plots of flap force coefficient for Models 301A and 301. The data shown by Figures 69 and 70 indicates that the flap forces for Models 301 and 301A are comparable and therefore the more complete set of data shown in Figure 69 can be considered correct for use with Model 301. Figures 71 and 72 are plots of reefing line force coefficient as a function of percent reefing for the front and side lobes of Model 301.

1.2.2 Model 302

Figure 73 gives L/D versus flap extension for Model 302. This figure represents the only useable L/D data available for this model from the Ames tests. The small amount of data

is again due to the difficulties experienced with wind tunnel instrumentation. Figure 74 is a plot of reefing line force coefficients versus percent reefing. Figures 83 and 84 are photos of Model 302 flying vertically.

1.2.3 Model 303

Figure 75 is a plot of L/D versus flap extension for Model 303. The test results for three velocities are presented in this figure. Although Model 303 did not exhibit values of L/D as high as some of the other models tested it was one of the most stable, and as can be seen from Figure 75 its performance was not greatly reduced by velocity increases.

1.2.4 Model 304

Figure 76 presents the data for Model 304. This model was rigged so that as the flaps were extended the interior lines attached to the canopy pulled the forward roof of the canopy down giving a flatter canopy profile and balancing the falp riser loads.

1.2.5 Model 402

Model 402 is a 16-ft D_o version of Model 302. As shown by Figure 77 this model did not show the improvement in performance over Model 302 that was shown in the tow truck tests. This may not have been the fault of the model as difficulties with the control mechanism and lack of time prevented the obtaining of data at optimum interior line setting when the Model was flown vertically.

1.2.6 Cluster of 3 Model 302's

Figure 78 gives the data obtained from the cluster of Model 302's. The performance of this cluster was disappointing compared to the cluster performance reported in Ref. 1. The corrected L/D max value for the cluster that give maximum performance in Ref. 1 was 1.51.

1.2.7 Model 101 (Aerosail)

Figure 79 is a plot of L/D versus flap extension for Model 101. Five test runs are shown. The higher values were obtained with the model flying vertical. Reference 1 quotes an L/D max of 1.75 for this model. Corrected data from the same tests give an L/D max of 1.54.

1.2.8 Model 105 (Aerosail)

Figure 80 is plot of L/D versus flap extension for Model 105. Reference 1 quotes on L/D max of 1.63 for this model. This value has been corrected to L/D max = 1.12.

1.2.9 Model 107 (Aerosail)

Figure 81 is a plot of L/D versus flap extension for Model 107. Reference 1 quotes on L/D max of 1.67, this has been corrected to L/D max = 1.09.

1.2.10 Model 113 (Aerosail)

Figure 82 is a plot of L/D versus flap extension for Model 113. Reference 1 quotes on L/D max of 1.55, this has been corrected to L/D max = 1.13.

Reproduced From Best Available Copy